Fatty acid induced changes in gene expression in cultured L6 rat muscle cells

An *in vitro* model on high dietary fat-induced insulin resistance in red gastrocnemius rat muscle *in vivo*

Thesis submitted to Dept. of Pharmacology, School of Pharmacy,
Faculty of Mathematics and Natural Sciences, University of Oslo
for the degree Candidata pharmaciae

By Børge Breivik
Dept. of Pharmacology, School of Pharmacy,
Faculty of Mathematics and Natural Sciences, University of Oslo
2003

Dedicated to Nicola Kaarina Breivik

TABLE OF CONTENTS

ABSTRACT

Type 2 diabetes is a serious cause of morbidity and mortality and the disease is reaching epidemic proportions in the developed world. A core defect in type 2 diabetes is insulin resistance in skeletal muscle. Previous global gene expression experiments conducted at the Garvan Medical Research Institute has shown that 3 weeks high fat feeding induced increased expression of stress related genes in rat muscle. These stress-related genes could be involved in the development of insulin resistance in rat muscle *in vivo*. However, it is not known whether the observed effect on stress associated gene expression in rat muscle is a direct effect of increased fatty acid availability or if the change in gene expression in rat muscle are a secondary effect of increased dietary fat intake.
To investigate the direct action of free fatty acids on gene expression we examined the effect of 24 and 48 h exposure to 1mM linoleate on gene expression on a cultured muscle cell line (cultured L6 myotubes).

RT-PCR results showed that linoleate did not upregulate any of the stress-genes measured in L6 rat muscle cells neither after 24 nor 48 hours. This indicates that either free fatty acids have a secondary effect on upregulation of stress-associated genes in rat muscle *in vivo* or that L6 myotubes may not be an appropriate model for comparison with *in vivo* effects.
To further investigate the impact on gene expression on muscle imposed by exposure to free fatty acids, an Affymetrix™ global gene expression analysis was conducted on mRNA from 24 hour linoleate treated L6 rat muscle cells and appropriate control cells. This experiment confirmed the previous RT-PCR measurements, but also revealed that there is a substantial difference in gene expression between cultured L6 rat muscle cells and red gastroc rat muscle *in vivo*.

ACKNOWLEDGEMENTS

I have finally come to the point of submitting and there are several people to thank. First of all, my Australian supervisor Greg Cooney at the Garvan Institute of Medical Research. Thank you for being supportive and always taking time to answer my questions in a thoughtful way.
Secondly, I want to thank Mercedes Ballesteros for helping me getting started and for her efforts to teach me general lab and tissue culture techniques.
I also want to thank my wonderful wife for correcting my many spelling mistakes.
Finally, I want to thank my co-supervisor professor Arild Rustan for making it possible for me to come to the Garvan and for reading through my thesis.

1. INTRODUCTION

1.0 Insulin

Insulin is the key anabolic hormone involved in the storage and controlled release of energy in the body. Deficiency in its secretion and action is central in all types of diabetes.
Insulin is a pancreatic polypeptide hormone consisting of one 21 and one 30-aminoacid chain joined by disulphide bonds. Increased blood concentrations of glucose, arginine and glucagon lead to increased insulin production and release from the β-cells of the pancreatic islets of Langerhans. This leads to a wide array of effects including increased glucose uptake in skeletal muscle and adipose tissue, increased glycogen synthesis in liver and muscle and increased triglyceride storage in adipose tissue. Insulin also affects protein synthesis.

1.1 Type 2 diabetes

Type 2 diabetes (also known as Non-Insulin Dependent Diabetes Mellitus; NIDDM) affects over 150 million adults worldwide and the incidence of this condition is expected to double over the next 25 years (1). The prevalence of diabetes in adults worldwide was estimated to be 4.0% in 1995, and with this figure expected to rise to 5.4% the year 2025 (2) there is no doubt as to the epidemic nature of diabetes (3).
Type 2 diabetes normally affects older adults, although it has been reported that type 2 diabetes is becoming more common among children and young adults in some developed countries (4). The underlying causes of type-2 have not been fully elucidated; however, type 2 diabetes is clearly a heterogeneous disorder with genetic and acquired components (5). The environmental factor is supported by the fact that the geographical distribution of the disease is highly shifted towards the developed world. The presence of a proven correlation between obesity and type 2 diabetes also supports the environmental component in the development of the disease (6). It is only recently that obesity has become a medical problem for the developed countries. It is also interesting that some ethnic groups, such as the Pima Indians are far more disposed to type 2 diabetes than most people, which clearly imply that there is a genetic component in the

development of the disease (7). Type-2 diabetes is a serious cause of mortality and morbidity and is strongly related to complications such as risk of cardiovascular disease, retinopathy, neuropathy and nephropathy.

1.2 A simplified model of insulin signalling in skeletal muscle

The insulin receptor is a tyrosine kinase that undergoes autophosphorylation upon insuln binding. When phosphorylated, the receptor catalyses the phosphorylation of several proteins resulting in a wide array of effects. The insulin receptor substrate (IRS) family is among these phosphorylated proteins. IRS binds and activates phosphatidylinositol-3-OH kinase (PI(3)K) which catalyses phosphorylation of phosphatidylinositol (PI) in the membrane generating PI 3,4,5 triphosphate, which in turn activates phosphoinositide-dependent kinase-1 (PDK-1).

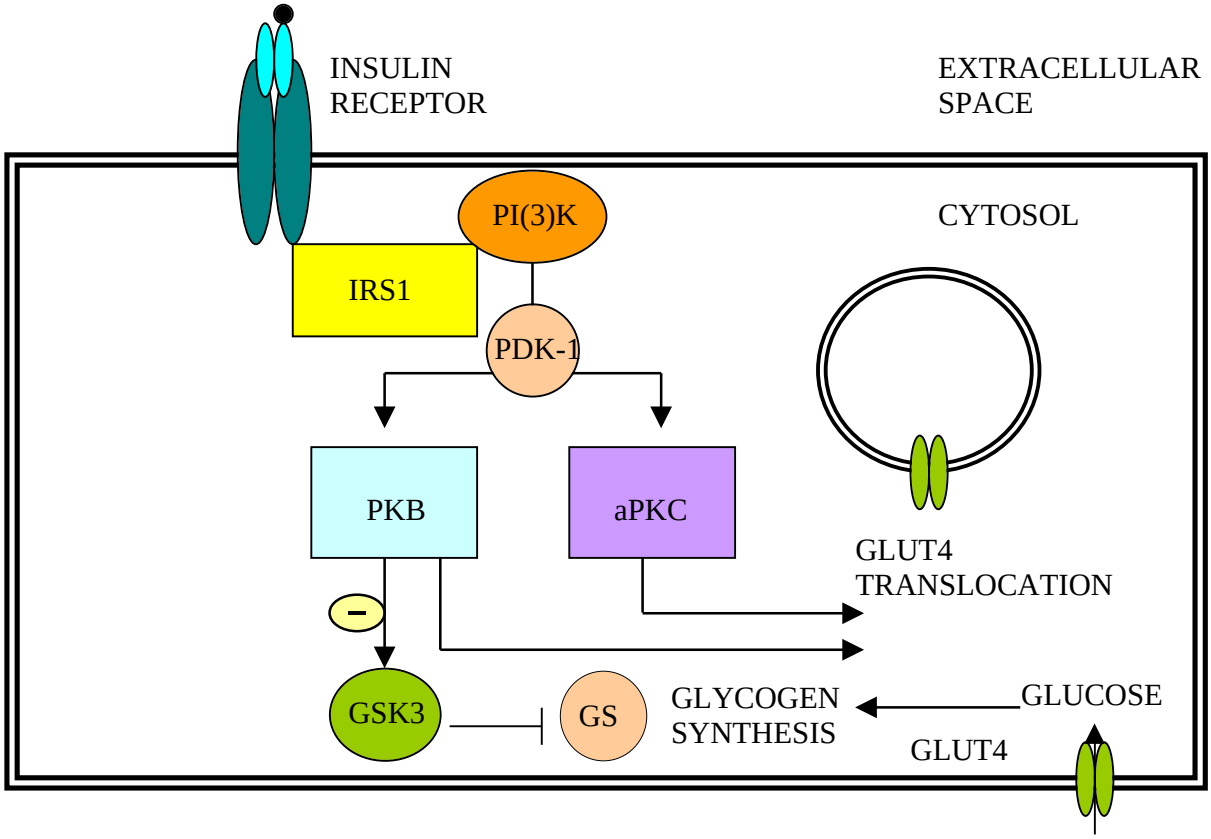

Figure 1.2.1 A schematic overview of glucose related insulin signaling. PI(3)K, phosphatidylinositol-3-OH kinase; IRS1, insulin receptor substrate-1; PKB, protein kinase B; aPKC atypical protein kinase C; GLUT4, glucose transporter 4,; GSK3, glycogen syntase kinase 3; GS, glycogen synthase

.

PDK-1 activates protein kinase B (PKB), also known as v-akt and atypical protein kinase C (aPKC) ultimately leading to several effects. These effects includes increased glucose influx as a result of translocation of glucose transport protein 4 (GLUT4) containing vesicles to the cell membrane, as well as stimulation of glycogen synthesis (8).

1.3 The pathogenesis of type 2 diabetes

Type 2 diabetes is characterised by excessive hepatic glucose production, decreased or inappropriate insulin secretion as a result of progressive β-cell dysfunction, and insulin resistance (9).

The first measurable sign of type 2 diabetes development is insulin resistance. Insulin resistance, or the failure of target tissue to respond appropriately to physiological concentrations of insulin, can appear in tissues such as liver and muscle 10-20 years before the onset of type 2 diabetes, although not everyone with insulin resistance develops type 2 diabetes. During the early stages of insulin resistance the decreased tissue response to insulin is compensated for by increased insulin secretion by β-cells in the pancreas (10). After some time, the insulin resistance becomes so severe that it can not longer be compensated for by increased insulin secretion, and glucose intolerance occurs (11, 12).

Impaired β-cell function is often the long-term consequence of the hyperinsulinaemic/insulin resistant state, leading to elevated blood glucose concentration and development of type 2 diabetes. Although there is evidence for a genetic predisposition to β-cell failure, there are also other parameters that influence β-cell function. Amongst these is the prolonged elevation in free fatty acid blood concentration, which is thought to impair β-cell function by specifically desensitising the β-cell response to glucose (13).

There are several physiological parameters that change as type 2 diabetes develops. An increased glucose production and approximately 60% down regulation in glycogen formation by the liver is seen in type 2 diabetics owing to inadequate suppression of glucose synthesis and inhibition of glycogen synthesis by insulin. This, together with impaired glucose uptake and glucose catabolism in the peripheral tissues leads to an elevated blood glucose concentration and an

impaired glucose tolerance (10, 14). Muscle accounts for up to 75 % of insulin-stimulated glucose whole body uptake via regulation of GLUT 4 transporter, whereas adipose tissue accounts for only a small fraction. This implies that insulin resistance in muscle plays a central role in the development of hyperglycaemia in type 2 diabetics.
Insulin resistance in adipocytes leads to increased lipolysis, which results in an elevated circulating free fatty acid concentration. A high free fatty acid concentration stimulates the production of very low-density lipoprotein (VLDL) in the liver, and its release into the circulation. Dyslipidaemia can result in vascular complications and also increases the insulin resistance by reducing glucose muscle clearance and increasing glucose output from the liver (15).

1.4 Possible mechanisms in the development of insulin resistance

There are several factors in addition to the genetic predisposition that can cause insulin resistance; such as obesity, pregnancy and a hormone excess (16). There is a strong link between excessive body fat, especially central abdominal fat, and insulin insensitivity (17).
In 1963, Randle et. al.proposed a mechanism known as the Randle cycle, which implied that increased fatty acid oxidation caused the inactivation of mitochondrial pyruvate dehydrogenase, ultimately leading to decreased glucose uptake (18).
Since then there have been several other proposed underlying mechanisms for the fatty acid induced development of insulin resistance, and several of these mechanisms are overlapping. In the following some of these mechanisms are outlined:

1.4.1 LCACoA

The first step in the metabolism of free fatty acids after they have entered the muscle cell, is the covalent attachment of coenzyme A (CoA) by acyl-CoA synthase (ACS), forming long-chain acyl CoA (LCACoA) (19). The activated fatty acids have several fates; including β-oxidation in the mitochondria and conversion to intramuscular triglyceride initiated by glycerol-3-phosphate acyl transferase (GPAT). There is evidence that accumulated intramuscular fat, in the form of

activated LCACoA or stored triglycerides, is linked with insulin resistance in animals and humans (20, 21).

This muscle cell lipid accumulation can be caused by an increased uptake of systemic available fatty acids, but the most probable reason is a reduced import into the mitochondria and a reduced β -oxidation, leading to an increased cytosolic LCACoA concentration (19).

LCACoA has direct effects on muscle cell metabolism through modulation of enzyme activity of several key enzymes, including inhibition of hexokinase (22), a key enzyme in glucose metabolism.

Palmitoyl-CoA is a precursor for *de novo* synthesis of ceramide, a signal molecule known to influence insulin sensitivity, as described in more detail below, and it has been speculated whether increased ceramide synthesis through increased substrate availability could have an indirect effect on insulin signalling.

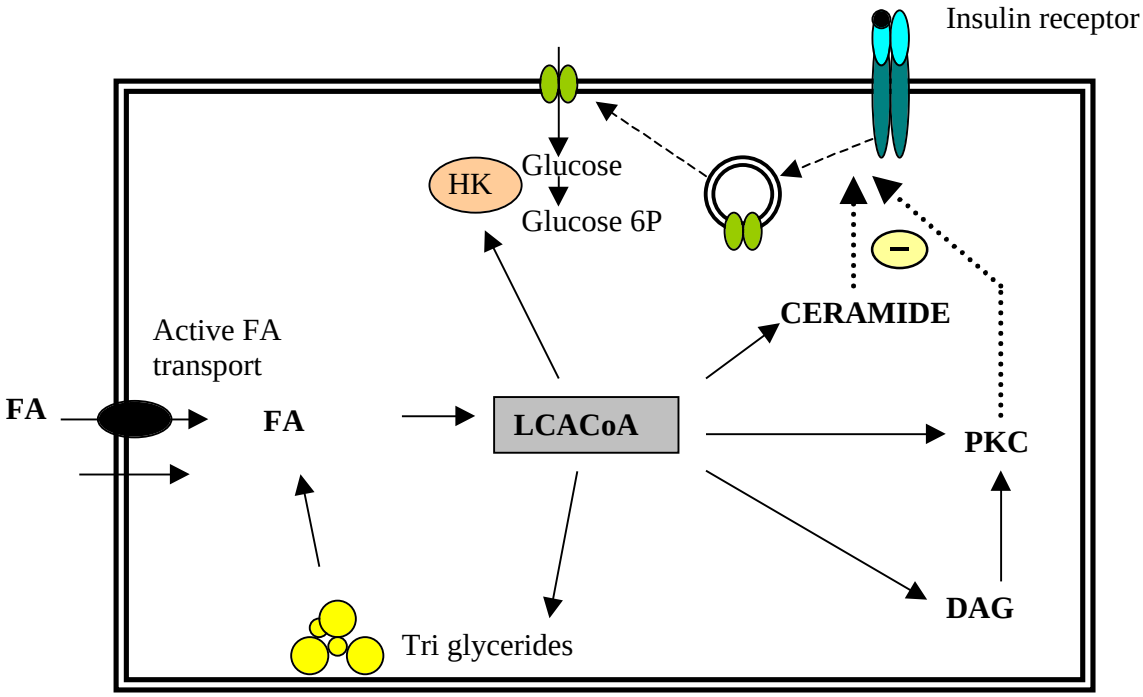

Figure 1.4.2 Effects of elevated intracellular long chain acyl coA (LCACoA). HK, hexokinase; DAG, diacyl glycerol; PKC, protein kinase C; FA, fatty acid

There is also evidence that LCACoAs can activate specific subtypes of protein kinase C (PKC) either directly or by acting as a percursor for increased 1,2-diacylglycerol (DAG) (as described in more detail below).

1.4.2 PKC

The Protein Kinase C (PKC) family consists of several isoenzymes divided into classical, novel and atypical subclasses. The PKCs translocate to the membrane upon activation and phosphorylate serine threonine residues on target proteins, including the insulin receptor and insulin receptor substrate-1 (IRS-1). Activation of certain PKCs, such as the novel PKCε and PKCθ by increased lipid availability in muscle, is strongly associated with insulin resistance (23).

Experiments have shown a decrease in the phosphorylation of tyrosine in the insulin receptor (IR) and the IR substrate (IRS)-1 in muscle from rats after treatment with free fatty acids. Pre-treatment with a PKC inhibitor prevented this effect, suggesting that PKC has a central role in fatty acid influence on insulin signalling (24).

Recently, it has been shown that not only activation of classical and novel but also atypical PKCs (aPKCs), involved in GLUT4 translocation, are important in the regulation of insulin sensitivity. In 2003, Beeson et al. (25) demonstrated a decrease (70-80%) in insulin stimulated aPKC activation in subjects with impaired glucose tolerance and in type 2 diabetics compared to control subjects. This implies that aPKC activation and skeletal muscle insulin sensitivity are linked. Another study (26) supports this, showing an insulin stimulated decrease in activation of the aPKC isoforms PKCλ/ζ in obese and diabetic subjects compared to PKCλ/ζ activation in lean subjects.

1,2-diacylglycerol (DAG), an intermediate in triglyceride and phospholipid metabolism, has been found to accumulate in insulin resistant muscle. DAG is a widespread intracellular second messenger and it has been suggested that there is a link between accumulation of DAG in muscle and decreasing insulin sensitivity through DAG activation of PKC (27)

1.4.3 Ceramide

Ceramide is known to be involved in intracellular signalling (28) and it has been suggested that intracellular ceramide concentration is linked to insulin sensitivity (29). Ceramide is generated by sphingomyelinase from sphingomyelin, a widely distributed cell membrane component, or synthesised *de novo* from serine and palmitoyl-CoA (30).

Interestingly, there is evidence that TNFα is an activator of sphingomyelinase, and that ceramide may be a second messenger in TNFα signalling (figure 1.4.3) (23).

Ceramide appears to be act via phosphatase 2A(PP2A). PP2A is reported to inhibit the synthesis of glycogen through inhibiting regulatory phosphorylation by protein phosphatase-1 (PP1). In addition, dephosphorylation, and hence deactivation of PKB mediated by PP2A, can lead to impaired insulin sensitivity. Incubation of adipocytes with ceramide has shown a 50% decrease in the insulin-stimulated glucose transport by inhibiting GLUT4 translocation and activation of PKB(31).

Finally, some isoforms of PKC including PKCζ, have been reported to be directly activated by ceramide leading to interference with insulin signalling (32).

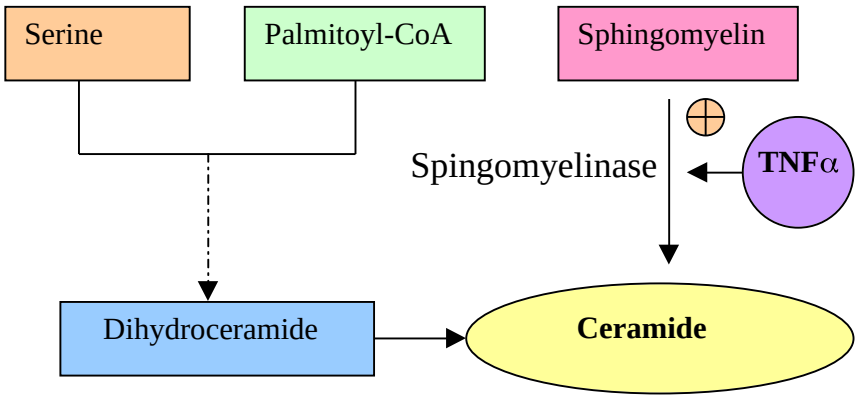

Figure 1.4.3 Intracellular ceramide synthesis and activation of sphingomyelinase by tumour necrosis factor-α (TNF-α). Figure adapted from (23).

1.4.4 Hexosamine pathway

The hexoamine pathway is the conversion of fructose-6-phosphate into UDP-N-acetyl-glucosamine initiated by the rate limiting enzyme glutamine:fructose-6-phosphate amidotransferase (GFAT). The hexosamine pathway is thought to be involved in nutrient sensing, and an increased flux through the pathway, initiated by for example increased fatty acid availability, is associated with decreased insulin sensitivity (33, 34).

The underlying mechanisms for the effect of hexosamines are not fully understood. One possibility is that increased production of protein glycosylation substrate by the hexosamine pathway affects the specific O-glycosylation of proteins (34). Several proteins are O-glycosylated, including IRS-1 (35) and glycogen synthase (36) and although the precise functional consequences of O-glycosylation are unclear it seems reasonably to assume it has some functional significance.

It has been demonstrated that glucosamine exposure increased the activity of PKC in rat adipocytes, which could also be an explanation for the hexosamine-pathway-effect on insulin

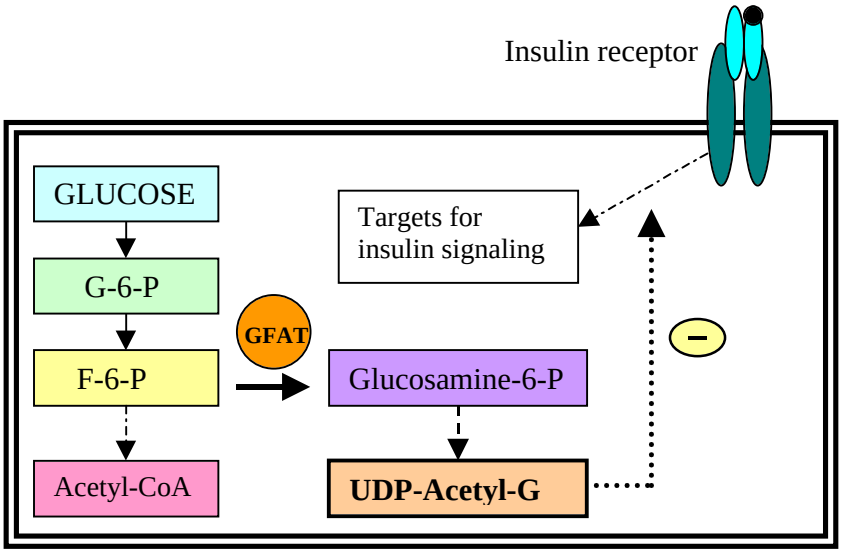

Figure 1.4.5 Overview of the hexosamine pathway. G-6-P, glucose-6-phosphate; F-6-P, Fructose-6-phosphate; GFAT, glutamine:fructose-6-phosphate amidotransferase; UDP-acetyl-G. UDP-acetyl-gucosamine.

signalling in muscle. In addition *in vitro* studies has also demonstrated that a PKC inhibitor reversed, glycosamine induced insulin resistance in adipocytes (37).
Hexosamines are also known to stimulate transforming growth factor-β (TGFβ) transcription and and hence production of extracellular matrix which, in turn can inhibit insulin signalling (38). This could be an alternative explanation on the hexosamine effect on insulin sensitivity in muscle.

1.4.5 TNFα

Tumour necrosis factor-α (TNFα) together with, adiponectin, resistin and others, forms a class of biologically active message molecules known as adipokines. While adiponectin and leptin, a hormone secreted from the adipocytes are associated with increased insulin sensitivity (39, 40), TNFα and resistin are associated with the development of insulin resistance (41, 42). TNFα is secreted from several cell-types including adipocytes and is found to be overexpressed in obese humans (43). Since TNFα stimulates lipolysis and inhibits lipogenesis in adipose tissue it is thought be an important mediator of insulin sensitivity, although knockout experiments of the TNFα gene provided only partial protection against obesity-induced insulin resistance (44). Insulin-stimulated glucose uptake and activation of glycogen synthase is reported to be decreased by TNFα in rat skeletal muscle *in vitro* (45), although others have reported that TNFα does not seem to have any effect on the ability of insulin to increase glycogen synthesis in cultured human muscle cells (46).
TNFα acts on the TNFα-receptor and initiates several signalling pathways (figure 1.4.1) including activation of the dimeric transcription factor Nuclear Factor-κB (NFκB) (41, 47). In its inactive form, NFκB is located in the cytoplasm bound to the inhibitor protein IκB. When the TNFα receptor is stimulated, a serine kinase cascade leads to phosphorylation of IκB by IκB Kinase (IKK), which leads to its protosome mediated degradation. This releases NFκB and it is translocated from the cytoplasm to the nucleus where it binds to DNA, initiating transcription of several genes including pro-inflammatory and pre-adipocyte genes. NFκB also regulates the expression of TNFα. IKK is built up of two subunits, IKK-α and IKK-β. Interestingly, the

β-subunit has been identified as the cellular kinase responsible for TNFα induced IRS-1 phosphorylation. (48).

A more indirect way in which TNFα can influence insulin sensitivity is by repression of adiponectin gene expression. Adiponectin is reported to have an enhancing effect on insulin sensitivity (40), and while insulin stimulates adiponectin secretion *in vitro*, TNFα potently represses adiponectin mRNA levels in adipocytes (49). Recently, two adiponectin receptors, adiponectin receptor 1 (AdipoR1) abundantly expressed in muscle and adiponectin receptor 2 (AdipoR2) present in the liver were cloned by Yamauchi et. al.(50). These receptors could be novel drug targets in the treatment of type 2 diabetes.

Several factors, other than TNFα can lead to activation and translocation of NF-κB, including p38 MAPK, oxidative stress and IL-1β exposure.

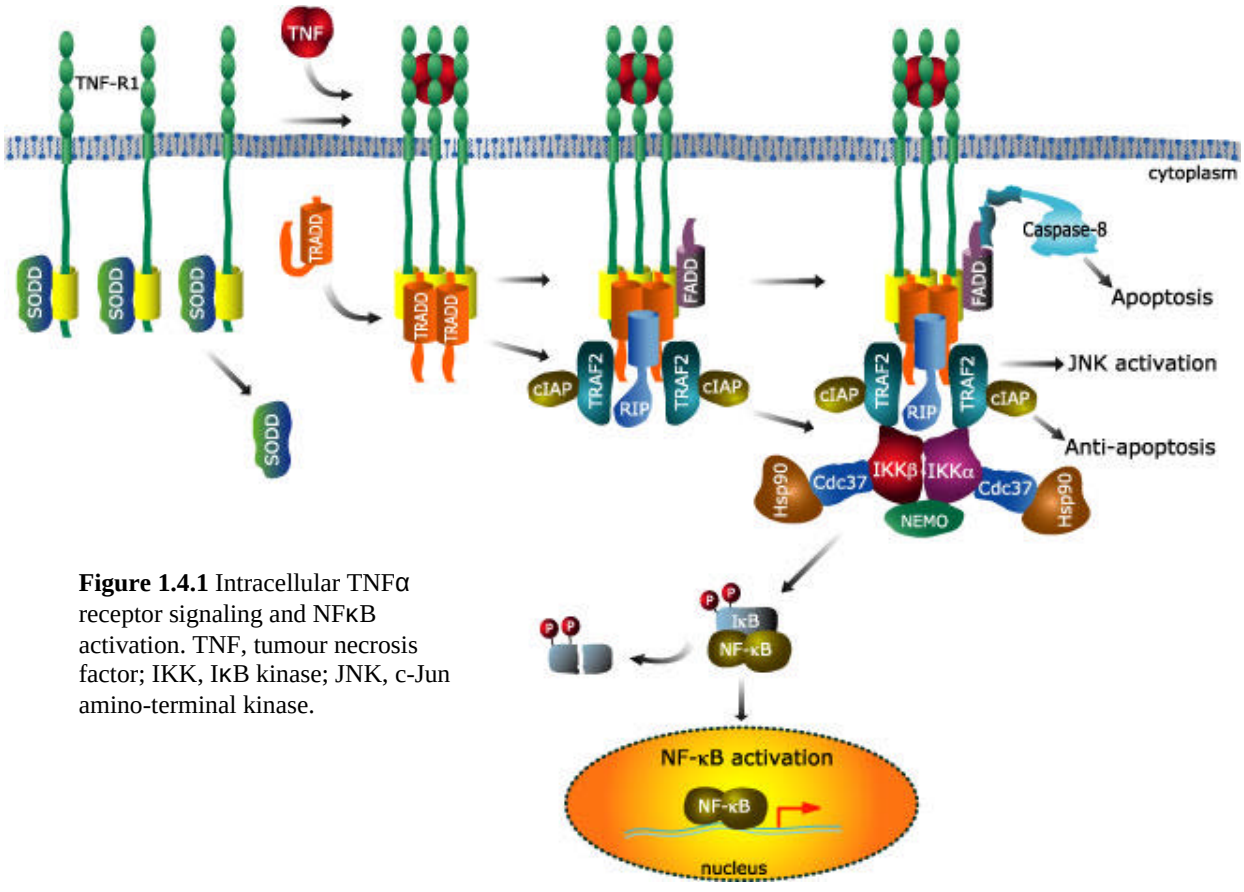

Figure 1.4.1 Intracellular TNFα receptor signaling and NFκB activation. TNF, tumour necrosis factor; IKK, IκB kinase; JNK, c-Jun amino-terminal kinase.

1.5 Oxidative stress and insulin resistance

There is an increasing body of evidence linking insulin resistance and stress-activated signalling pathways. Some of the findings implying that oxidative stress-sensitive gene expression and insulin sensitivity are related include:

· It has been reported in both animal models and in muscle cells *in vitro* that insulin resistance induced by either hyperglycaemia or by increased free fatty acids can be prevented by administration of antioxidants such as α-lipoic acid (LA), N-acetylcysteine and vitamin E (51),(52),(53). The acute and long-term protective effect of LA has also been demonstrated in humans with type 2 diabetes (54).

· It has recently been discovered that some genes involved in providing cellular protection against oxidative stress, are down regulated in skeletal muscle in people with type-2 diabetes (including heat shock protein 72 and oxygenase-1)(55).

· A major intracellular target of oxidative stress is the transcription factor NFκB. IKKβ, a kinase which regulates the NFκB pathway has been found to be increased in insulin resistant muscle (56). Salicylates which are known to inhibit IKKβ activity have been shown to protect against fat-induced insulin resistance and lower blood glucose in rats (57).

· The c-Jun amino-terminal kinase (JNK), a protein in the stress sensitive JNK/SAPK pathway has been shown to be substantially upregulated in obese and insulin resistant mice, whereas mice JNK1(-/-), but *not* JNK2(-/-) knock out mice had decreased weight and significantly improved insulin resistance. This suggests that the JNK/SAPK pathway plays a role in the pathogenesis of type 2 diabetes.

Mitochondria are the main site for the generation of free radicals. In the process of respiration a fraction of the oxygen used is converted into reactive oxygen species (ROS) (see figure 1.5.1). ROS are toxic to the cell but are normally quickly detoxified by several defence mechanisms, including, catalase, superoxide dismutase (SOD) and glutathione (GSH) peroxidase/reductase (Figure 1.5.1). Both increased free fatty acid concentrations and hyperglycaemia can increase ROS concentrations (47).

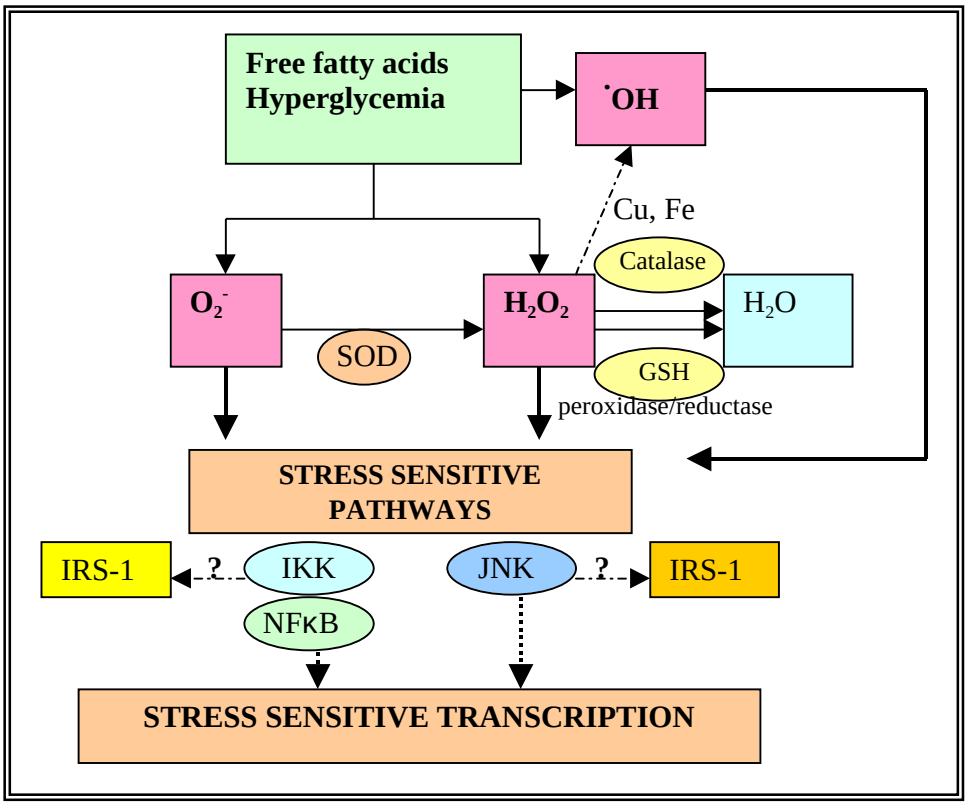

Figure 1.5.1 Overview of reactive oxygen species generation, degradation, influence on gene transcription and dephosphorylation of IRS-1(insulin-receptor-substrate-1). SOD, superoxide dismutase; GSH, glutathion; IKK, IκB Kinase; NFKB, Nuclear-factor-KB; JNK, c-Jun amino-terminal kinase

1.6 Lipid metabolism in skeletal muscle

As discussed in the previous section, it is well established that fatty acids influence insulin sensitivity in skeletal muscle although the exact mechanism behind this is not known. The impact of fatty acids may be direct or indirect through a lipid metabolite (such as diacyl glycerol (DAG)). In this section fatty acid metabolism in skeletal muscle is briefly reviewed.

1.6.1 Transport of fatty acids into muscle cells:

Fatty acids (FA) are highly hydrophobic, do not dissolve freely in blood and are bound to transport proteins (albumin and lipoproteins) while circulating in the bloodstream. When FAs are

transported from adipose tissue they are transported as non-esterified fatty acids (NEFA) bound to albumin, an abundant blood protein. Other protein-containing structures that transport FAs include lipoproteins such as chylomicrons which transport dietary fat taken up by the gut, and very low-density lipoproteins (VLDL) which are secreted from the liver. Both in chylomicrons and VLDLs fatty acids are transported esterified to glycerol (triacylglycerol). On reaching the muscle cell, triacylglycerol is hydrolysed into fatty acids by lipoprotein lipase, after which it enters the cell via simple diffusion or active transport. There is evidence of passive transport of FAs across the cell membrane through a “flip-flop” mechanism (58), and there is no doubt that this mechanism can contribute to the FA translocation, although views vary on the contributing effect of this compared to active transport.(58, 59)

There are several suggested mechanisms for active FA transport across the cell membrane. One paper (60) suggests that long-chain FAs (LCFA) are actively transported either directly through fatty acid transport proteins (FATPs) or by first attaching to fatty acid transporter (FAT/CD36), which then hands over the FFA to the FATPs (as illustrated in figure1.6.1).

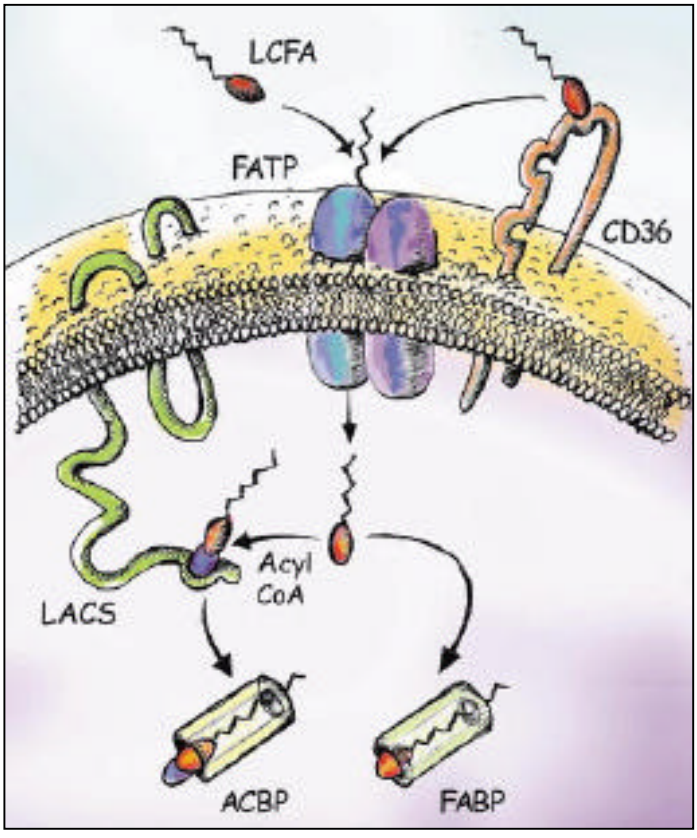

Figure 1.6.1 Proposed mechanism for active fatty acid translocation. LCFA, long-chain fatty acid; FABP, fatty acid binding protein; ACBP, acyl CoA binding protein; LCACS, long-chain fatty acyl-CoA synthetase; FATP, fatty acid transport protein.

It has been reported that overexpression of FAT/CD36 in mice skeletal muscle leads to enhanced fatty acid oxidation and reduced circulating triglycerides and fatty acids (61), while FAT/CD36 deficiency in mice increases insulin sensitivity in muscle and decreases insulin sensitivity in liver(62). It has also been reported that insulin can stimulate uptake of FAs through cellular redistribution of FAT/CD36 (63). Together, these findings imply that FAT/CD36 has a central role in the translocation of FAs into the cytosol in muscle. Peroxisomal proliferator-activated receptors (PPARs), which can be activated by fatty acids, seem to regulate the expression of FAT/CD36 and FATPs.

Once inside the cell, the FAs are esterified by long-chain fatty acyl-CoA synthetase (LACS) or fatty acyl-CoA synthetase (ACS) to coenzyme A (CoA), which activates the FAs for mitochondrial transport and oxidation. The esterified FA are also more hydrophilic than FAs, which prevents passive leak of FAs into the extracellular space. Fatty acid binding proteins (FABP)s and acyl CoA binding protein (ACBP) respectively bind FAs and the esterified LCACoAs, increasing their cytosolic solubility.

1.6.2 Fatty acid storage in muscle cells

The main site for fatty acid storage is as triglyceride in adipose tissue. Lipids can also be stored in muscle, although only to a limited extent compared to adipose tissue. Intramuscular accumulation of triglycerides has been found to correlate with decreased muscle insulin sensitivity (64, 65). The first step of triglyceride synthesis *de novo* is the esterification of LCACoA to glycerol-3-phosphate, catalysed by glycerol 3-phosphate acyl transferase (GPAT). Insulin influences the rate of triglyceride synthesis by regulating GPAT activity (66).

There is some evidence that reduced fatty acid oxidation rather than increased uptake is more important in elevating lipid (LCACoA) concentration in muscle (67, 68) and since *de novo* fatty acid synthesis is minimal in skeletal muscle (69) the rate of oxidation would also influence the rate of intramuscular triglyceride synthesis. Polyunsaturated fatty acids (PUFAs) have been shown to reduce triglyceride accumulation in skeletal muscle (70). This suggests that not only the concentration of intramuscular FA (LCACoA) but also the type of fatty acid influences the amount of intracellular triglyceride synthesised.

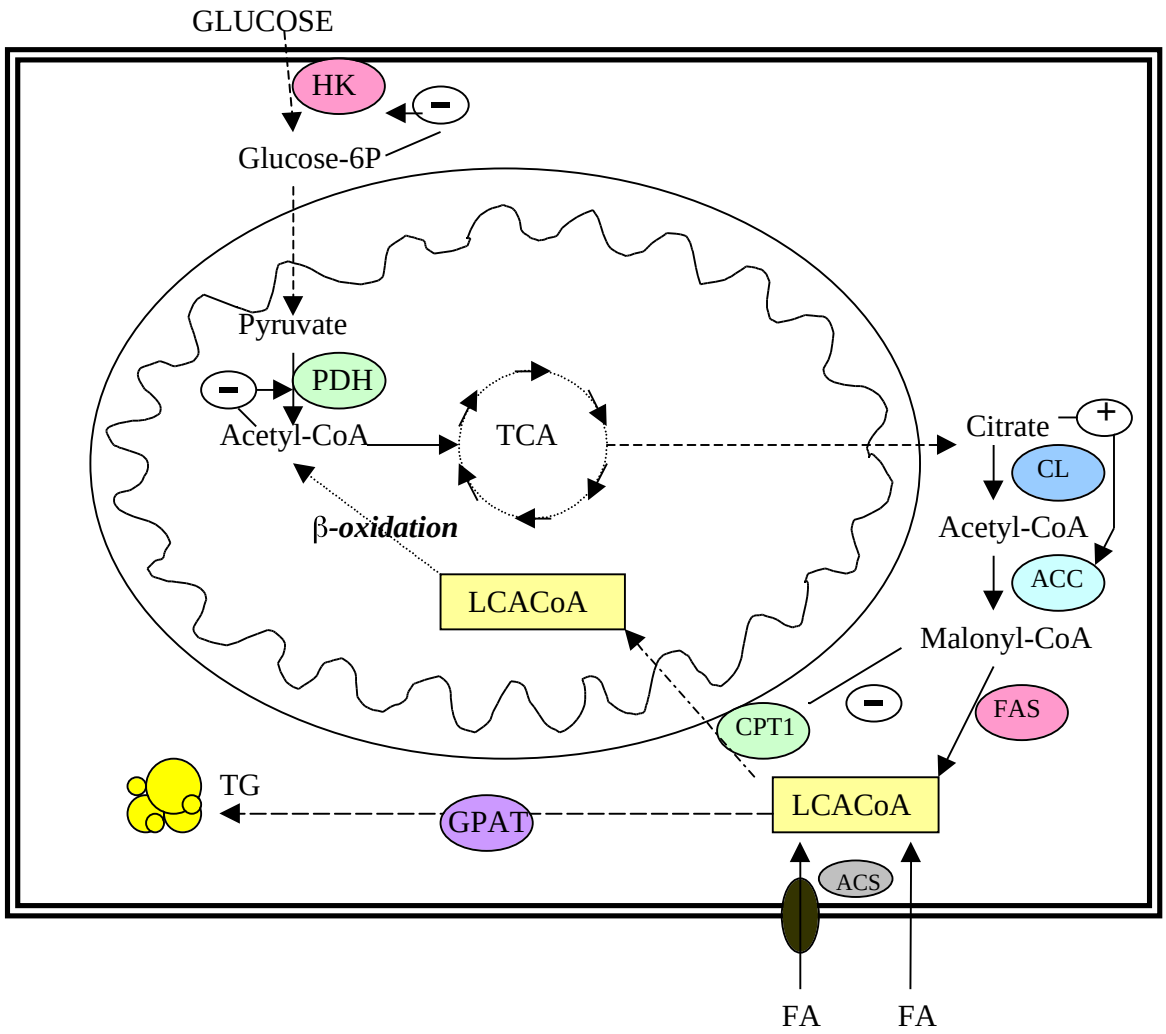

Figure 1.6.2 Overview of fatty metabolism. CPT1, carnitine palmitoyl transferase; ACC, acetyl CoA carboxylase, CL, citrate lyase; FAS, fatty acid synthase; GPAT, glycerol 3-phosphate acyl transferase; PDH pyruvate dehydrogenase complex; HK, hexokinase.

1.6.3 Fatty acid oxidation in muscle cells

Fatty acid oxidation in the muscle is predominantly located to the mitochondria, but fatty acid oxidation also occurs in peroxisomes (71). Before the LCACoA can be oxidised in the mitochondrion, it has to be transported across the mitochondrial membrane. Carnitine palmitoyl transferase (CPT) 1, which is located on the outside of the mitochondrial membrane, is thought to be the rate-limiting enzyme in this process. CPT1 converts LCACoA to acyl-carnitine (AC). AC is transported across the membrane and converted back to LCACoA by CPT2. Malonyl-CoA, an early intermediate in fatty acid synthesis, is an inhibitor of CPT1, and elevated

concentrations of malonyl-CoA can lead to cytosolic accumulation of LCACoAs which can by mechanisms previously described lead to insulin resistance (69).
Once inside the mitochondrion the LCACoA is fully oxidised by β-oxidation to water, CO_2 and energy.

1.6.4 Transcriptional regulation of fatty acid metabolism by PPARs

The peroxisome proliferator-activated receptors (PPARs) are a family of ligand-activated transcription factors that are activated by several agonists including some lipids, for example polyunsaturated fatty acids (PUFAs). There are several isoforms of PPARs; PPARα, highly expressed in many tissues including liver, muscle, and heart; PPARδ, which is ubiquitously expressed and PPARγ highly expressed in adipose tissue. All three PPAR subtypes bind to DNA, as hetrodimers with retinoid X receptor (RXR) subtypes upon agonist activation (72) and regulate the expression of genes involved in lipid metabolism (73). Some of these genes include FATP, CD36/FAT (74), acyl-CoA synthase (75) and CPT1 (76). PPAR activity has been more thoroughly studied in adipose tissue and liver than in skeletal muscle but, studies show that the expression of PPAR-responsive genes are enhanced when cultured skeletal muscle cells are incubated with fatty acids or specific synthetic ligands for PPAR isoforms. This demonstrates that PPARs may also have a regulating role in muscle energy metabolism (77). Both PPARα and PPARγ are abundantly expressed in skeletal muscle and it has been demonstrated that PPARα plays a role in regulating lipid homeostasis in human muscle cells.
PPARδ is also expressed in muscle cells and has been shown to be at least partially responsible for the dual effect of long chain fatty acids, both as inhibitors of myogenesis and inducers of transdifferentiation into preadipose-like cells. This is for example seen in cultured C2C12 mouse muscle cells (78). Recent in vitro studies suggests that PPARδ plays a central role in the regulation of fatty acid oxidation in skeletal muscle. It has been demonstrated that fatty acid treatment or treatment with synthetic PPARδ -agonist induces genes involved in lipid metabolism in C2C12 mouse muscle cells (79, 80).

1.7 Aims

Previous microarray data from research at the Garvan Institute of Medical Research has revealed that mRNA expression of genes that are involved in stress pathways are upregulated in insulin resistant skeletal (red gastroc) muscle from high-fat fed rats compared to normal (chow fed) rats. It is not known whether the dietary fatty acids have a direct effect on stress pathways in muscle cells or if the changes in the stress-associated gene expression observed are due to an indirect effect of the high fat diet.

The purpose of the study is firstly to see whether exposure of cultured L6 rat muscle cells to 1mM fatty acid (linoleate) gives a similar change in stress associated gene expression as seen in high-fat-fed rat muscle *in vivo*. The modulating effect of the cytokine TNFα and the PPARγ agonist rosiglitazone on stress associated gene expression in L6 cells is also investigated.

A second goal is to examine the degree of similarity in gene expression between a cultured differentiated rat muscle cell line and red gastroc rat muscle *in vivo.*

Finally, this study aims at evaluating whether cultured L6 rat muscle cells would be a suitable *in vitro* model for further research on the mechanisms behind modulation of stress sensitive gene expression in muscle from high-fat-fed rats.

2.1 ABBREVIATIONS

ACBP - acyl CoA binding protein
ACC - acetyl CoA carboxylase
ACS - acyl-CoA synthase
ADD1- adipocyte determination- and differentiation-dependent factor 1
AdipoR1 - adiponectin receptor 1
AdipoR2 - adiponectin receptor 2
aPKC – atypical protein kinase C
BSA - bovine serum albumin
BTEB - basic transcription element binding protein
CL - citrate lyase
CL-6 - growth responce protein
CoA - coenzyme A
COX-2 - prostaglandine-endoperoxide synthase 2
CPT1 - carnitine palmitoyl transferase
DAG - 1,2-diacylglycerol
DMSO – dimethyl sulfoxide
DNA b.p. - DNA binding protein
dNTP – deoxyribonucleotide triphosphate
ERK – early responce kinase
EST - expressed Sequence Tags
FA - fatty acid
FABP - fatty acid binding protein
FAT/CD36 - fatty acid transporter
FATP - fatty acid transport protein
FCS- fetal chalf serum
GAPDH – glyceraldehyde-3-phosphate-dehydrogenase
Gastroc - gastrocnemius
GLUT1 - glucose transporter 1
GLUT4 - glucose transport protein 4
GMA - Growth Medium A
GMB - Growth Medium B
GO - Gene Ontology
GPAT - glycerol-3-phosphate acyl transferase
GS - glycogen synthase
GSH - glutathione
GSK3 - glycogen syntase kinase 3
HK - hexokinase
HMG-hydroxy-methylglutaryl
IKK - IκB Kinase
IR - insulin receptor
IRS - insulin receptor substrate

IVT - in vitro transcription
JAK2 - Janus kinase 2
JNK - c-Jun amino-terminal kinase
LA - α-lipoic acid
LCACoA - long-chain acyl CoA
LCACS - long-chain fatty acyl-CoA synthetase
LDL – low density lipoprotein
MAPK - mitogen activated protein kinase
MAS - The Micro Array Suite™
MEM- minimal Essential Medium
mRNA – messenger ribonucleic acid
NEFA - non-esterified fatty acids
NFκB - nuclear Factor-κB
NGFI-B – nerve growth factor I-B
NIDDM - Non-Insulin Dependent Diabetes Mellitus
PBS – phosphate buffer
PCR - polymerase chain reaction
PDH - pyruvate dehydrogenase complex
PDK-1 - phosphoinositide-dependent kinase-1
PI(3)K - phosphatidylinositol-3-OH kinase
PKB - protein kinase B
PP1 - protein phosphatase-1
PP2A - phosphatase 2A
PPARs - peroxisomal proliferator-activated receptors
PUFAs - Polyunsaturated fatty acids
ROS - reactive oxygen species
RT - reverse transcriptase
RXR - retinoid X receptor
SAPE - streptavidin phycoerythrin
SOD - superoxide dismutase
SREBP-1 - sterol regulatory element-binding transcription factor 1
TGFβ - transforming growth factor-β
TNF-α - tumour necrosis factor-α
UCP3 - uncoupling Protein-3
VLDL - very low-density lipoprotein

2.2 MATERIALS AND METHOD:

2.2.1 L6 cell growing, splitting and differentiation

Establishing tissue culture of L6 myoblasts

In sterile conditions, an ampoule of L6 myoblasts cells was thawed rapidly at 37 °C. The cells were carefully resuspended in a 150cm^2 flask containing Growth Medium A (GMA) (MEM/10% FCS/10% Antibiotic/antimyotic) equilabratid to 37 °C. The cells were incubated at 37°C in a 5% CO_2 atmosphere. The medium was carefully decanted and replaced with another 20ml GMA after 2 hours of incubation to remove DMSO originating from the L6 freezing medium. The cells were then further incubated until they were 60-80% confluent. The flasks were inspected daily under a microscope.

Splitting of cells

At 60-80% confluence, usually every 3-4 days, the cells were split to avoid cell differentiation and maintain passages. After removing the growth medium by vacuum, the cells where washed twice using 2x20ml PBS (0.36% Disodium Hydrogen Ortophosphate, 0.02% Potassium Chloride, 0.024% Potassium Dihydrogen Phosphate, 0.8% Sodium Chloride). The cells were detached from the flask by adding 5mL trypsin (Gibco) for about 10 seconds. The trypsin was carefully decanted and replaced with 10ml Growth Medium B (GMB) (MEM/2% FCS (Gibco)/ 10%Antibiotic/antimyotic (Gibco)). The cells came into suspension by gently tapping the side-walls of the flask. The cell suspension was then decanted into a sterile 50ml tube and 20ml GMA was added. The serum in the medium deactivates the trypsin. 0.3ml of the cell suspension was added to a new 150 cm^2 flask containing 20ml GMA and incubated at 37°C in a 5% CO_2 atmosphere until the cells had grown to 60-80% confluence.

Seeding of cells on plates

After 2 passages there were enough cells to seed them into 10cm plates.
The growth medium was removed by vacuum and the cells were washed twice with 20ml PBS. 5ml trypsin was added to detach the cells. The trypsin was carefully removed and replaced with 10ml GMA. The cell suspension was then decanted to a sterile 50ml tube and the cell concentration was determined using a haemocytometer. 10ml GMA was added to each plate (10cm). The cell suspension volume containing $4x10^5$ cells was calculated and added to the plates. The plates were gently swirled and then incubated at 37°C in a 5% CO_2 atmosphere for 48 hours.

Differentiation of cells

The L6 muscle cells differentiate into myotubes when treated with a low serum content medium. The GMA medium was removed from the plates by vacuum and replaced with 7.5ml GMB and incubated at 37°C in a 5% CO_2 atmosphere for 10 days. The GMB was replaced every 24 hours and the plates were inspected under a microscope daily.

2.2.2 Preparation of treatment solutions

Linoleate solution

1.87g BSA (Bovine Serum Albumin, Fatty acid free, SIGMA) was dissolved in 9.37ml medium (2% FCS MEM) on a roller for 30 min at room temperature to make a 20% BSA solution. A 28mg/ml solution of linoleate (18:2 (n-6)) in ethanol was made from freshly thawed pure linoleate. The linoleate stock was stored at –80°C under an argon atmosphere to avoid oxidation. 375µl 28mg/ml linoleate solution was added into the freshly made 20% BSA solution in sterile conditions. The BSA solution was pre-heated to approximately 37°C to avoid linoleate from coming out of solution. The combined linoleate and BSA solution was then filtered (0,22µm) into 28,1ml sterile 2% FCS MEM to give a final linoleate concentration of 1mM in 5% BSA 2% FCS MEM.

Rosiglitazone control solution

10mg of Rosiglitazone (Rosiglitazone-maleate, GlaxoSmithCline) was dissolved in 211 µl DMSO and 20µl of this solution was added into 20 ml 2% FCS MEM. 20ml of the combined solutions were filtered (0.22µm) into 20ml media (2% FCS MEM) under sterile conditions. Finally 16µl of this solution was added into 8ml 5% BSA 2% FCS MEM under sterile conditions to give a final Rosiglitazone concentration of $2x10^{-7}$M.

Rosiglitazone linoleate solution

10mg of Rosiglitazone was desolved in DMSO and in into 20 ml 2% FCS MEM as described above. 16µl of this solution was added into 1mM linoleate 5% BSA 2% FCS MEM prepared as described above, to give a final Rosiglitazone concentration of $2*10^{-7}$M and a final linoleate concentration of 1mM.

TNFα solution

4ml of TNFα stock solution (10µg/ml, Recombinant Human, R&D System) was added into 8ml 2% FCS MEM to give a final TNFα concentration of 5ng/ml. The solution was filtered (0.22µm) in sterile conditions.

2.2.3 L6 rat muscle cell treatment

Growth medium was removed from the differentiated L6 muscle cells by vacuum and replaced by the treatment medium. Each treatment solution was added to two separate plates with differentiated L6 rat muscle cells (Figure 2.2.3.1). One was incubated at 37°C in a 5% CO_2 atmosphere for 24 hours and the other was incubated at the same conditions for 48 hours.

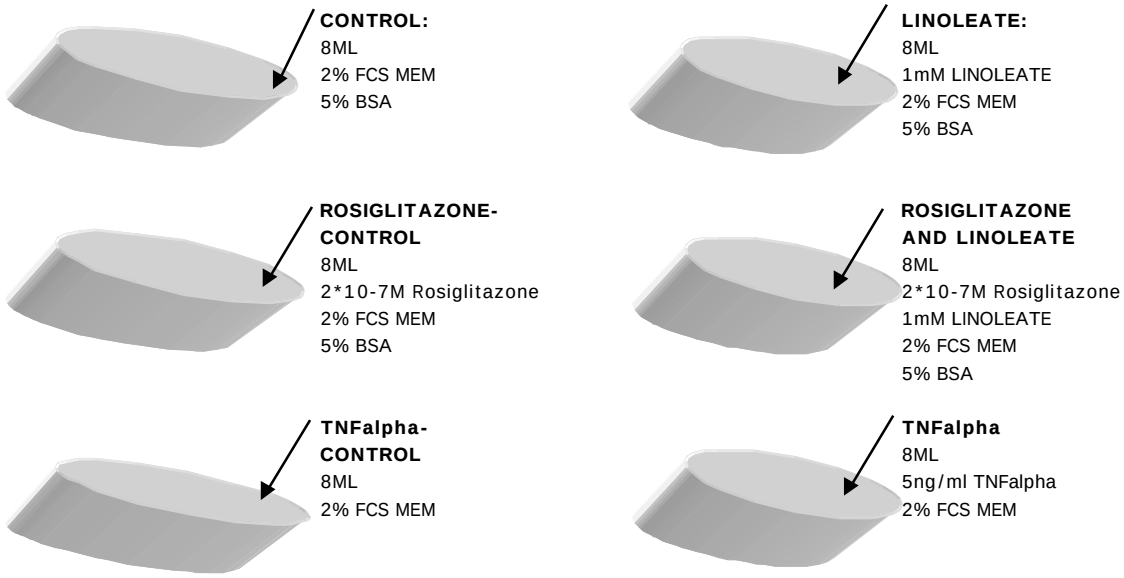

Figure 2.2.3.1 L6 cell treatment overview. FCS, Fetal Calf Serum;BSA,Bovine Serum Albumin ;MEM, α-Minimal Essential Medium

2.2.4 Total RNA Isolation and quantification

Total RNA was isolated from the treated L6 rat muscle cells by using Tri Reagent® (Sigma). The medium was removed from the plates and the cells were washed twice with 10ml PBS. 1.5ml of Tri Reagent was added to the plates in a fume hood and the lysed cells were immediately harvested using a cell scrape. The lysate was passed through a syringe to make it homogenous and the RNA was extracted according to manufacturers instructions. The isolated RNA was stored as a pellet in absolute ethanol at –80°C.

The amount of RNA isolated from the L6 rat muscle cells was measured by fluorometry using a SYBR Green II assay (81).

The RNA stocks stored at -80°C were washed with 1ml 75% ethanol and the pellets were then resuspended in 50µl RNase free H_2O (AmResco). 5µl of this RNA solution was added to 45µl RNase free H_2O. The stock solutions were stored at -80°C. 2µl and 3µl of the 1:10 RNA dilutions were added to 1ml freshly made 1:10000 dilution of SYBR green II dye (Molecular Probes) in 1xTE buffer (10x, 1,2% Tris HCL 10mM, 0.3% EDTA). Standard RNA solutions (50, 100, 200, 400, 600 and 800ng) were made up and 1ml of the same SYBR green II solution was

also added. The intensity of emitted light was measured using a fluorometer (excitation wavelength: 468nm; emission wavelength: 525nm), and the RNA concentration of the stock was measured as the mean value of the two samples calculated from the standards by linear regression. The 1:10 RNA dilutions were stored at -20°C.

2.2.5 RT-PCR

Reverse Transcriptase

cDNA was made from 1:10 total RNA dilutions stored at -20°C. A volume of dillution equal to 200ng RNA was added to the master mix (1µl Omniscript, 2µl 10x Buffer, 2µl dNTP, 1µl oligoprimer (20µM), 0.25µl RNase inhibitor 40u/µl; Quiagen) and RNase free H_2O to give a total volume of 20µl. The mix was incubated for 1 hour in water bath at 37°C. The cDNA made from the reaction was stored at –20°C.

PCR

PCR primers:

CD36 1 Rat	Forward:	TTG TTC TTC CAG CCA ACG CC
	Reverse:	CCA GTT ATG GGT TCC ACA TCC AAG
CD36 2 Rat	Forward:	GGG`AAA GTT ATT GCG ACA T
	Reverse:	CAG ATT CAA ACA CAG CAT AGA
cJUN Rat	Forward:	AGC AAT GGG CAC ATC ACC AC
	Reverse:	TGG GCA GCG TAT TCT GGC TAT G
DBP Rat	Forward:	CAA GAA CAA TGA AGC AGC CAA GAG
	Reverse:	TGA AAG CAC AGC ACG GTA GTG G
NFkB Rat	Forward:	AAG CAG GAA GAT GTG GTG GAG G
	Reverse:	GAG TAG GAC CCC GAG GAT TTT ATC
FATP Rat	Forward:	ATC CGT CTG GTC AAG GTC AAC G
	Reverse:	AAC ACG CTG TGG GCA ATC TTC
Ikkb Rat	Forward:	TGG AAG TGA TTG GTC AGG TGA AG
	Reverse:	GGC AAG ATG GAG AGG GGT ATT TC

PCR was performed with 1µl RT product, 5µl 10x PCR buffer (Roche), 2µl 25mM $MgCl_2$ (Roche)solution (1mM final concentration), 1µl forward primer, 1µl reverse primer (Proligo®), 0,3µl AmliTaq Gold enzyme (Promega) and RNase free H_2O to a final volume of 50µl.

Table 2.2.5.1 Thermocycler parameters for PCR-reaction:

Step	Temperature (°C)	Number of cycles
1	94	1
2	94	"Cycle number"
2	Annealing temperature "AT"	"Cycle number"
2	72	"Cycle number"
3	72	1

Table 2.2.5.2 Primer parameters:

Primer	Product size	AT	Cycle number
Cyclophillin	189	53	22
IKK	182	53	26
DNAbinding	160	53	26
FATP	188	55	37
cJun	136	55	28
NFK	129	55	29
UCP3	154	53	31

PCR products were separated by agarose (LE Analytical Grade, Promega) gel electrophoresis. Gel concentration was 2% agarose in TAE (4.84% tris acetate, 40mM, 1.15% glacial acetic acid, 2% EDTA 0.5M) buffer and the applied field was 90V for ~1 hour. The cDNA product size was approximated using a DNA ladder and the DNA bands were detected by UV using ethidium bromide staining (0.5µg/ml) for 10 minutes followed by a wash in water for 10 minutes. The relative densities of the visualised PCR products were measured using NIH Image® software.

2.2.6 LightCycler

Real-time PCR was performed using cDNA from some samples. This was carried out under standard PCR conditions using 0.6mM of each primer, 3mM $MgCl_2$ and 1µl of purified PCR product as standard with added water to a final volume of 10µl. The amplification program was

initially started at 95°C for 10min., then 40 cycles of three steps each, comprised of 95°C for 15s, 55°C for 5s and 72°C for 10s. The fluorescence of the products was measured (494nm excitation wavelength and 523nm emission wavelength) during each run and for specificity determination the melting curves for each sample were acquired at the end of each run. The standard concentrations used was 10^{-2}, 10^{-4} and 10^{-5}.

2.2.7 Affymetrix™ GeneChip

Introduction

High density microarray gene expression gives an unique opportunity to simultaneously obtain gene expression results from thousands of genes and to make comparisons between gene expression under different conditions.

On an array millions of copies of a single 25 base oligonucleotide probe are grouped as a probe cell. Each perfect match probe cell has its mismatch match probe cell with an oligonucleotide sequence similar to the perfect match. There are at least 16 probe pairs for each probe set and each gene or Expressed Sequence Tags (EST) clusters on the gene chip is represented by at least one gene set. The U34A genechip contains 8,800 probe sets and provides gene expression data for approximately 7,000 full-length sequences and approximately 1,000 (EST) clusters (82).

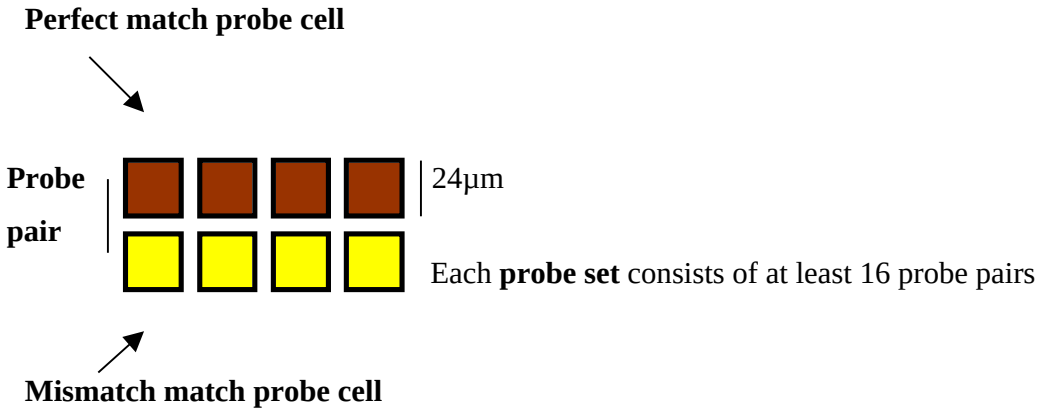

Figure 2.2.7.1 GeneChip®, probe set illustration.

After staining, the intensity of the light emitted from each probe is proportional to the amount of RNA bound, giving a measure of gene expression. The probe pairs are compared, and probability

algorithms are used to calculate whether or not an mRNA sequence representing a gene or an EST is likely to be present, not present or marginally present, and then calculates the abundance of the mRNA.

Before the mRNA can be hybridised to a gene chip the total RNA has to be purified, labelled, amplified and fragmented as illustrated below.

RNA from five different 24-hour 1mM linoleate treated L6 rat muscle cells and their controls were pooled and analysed on two U34A gene chips.

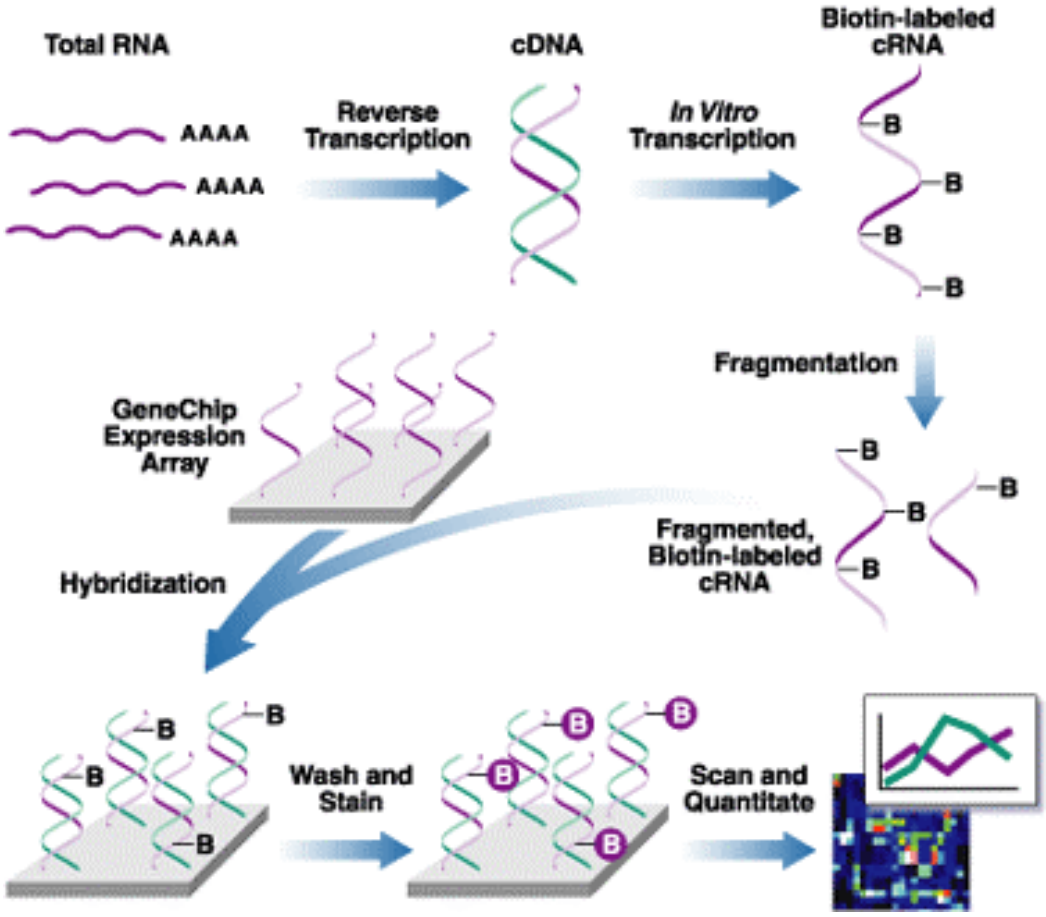

Figure 2.2.7.2 Illustration of the Affymetrix genechip processing.

Pooling of RNA

The quality of the total RNA from five different 24-hour 1mM linoleate treated L6 cell experiments and their controls were checked by UV-visualisation on a 1% agarose gel, TBE (10.8% tris base 89mM, 5.5% boric acid 89mMm, 0.7% EDTA, 2mM), ran at 50V for 1 hour and developed using ethidium bromide.

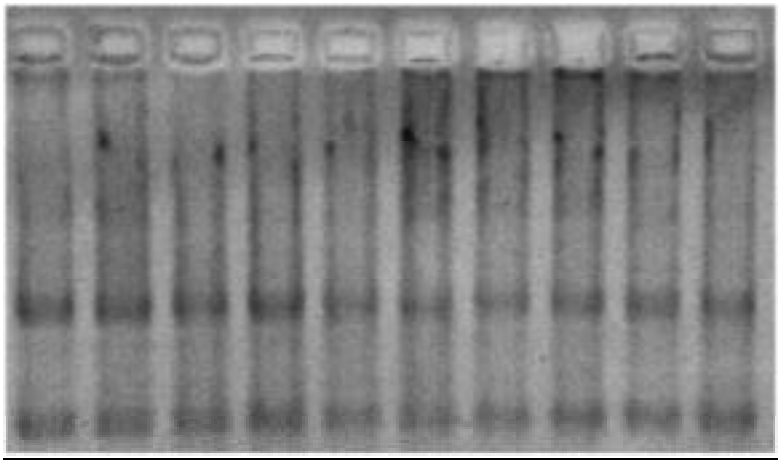

C1 C2 C3 C4 C5 F1 F2 F3 F4 F5

Figure 2.2.7.3 1% agarose visualisation of control (C) and linoleate (F) treated L6 muscle cell total mRNA before pooling.

The total RNA concentration was determined for all 10 samples using a SYBR green II assay as previously described. Volume equal to 6µg total RNA was for each of the linoleate treated samples pooled and RNase free water was added to a total volume of 100µl. The same procedure was carried out for the five control total RNA samples.

To remove traces of DNA the pooled samples were cleaned on an RNEasy column according to manufacturers instructions. Total RNA concentration was determined for the pooled and cleaned samples using the SYBR green II assay previously described.

The pooled RNA samples were diluted to a concentration of 5µg/ml and were prepared for hybridisation according to the Affymetrix™ genechip Expression Analysis technical Manual as briefly described below.

Double stranded DNA synthesis:

First strand and second stand cDNA synthesis was performed using T7-$(dT)_{24}$ primer (Proligo) and SuperScript Choice system as described in the Affymetrix™ protocol.

T7-$(dT)_{24}$ sequence: GGCCAGTGAATTGTAATACGACTCACTATAGGGAGGCGG-$(dT)_{24}$

The double stranded cDNA was cleaned up by phenol:chlorophorm:isoamyl alcohol (saturated with 10mM Tris-HCl, pH 8.1, 1 mM EDTA) extraction using a PGL-Light tube (Bio-Rad) to prevent phenol contamination and was then applied and spun through a BioGel column (Bio-Rad). The cDNA was then precipitated with absolute ethanol and ammonium acetate and the pellet washed as described in the Affymetrix™ protocol. The pellet was resuspended in 23µl RNase free H_2O and the cDNA quality ensured by running 3µl of the cDNA solution on a 1% agarose gel.

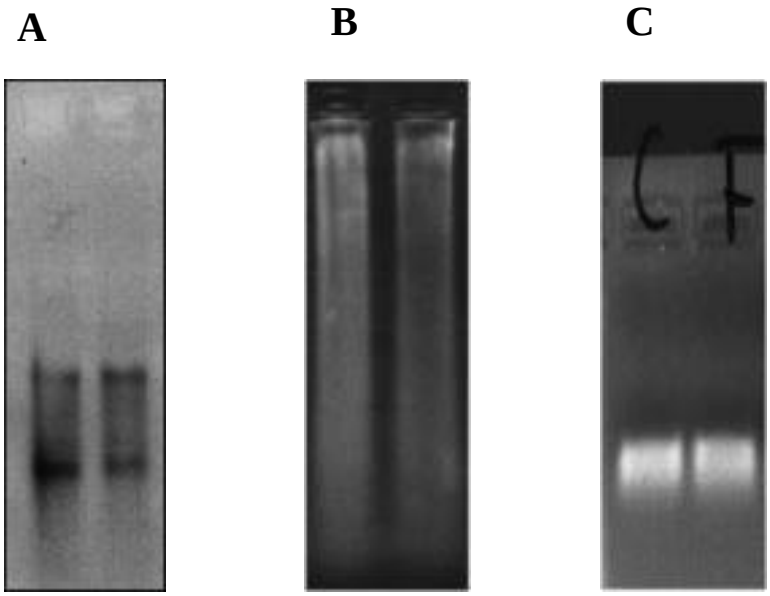

Figure 2.2.7.4 Visualisation of synthesised double stranded DNA (A), IVT product (B) and fragmented cRNA (C) from the control and linoleate treated L6 cells.

In vitro transcription:

In vitro transcription (IVT) was performed by using Enzo Bioarray HighYield Transcript Labelling Kit according to manufacturers' procedure. Biotin labelled UTPs and CTPs were incorporated in to the synthesised RNA made form the cDNA template. The IVT product was split into two RNEasy columns to optimise the yield and the unincorporated dNTPs was removed according to manufacturers procedure. 30µl of RNase free H_2O was used to elute the RNA. The total elute volume was reduced to a about 10µl by vacuum centrifuging and the volume was corrected to 12µl with RNase free H_2O. The yield from the IVT reaction was determined by the SYBR green II RNA quantification assay described above.

Fragmentation

Fragmentation of the cRNA to a base pair length to approximately 35 to 200 pieces of 35 to 200 base pair length was performed on 20µg cRNA by adding 5x fragmentation buffer (4.0mL 1M Tris acetate pH 8.1 (Trizma Base, 0.64g MgOAc, 0.98g KOAc, RNase free water to 20mL, pH adjusted with glacial acetic acid) and incubating at 95°C for 35 minutes. This was carried out in order to make the cRNA suitable to bind to the 25 base pair oligonucleotides on the gene array.

Gene chip processing

The fragmented target cRNA was diluted with 101µl RNase free H_2O and 100x Cocktail Spike, 2x Hybridisation buffer, 1µl control oligotide B2, 3µl Herring Sperm DNA (10mg/ml, Promega) and 3µl acetylated BSA (50mg/ml, Invitrogen) was added RNase-free H_2O to give a total volume of 300µl, as described in the Affymetrix™ technical protocol. This hybridisation cocktail was then hybridised to an Affymetrix™Test3 gene chip in a hybridisation oven at 45°C, 60rpm for 16 hours to test the quality of the RNA.

After incubation the hybridisation cocktail was removed from the chip and stored at -80°C for later use. The gene chip was washed and the biotinylated cRNA was stained with streptavidin phycoerythrin (SAPE) and double stained using normal goat IgG, biotinylated antibody and SAPE. The procedures were performed using Affymetrix™ Fluidics Station.

The control and linoleate Test3 chips were then scanned twice with a Hewlett-Packard GeneArray Scanner at excitation and emission wavelengths of 488nm and 570nm respectively. After the results from the Test3 chip confirmed the quality of the RNA the hybridisation cocktail was applied to a pre-wetted Affymetrix™ U34A rat genome gene chip and the hybridisation, washing/staining and scanning processes described above were performed.

Data analysis:

*Test chip results**:***

Five criteria were met before applying the cRNA hybridisation cocktail to the U34A rat genome chip:

a) The background noise was less than 150.

b) The applied standards (bioB, bioC, bioD and cre, all genes from E.Coli biotin synthesis pathway) were present.

c) The probe sets that corresponds to the 3' and 5' ends for the mRNA from the housekeeping genes β-actin and GAPDH did not differ by more than two-fold.

d) The scaled noise, the scale factor and the normalization factor were comparable between the two test chips.

The above criteria were also met for the U34A gene chip.

Raw data extraction

The expression raw data was calculated from the generated gene chip picture using Affymetrix™ Microarray Suite 5. The raw data from the two gene chips were compared using the same software.

Affy Analysis Tool

The raw data from the two chips and their comparison were exported to Affy Analysis Tool v0511 (Dr. Gareth Denyer, The University of Sydney) and were compared to data from previously performed gene chips on high fat fed rat muscle and liver as described below. Analysis of the expressed sequence tags (ESTs) is beyond the scope of this project and were therefore excluded at this stage. The up- or downregulated ESTs are included in appendix II.

MAPPFinder and GenMAP

Further analysis of the microarray results were performed using MAPPFinder and GenMAP software. MAPPFinder is a tool that creates a global gene-expression profile by integrating the annotations of the Gene Ontology (GO) project with pathway maps from the GenMAPP software (83).

Presentation of data:

Results are presented in tables as fold change in the gene expression of the linoleate treated L6 rat muscle cells relative to the control. Since fold change can some times be a misleading measurement of change, the measured signal intensities are also included to assist in the interpretation of the result.

Comparison of microarray results to data from previously conducted experiments at the Garvan Institute of Medical research.

A combined search where conducted on the gene-chip-data from the L6 linoleate-control comparison and gene-chip-data on muscle and liver from high-fat-fed rat experiments previously conducted at the Garvan Institute of medical research. The expreiment where conducted with adult male Wistar rats. The rats where fed chow diet or high-fat diet for $3\ ^{1}/_{2}$weeks prior to the tissue collection. The combined search where preformed using Affy Analysis Tool v0511.

3. RESULTS

3.0 L6 rat muscle cells

L6 rat muscle cells were used to mimic rat muscle cells *in vitro*. L6 rat muscle cells were selected for high fusion (84) and the development of a insulin responsive pool that contained GLUT4 was characterised (85, 86). The L6 rat muscle cell culture were started, grown and differentiated (see figure 3.0.1) as described in the 'Materials and methods'-chapter.

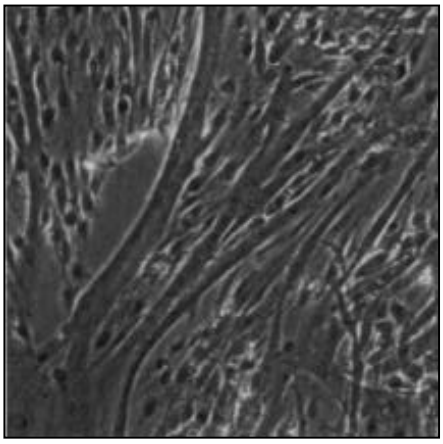

Figure 3.0.1 Differentiated L6 rat muscle cells

3.1 RT-PCR

3.1.1 Expression of genes involved in lipid metabolism

Previous experiments conducted at the Garvan Institute of Medical Research, Sydney, Australia have shown that rats fed a high fat diet have a significant increased FAT/CD36 (1.5 fold) and FATP (8.5 fold) mRNA gene expression in muscle (red gastroc) compared to chow fed rats.

FATP

To test whether this also applies *in vitro* the relative FATP mRNA expression was measured in 24 and 48 hour incubated L6 rat muscle cells by quantitative RT-PCR. Surprisingly, the result showed that there was no significant change in FATP expression between the different treatments and their controls, either after neither 24- nor 48-h incubation. To obtain easily detectable PCR cDNA products, the FATP samples were ran at 38 cycles. This may indicate that the FATP gene is not very abundantly expressed in L6 rat muscle cells.

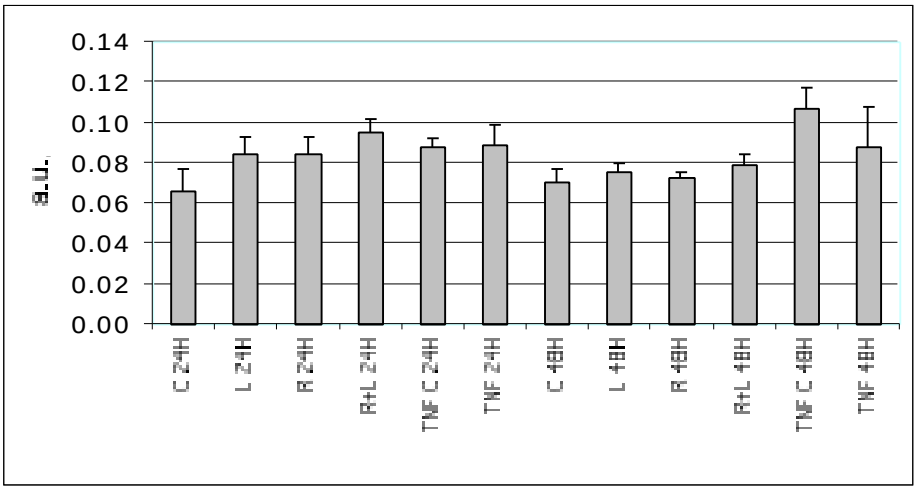

Figure 3.1.1.1
FATP expression...
Cyclophillin corrected FATP gene expression in L6 rat muscle cells
C, Control; L, Linoleate treated; R, Rosiglitazone; TNF, tumor necrosis factor-α
n=3

CD36/FAT

Attempts with several different, previously tested CD36/FAT primers under several different conditions did not give any PCR product. This raised doubt as to whether CD36/FAT is expressed in L6 rat muscle cells. The expression of CD36/FAT was further investigated using real-time PCR (LightCycler) without formation of a PCR product.

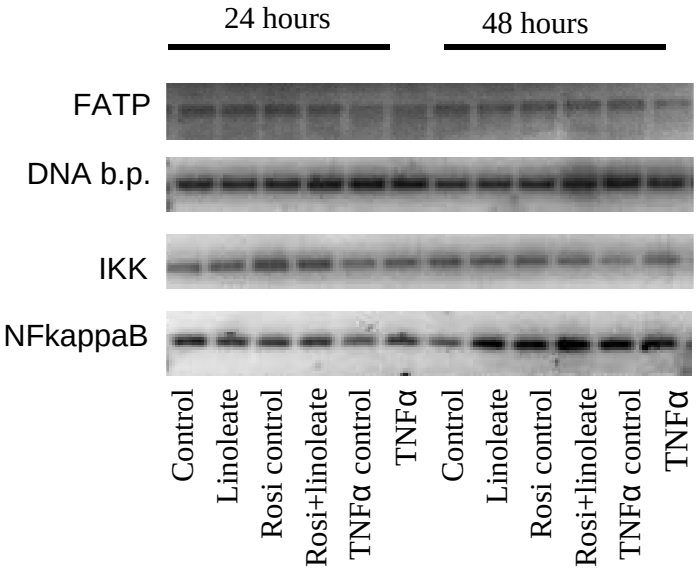

Figure 3.1.2.1 Visualisation of FATP (Fatty Acid Transport Protein), DNA b.p.(DNA binding protein), IKK and NFκB gene expression in L6 rat muscle cells

3.1.2 Expression of genes involved in stress related pathways

*IKK*β

IKKβ is, involved in the activation of the oxidative stress responsive transcription-factor NFκB. Although the density measured shows some variation, the IKKβ gene expression was not significantly changed by linoleate treatment or any of the other treatments (n=2, figure 3.1.2.1).

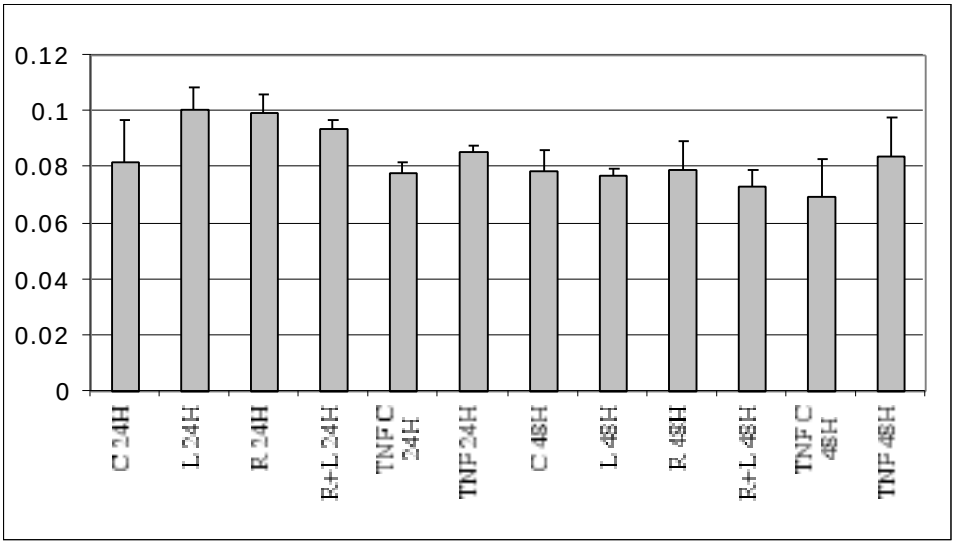

Figure 3.1.2.1
Cyclophillin corrected IKK gene expression in L6 rat muscle cells
C, Control; L, Linoleate treated; R, Rosiglitazone; TNF, tumor necrosis factor-α
n=2

*NF*κ*B*

NFκB is reported to be activated by degradation of the inhibitory sub-unit IκB. Several stimuli, including increased oxidative stress are known to activate NFκB, which, upon activation translocates into the cell nucleus and initiates gene transcription. The RT-PCR results did not show any significant change in gene in NFκB gene expression in any of the treatments compared to their controls.

cJun

c-Jun, a member of the bZIP protein family, can form hetrodimers with other proteins, including cFos. After dimerisation it can bind to DNA and initiate transcription. cJun is activated by an upstream signal delivered by the Jun N-terminal kinase (JNK) (87).

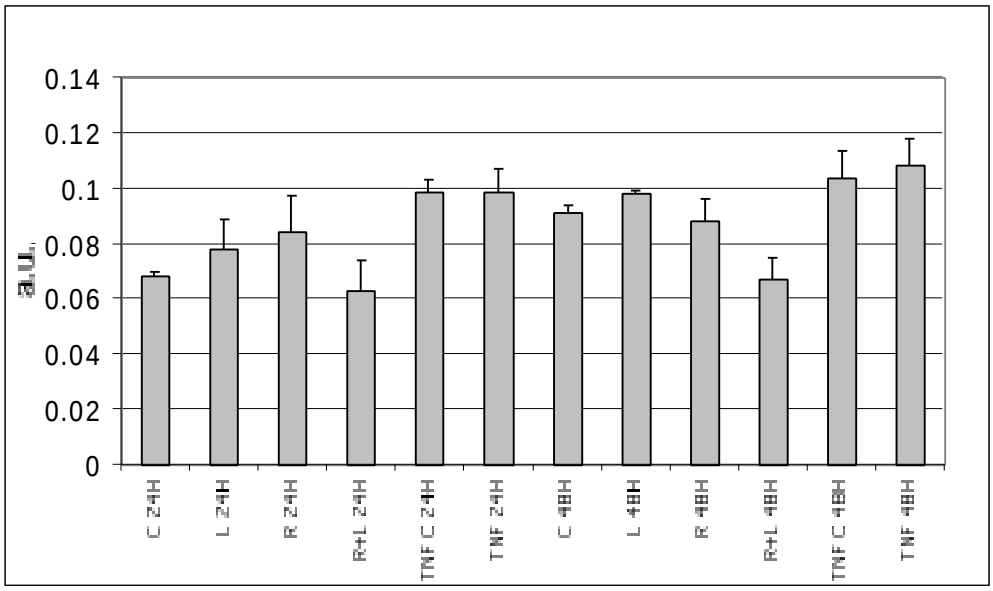

Figure 3.1.2.2
Cyclophilllin corrected c-Jun gene expression in L6 rat muscle cells
C, Control; L, Linoleate treated; R, Rosiglitazone.
TNF, tumor necrosis factor-α.
n=3

Microarray expression analysis conducted at the Garvan Institute of Medical Research showed that cJun was upregulated by >2-fold in rats fed a high-fat diet compared to chow fed rats.
The results from quantitative RT-PCR measurements show that the c-Jun mRNA expression in L6 rat muscle cells was not significantly affected by 1mM linoleate treatment or any of the other treatments compared to their controls.(figure 3.1.2.2)

dbp

The gene expression of DNA-binding protein, a transcription factor, that previously has been shown to increase by 5 fold in high-fat fed rat muscle, did not increase in L6 cells after linoleate incubation or in any of the other treatments (data not shown).

3.1.3 Positive control

UCP3

Uncoupling Protein-3 (UCP3) mRNA has been reported to be upregulated in 24-h fatty acid treated L6 myotubes (88, 89), an effect reported not to be reversed by rosiglitazone, and was used as a positive control.

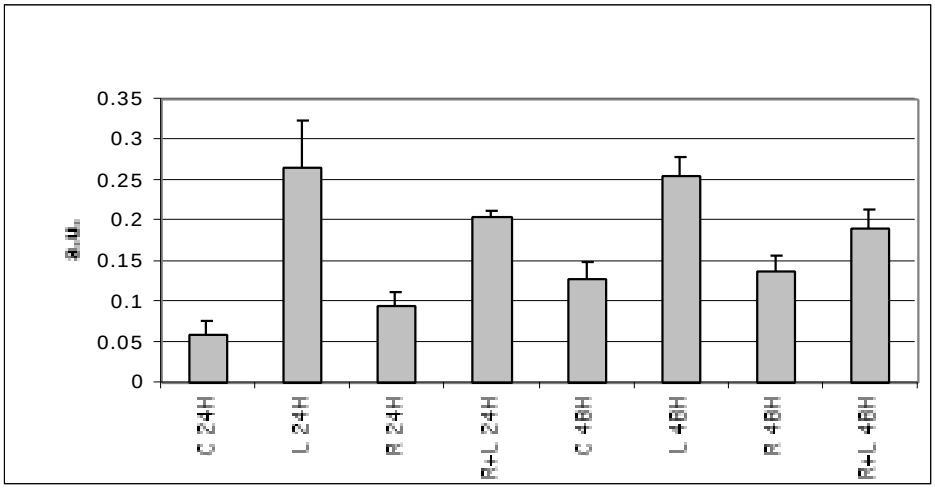

Figure 3.1.3.1
Positive control, Cyclophillin corrected UCP3 gene expression in L6 rat muscle cells after 1mM linoleate treatment. C, Contol; L, Linoleate; R, Rosiglitazone $2*10^{-7}$M. n=4

The PCR results (figure 3.1.3.1 and figure 3.1.3.2) showed that the linoleate treatment increased UCP3 mRNA expression significantly by 2 fold after 48 h incubation (n=4, p=0.0067) and close to a significant by 4.5 fold (n=4, p=0.058) after 24 h treatment. The increase was confirmed by real-time PCR (see LightCycler). Linoleate treatment also significantly upregulated UCP3 gene expression by >2 fold in rosiglitazone treated L6 cells (n=4, p=0.024) after 48 hours. This confirms that the linoleate treatment has had an impact on cultured L6 cells.

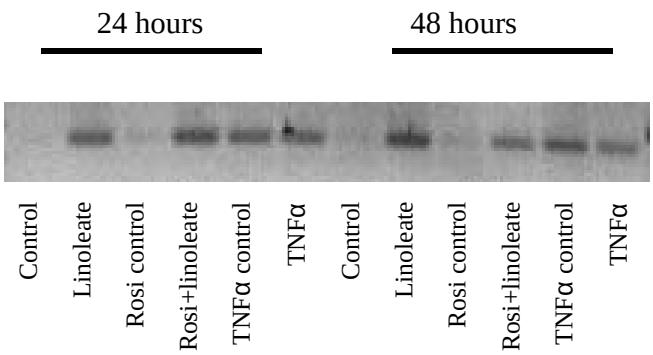

Figure 3.1.3.2
UCP3 RT-PCR product visualised on a 1.5% agarose gel

3.1.4 Real-time-PCR (LightCycler™)

Real-time PCR measurements were conducted to confirm the RT-PCR results that showed an up-regulation in UCP3 gene expression in L6 muscle cells after 1mM linoleate treatment (see section 3.1.3). The LightCycler results showed a highly significant increase in UCP3 gene expression in L6 cells after both 24- and 48-h linoleate incubation, although a high cycle number indicates that UCP3 probably is not very highly expressed in L6 rat muscle cells.

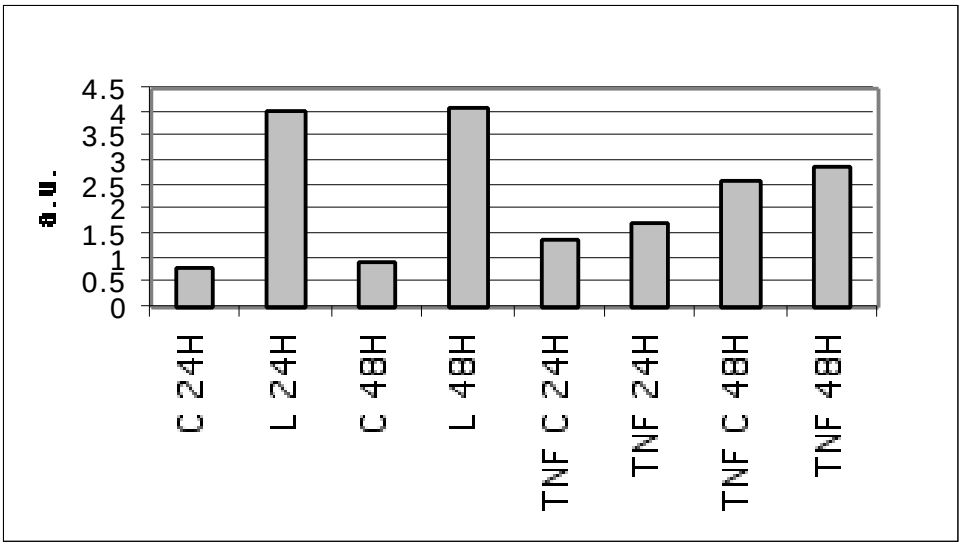

Figure 3.1.4.1
UCP3 gene expression in L6 rat muscle cells. Real time PCR (LightCycler)
n=1

3.2 Micro array gene expression analysis

Control and 24-h linoleate treated total mRNA from five experiments were pooled, processed according to the Affymetrix™ protocol as described in the 'Methods and materials', and analysed using two Affymetrix™ U34A GeneChips.

Both gene chips showed an acceptable background noise, and all housekeeping mRNA controls and added mRNA controls were present with an acceptable 3'/5' ratio which indicates good starting mRNA quality and reliable results.

The Micro Array Suite™ (MAS) v5 software measured, by probability algorithms, that 4061 out of 8784 probe sets where present in the linoleate chip, and that 4196 probe sets were present in the control-chip. When data from the two chips were compared, MAS5 calculated that the linoleate treatment upregulated 358 probe sets and down-regulated 310 whereas 19 were marginally increased and 12 marginally decreased.

As shown in figure 3.2.1, the magnitude of the change is widely distributed, with the majority (>85%) of the probe sets changing two fold or less, and more than half of the probe sets changing only 1.3 fold or less.

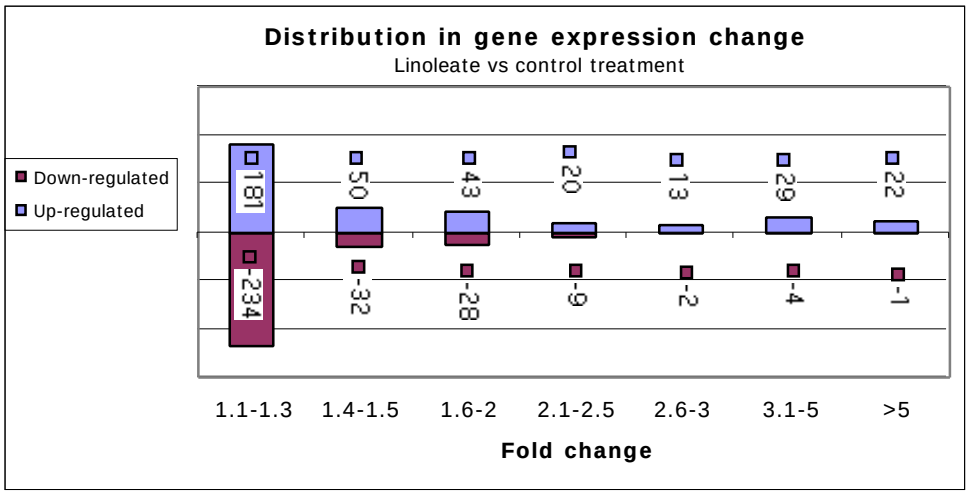

Figure 3.2.1
Distribution in the magnitude of change in gene expression between linoleate treated and control L6 rat muscle cells

The magnitude of the change is presented in fold-change. This unit can sometimes, especially at low abundances be a misleading measurement of change, and signal intensity is therefore included in the tables.

There are >1000 probe sets on the U34A GeneChip, called expressed sequence tags (ESTs), which represent unknown genes. Around 190 ESTs were up- or down regulated when the two chips were compared and these were, although included in the appendix (Appendix II), excluded from further analysis.

Some of the genes that changed are commented on below. The complete list of probe sets that showed an altered expression between the linoleate treated L6 rat muscle cells and the control are included in 'Appendix I'.

3.2.1. Genes involved in lipid metabolism

The expression microarray data showed that several probe sets encoding for genes involved in lipid metabolism changed with linoleate treatment. Genes involved in lipid degradation (β-oxidation) such as acyl-CoA acyltransferase 2 and acyl-CoA dehydrogenase, showed as expected an overall increased expression. Some of these genes are presented in table 3.2.1.1 (illustrated in figure 3.2.1.1).

Table 3.2.1.1 Genes involved in lipid activation and β-oxidation:

GENE_ID	NAME	Fold ch	Sig. Lin.	Sig. Con	Swissprot
L07736	carnitine palmitoyltransferase 1	4.6	198	40	P32198
X05341_at	acetyl-Coenzyme A acyltransferase 2 (mitochondrial 3-oxoacyl-Coenzyme A thiolase)	1.7	343.3	177.5	
J02791	acetyl-coenzyme A dehydrogenase, medium chain	1.2	236	171	P08503
J05029_s_at	acetyl-Coenzyme A dehydrogenase, long-chain	1.6	262.7	152.9	P10608
rc_AA893242	fatty acid Coenzyme A ligase, long chain 2	-1.3	72	101	P18163
D30666	fatty acid Coenzyme A ligase, long chain 3	-1.5	675	1105	Q63151
D85189	fatty acid Coenzyme A ligase, long chain 4	-1.3	326	430	O35547
rc_AI236284	fatty acid Coenzyme A ligase, long chain 4	-1.3	137	209	O35547

Genes involved in ATP-production, including ATP-synthase (gene id AA799778, increased 13 fold) were generally increased in L6 cells after linoleate incubation.

Table 3.2.1.2 Genes involved in lipid synthesis:

GENE_ID	NAME	Fold ch	Sig. Lin.	Sig. Con	Swissprot
J05210	ATP citrate lyase	-1.5	200	321	P16638
J05210	ATP citrate lyase	-1.3	574	740	P16638
rc_AA892832	fatty acid elongase 1	-1.1	724		Q920L7
X13527cds	fatty acid synthase	-1.2	397	505	P12785

Surprisingly, expression of CPT1, the enzyme transporting acyl-CoA into the mitochondrion, did not change for the muscle isoform (CPT1b), whereas linoleate treatment upregulated expression of the liver CPT1a isoform in L6 cells more than 4 fold. On the other hand, expression of genes involved in *de novo* fatty acid synthesis, including ATP citrate lyase and fatty acid synthase were generally slightly decreased after linoleate incubation (see table 3.2.1.2).

Table 3.2.1.3 Genes involved in cholesterol biosynthesis:

GENE_ID	NAME	Fold ch	Sig. Lin.	Sig. Con	Swissprot
D45252	2,3-oxidosqualene: lanosterol cyclase	-1.3	68	86	P48450
rc_AI171090	3-hydroxy-3-methylglutaryl CoA lyase	1.9	84	54	P97519
M29249cds	3-hydroxy-3-methylglutaryl-Coenzyme A reductase	-1.9	30	67	P51639
X55286	3-hydroxy-3-methylglutaryl-Coenzyme A reductase	-1.7	22	51	P51639
X52625	3-hydroxy-3-methylglutaryl-Coenzyme A synthase 1	-1.9	450	805	P17425
rc_AI177004	3-hydroxy-3-methylglutaryl-Coenzyme A synthase 1	-2.3	193	439	P17425
AB016800	7-dehydrocholesterol reductase	-1.7	121	160	Q9Z2Z8
AB016800	7-dehydrocholesterol reductase	-1.5	146	199	Q9Z2Z8
M89945mRNA	farensyl diphosphate synthase	-1.9	572	1261	P05369
rc_AI180442	farensyl diphosphate synthase	-2.3	208	471	P05369
M89945mRNA	farensyl diphosphate synthase	-1.7	639	1113	
M95591	farnesyl diphosphate farnesyl transferase 1	-1.9	247	393	Q02769
M95591	farnesyl diphosphate farnesyl transferase 1	-1.9	150	223	Q02769
AF003835	isopentenyl-diphosphate delta isomerase	-2.1	80	203	O35760
M29472	mevalonate kinase	1.3	87	88	P17256
rc_AA924198	mevalonate kinase	-1.5	77	118	P17256
D37920	squalene epoxidase	-1.4	249	361	P52020

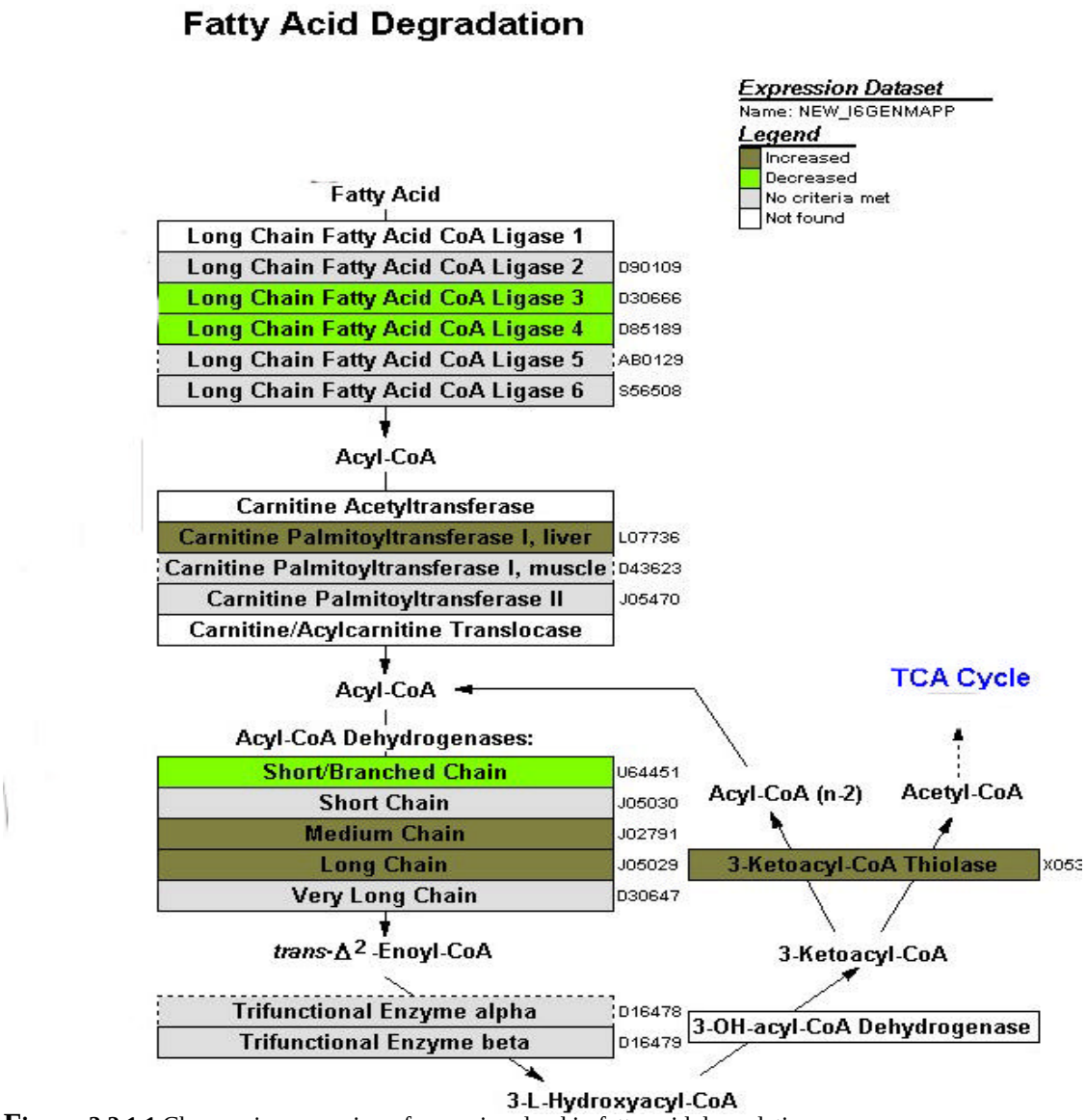

Figure 3.2.1.1 Changes in expression of genes involved in fatty acid degradation.

Several genes involved in cholesterol synthesis were, as illustrated in figure 3.2.1.2, abundantly present and decreased after linoleate treatment. The expression of the LDL-receptor was also reduced with linoleate incubation. These observations are discussed in more detail in the discussion chapter.

The microarray results showed that FAT/CD36 mRNA was absent in L6 rat muscle cells. This explains why the conducted RT-PCR and real-time-RT-PCR did not give any PCR product.

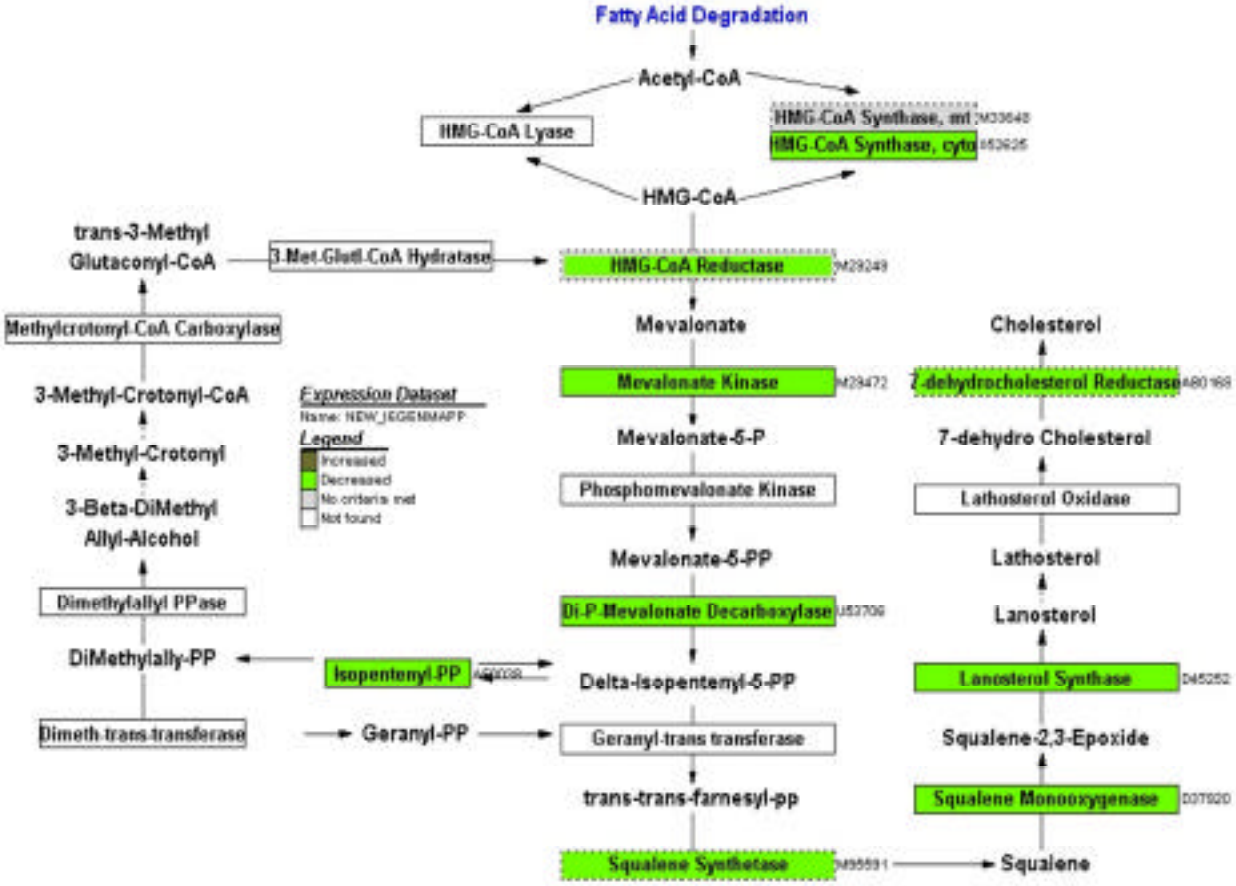

Figure 3.2.1.2 Changes in expression of genes involved in cholesterol biosynthesis in L6 rat muscle cells after linoleate incubation.

3.2.2 Genes involved in insulin signalling:

Table 3.2.2.1

Gene ID	Name	Sign. Con.	Sign. Lin.	Fold change	Swissprot
X58375_at	Insulin receptor substrate 1	36.9	24.7	-1.4	P14423
rc_AI105076_	Murine thymoma viral (v-akt) oncogene homolog 2	120.5	86.6	-1.3	P48317

Although not a large change, expression of insulin receptor substrate 1(IRS1) and Protein Kinase B beta (PKB beta/v-akt2) both important in insulin signalling changed with linoleate incubation

(figure 1.2.1 in the introduction chapter). Mice lacking the IRS1 are insulin resistant (90), and recently it has been demonstrated that mice lacking the PKB beta gene exhibit mild growth deficiency and are insulin resistant. (91)

3.2.3 Genes involved in oxidative-stress-protection:

Table 3.2.3.1

Gene ID	Name	Sign. Con	Sign. Lin.	Fold ch	Swissprot
M11670_at	Catalase	71.6	84.7	1.1	Q923V7
rc_AA926149_	Catalase	127.5	138	1.2	Q923V7
X60328_g_at	cytosolic epoxide hydrolase	52.8	64.8	1.3	
X12367cds_s_a	Gluathione peroxidase 1	1626.2	1439.1	-1.1	O35823
J02679_s_at	NAD(P)H dehydrogenase, quinone 1	1536.9	1980	1.3	

As shown in table 3.2.3.1, both catalase and gluthatione peroxidase play an important role in protecting the cell against oxidative stress. The microarray results show that catalase is slightly increased in the linoleate treated L6 cells, whereas the gluthatione peroxidase 1 gene expression is slightly decreased. Cytosolic epoxide hydrolase and quione 1 are also involved in protection against oxidative stress.

3.2.4 Genes involved in stress associated signalling:

Table 3.2.4.1:

Gene ID	Name	Sign. Con	Sign. Lin.	Fold ch	Swissprot
AJ000557cds	Janus kinase 2 (a protein tyrosine kinase)	78.2	49	-1.2	O35804
U13396_at	Janus kinase 2 (a protein tyrosine kinase)	111.2	59.8	-1.5	P49088
U13396_g_at	Janus kinase 2 (a protein tyrosine kinase)	120.2	95.8	-1.3	Q62651
rc_AI171630_	mitogen activated protein kinase 14	190.6	278.5	1.3	P16232
U73142_g_at	mitogen activated protein kinase 14	188.7	244.3	1.2	O35854
rc_AI178835_	mitogen activated protein kinase kinase 1	25.7	11.3	-1.9	O35532
U35345_s_at	p21 (CDKN1A)-activated kinase 2	56.3	40.7	-1.3	Q8VHU3
U42627_at	dual specificity phosphatase 6	159.2	209.6	1.3	Q62784
X94185cds_s	dual specificity phosphatase 6	94.5	122.6	1.3	P18916

Expression of several genes involved in stress associated signalling pathways were altered in L6 cells after linoleate incubation. Some of these are included in the table above. Janus kinase 2 (JAK2) is a protein involved in the stress sensitive JAK/STAT pathway. There are three probe sets for the JAK2 gene on the U34A rat gene chip, and the fact that all of them show a slightly decreased expression adds to the reliability of the result. Mitogen activated protein kinase

(MAPK) 14 (also known as MAPK p38) is a member of the MAP serine/threonine protein kinases and is known to be a stress activated protein. Activation of MAPK 14 has been reported to cause inhibition of insulin mediated glucose transport in L6 cells (92). MAPK 14 expression was slightly upregulated in the L6 cells after linoleate incubation, whereas mitogen activated protein kinase kinase 1, a protein in the same pathway was down regulated. The dual specificity phosphatase 6 deactivates MAP kinases, with specificity for the ERK family (106).

3.2.5 Genes involved in cytokine pathways:

Table 3.2.5.1:

Gene ID	Name	Sign. Con	Sign. Lin.	Fold ch	Swissprot
AJ012603UTR#	a disintegrin and metalloproteinase dom 17	100	118	1.2	
M26744_at	Interleukin 6 (interferon, beta 2)	39.5	33.8	-1.3	P06536
rc_AI237535_s	LPS-induced TNF-alpha factor	283	238.3	-1.2	Q00918
X17053cds_s_a	small inducible cytokine A2	143.9	221.4	1.5	
X17053mRNA_s	small inducible cytokine A2	261.9	432	1.5	

LPS-induced TNF-alpha factor may have a role in regulating the transcription of TNFα (107) whereas a disintegrin and metalloproteinase domain 17, also known as TNF-alpha convertase, cleaves the membrane-bound precursor of TNFα to its mature soluble form.
Interleukin 6 changed in the L6 mRNA expression comparison, is a cytokine with a wide array of effects. Small incucible cytokine A2 is a chemotaktic factor that atracts monocytes but not neutrophiles.

3.2.6 Genes involved in gene transcription:

Gene expression of several transcription factors both involved in initiation and inhibition of gene transcription was increased with linoleate treatment. Some of these are included in the list below. Two genes (Kruppel-like factor 9 and immediate early transcription factor) are represented by two probe sets.
CCAAT/enhancer binding protein-δ (C/EBP-δ) was also increased (1.7 fold) after linoleate incubation. This transcription factor is a member of the bZIP family and is thought to be important in adipocyte development. Cells with C/EBP-δ deficiency has been shown have reduced IRS-2 and GLUT4 expression (108).

Table 3.2.6.1 Genes involved in gene transcription:

Gene ID	Name	Sig.Con	Sig.Lin.	Fld ch	Swissprot
rc_AA946292	CCAAT/enhancerbinding, protein (C/EBP) delta	41	59	1.7	Q01713
rc_AA800912	general transcription factor II I repeat domain-containing 1	97	82	-1.2	P41138
rc_AA944177	high mobility group box 1	19	23	1.2	Q01713
rc_AI029805	high mobility group box 1	18	79	3.2	P19335
U17254	immediate early gene transcription factor NGFI-B	33	49	1.5	Q63046
U17254	immediate early gene transcription factor NGFI-B	22	79	3.5	Q62655
L23148	Inhibitor of DNA binding 1, helix-loop-helix protein (splice variation)	22	32	1.5	AAF82799
rc_AI230256	Inhibitor of DNA binding 2, dominant negative helix-loop-helix protein	55	68	1.2	Q9R0W1
rc_AI171268	Inhibitor of DNA binding 3, dominant negative helix-loop-helix protein	24	98	2.8	O70185
D12769	Kruppel-like factor 9	46	62	1.3	
D12769	Kruppel-like factor 9	205	272	1.3	AAF82799
M27151	myogenic factor 6	13	25	1.6	P41137
rc_AI176488	nuclear factor I/B	56	65	1.1	O70189
AB012234	nuclear factor I/X	73	87	1.4	Q03484
M14053	nuclear receptor subfamily 3, group C, member 1	27	36	1.3	P41135
AF039832	paired-like homeodomain transcription factor 2	879	996	1.2	AAO32676
rc_AI180396	Retinoblastoma-related gene	94	107	1.2	P06536
rc_AI230602	Retinoblastoma-related gene	158	274	1.7	O55081
L35271	Runt related transcription factor 1	617	736	1.1	P22829
U09228	transcription factor 4	105	77	-1.3	O55081
U51583	transcription factor 8	83	173	1.4	Q08013
Z14030	TRAP-complex gamma subunit	47	200	3.5	P97659
U56242	v-maf musculoaponeurotic fibrosarcoma (avian) oncogene homolog (c-maf)	86	68	-1.2	P54844
U27186	zinc finger protein 111	65	73	1.2	Q62947
L16995_at	ADD1/sterol regulatory element binding factor 1	170.3	73	-2.5	

3.2.7 Genes involved in intracellular signalling:

Several of the probe sets that showed a changed gene expression in L6 cells after linoleate treatment are involved in intracellular signalling, and some of these are presented in table 3.2.7.1. Several of these genes where changed in two or more probe sets (including myristoylated alanine rich protein kinase C substrate, noggin, RAB11B and protein phosphatase 2C). Although the probe sets in table 3.2.7.1 represents genes involved in several different pathways, some of the genes are involved in the same pathway. Noggin, JAK2 (see figure 3.2.4.1), bone morphogenetic protein receptor (type 1A) and MAD homolog 1, 2 and 4 are all involved in transforming growth factor-β signalling pathway. Transforming growth factor beta 3 and TGFbβ Inducible Early Growth Response gene expression also changed after linoleate treatment (see Appendix I).

Other interesting genes that changed expression in L6 cells include prostaglandine-endoperoxide synthase 2 (COX-2), ras-related protein rab10 and the chemokine orphan receptor 1, also known as calcitonin/calcitonin-related polypeptide, alpha.

Table 3.2.7.1 Genes involved in intracellular signalling:

Gene ID	Name	Sign.con	Sign. Lin	F.ch	Swissprot
Y15748_at	3-phosphoinositide dependent protein kinase-1	53.7	39.1	1.4	O55173
M77850_at	6-pyruvoyl-tetrahydropterin synthase	148.9	6.7	12.1	P27213
U94904_s_at	abl-interactor 2	140.6	118.5	1.2	O35823
rc_AI176052_a	adenylate kinase 3	635	778.3	-1.1	P29411
M80550_at	adenylyl cyclase 2	416.9	340	1.1	P26769
rc_AA946251_	G protein-coupled receptor kinase 5	27.9	14.3	1.4	Q62833
U26397_at	inositol polyphosphate-4-phosphatase, type 1	106.6	90.2	1.1	Q62784
AF067727_s_at	MAD homolog 1 (Drosophila)	24.9	39.6	-1.4	P97588
AB017912_at	MAD homolog 2 (Drosophila)	184.4	245.3	-1.1	O70436
rc_AI228675_a	MAD homolog 2 (Drosophila)	26.4	37.8	-1.5	O70436
rc_AI008639_a	MAD homolog 4 (Drosophila)	91.3	22.1	3.2	O70437
rc_AA899253_	myristoylated alanine rich protein kinase C substrate	319.9	393	-1.2	P30009
rc_AA925762_	myristoylated alanine rich protein kinase C substrate	63.5	70.7	-1.2	P30009
rc_AA955167_	myristoylated alanine rich protein kinase C substrate	93.7	107.9	-1.2	P30009
rc_AA859752_	Noggin	21.9	31.5	-1.4	Q62809
U31203_at	Noggin	95.1	109.9	-1.2	Q62809
D64046_at	phosphatidylinositol 3-kinase, regulatory subunit, polypeptide 2	56.1	48.6	1.2	Q63788
D64046_g_at	phosphatidylinositol 3-kinase, regulatory subunit,pp2	76.6	19.8	3.7	Q63788
D88666_at	phosphatidylserine-specific phospholipase A1	432.9	302.3	1.4	P97535
X51529_at	phospholipase A2, group IIA (platelets, synovial fluid)	46.9	28.6	1.4	P14423
rc_AA998446_	phosphotidylinositol transfer protein, beta	177.9	242	-1.2	P53812
S67722_s_at	prostaglandin-endoperoxide synthase 2	35.2	68.5	-1.9	P35355
U63740_at	protein kinase C-binding protein Zeta1	15.6	39.3	-2.0	P97577
D26180_at	protein kinase C-like 1	40.8	24.1	1.9	Q63433
M12492mRNA#	protein kinase, cAMP dependent regulatory, type II beta	124.8	89.3	1.3	P12369
M12492mRNA#	protein kinase, cAMP dependent regulatory, type II beta	36.1	9.2	3.5	P12369
S78218_at	Protein phosphatase 1, catalytic subunit, beta isoform	1294.4	810.1	1.5	P37140
AF095927_at	protein phosphatase 2C	116.5	86.8	1.2	Q9Z1Z6
AF095927_g_a	protein phosphatase 2C	195.1	153.7	1.2	Q9Z1Z6
rc_AA799980_	Protein phosphatase type 1B (formely 2C), Mg-dependent, beta isoform	284.6	317.5	-1.1	CAC28067
D01046_at	RAB11B, member RAS oncogene family	278	245.7	1.1	O35509
AA891669	RAB11B, member RAS oncogene family	685	502	1.3	O35509
X06889cds_at	RAB3A, member RAS oncogene family	63.2	30.5	2.1	P05713
rc_AA851381	Ras homolog enriched in brain	45.2	9.6	3.0	Q62639
rc_AA851381_	Ras homolog enriched in brain	45	10	3	Q62639
rc_AA955306_	ras-related protein rab10	631.2	216.1	2.8	P35281
AF035151_s_at	regulator of G-protein signaling 12	608	431.7	1.3	O08774
AF084205_at	serine/threonine protein kinase TAO1	101.4	126.1	-1.2	O88664
U90312	Synaptojanin II	104	86	1.2	

It is worth noting that 6 pyruvoyl-tetrahydropterin synthase, an enzyme involved in the *de novo* synthesis of 5,6,7,8 tetrahydrobiopterin (BH_4), and thereby indirectly involved in signalling, was switched on by linoleate incunbation (12 fold increase, signal intensity 6.7 to 148). BH_4 is a

cofactor for several enzymes including the aromatic amino acid hyrdroxylases and tyrosine 3-monooxygenase and is also involved in the synthesis of NO.

3.2.8 Genes involved in transport:

Several probe sets encoding for genes involved in transport changed with linoleate treatment in L6 muscle cells. Some of them are included in table 3.2.7.1

Table 3.2.8.1 Genes involved in transport.

Probe_set	name	Sig. Con	Sig.Lin	F.Ch	Swisprot
rc_AA859975_at	2-oxoglutarate carrier	371.4	447.3	1.1	O70603
rc_AA799778_at	ATP synthase, H+ transporting, mitochondrial	99.6	1523.8	13.0	Q9Z2J3
M99223_at	ATPase, Ca++ transporting, cardiac muscle, fast twitch 1	61.5	119.6	1.5	P31232
AA799276_at	ATPase, Ca++ transporting, cardiac muscle, slow twitch 2	1443.5	1708.1	1.1	
M86621_at	calcium channel,voltage-dependent, alpha2/delta s.u.1	189.1	246.7	1.3	P26769
L07736_at	carnitine palmitoyltransferase 1	39.9	198	4.6	P09057
rc_AA799645_g_at	FXYD domain-containing ion transport regulator 1	32.7	78.6	1.7	P16632
rc_AA799645_at	FXYD domain-containing ion transport regulator 1	167.3	187.5	1.2	P54290
X66494_at	integrin alpha 7	110.7	158.4	1.3	P80299
rc_AA892810_at	low density lipoprotein receptor-related protein associated protein 1	67.8	78.9	1.1	P20294
rc_AA891045_at	nucleoporin p58	12.1	15.9	1.2	P28480
U69884_at	potassium intermediate/small conductance	18.6	28.9	1.5	Q62981
rc_AA799760_s_at	solute carrier family 2 , member 4	10	39.6	3.2	
S68135_s_at	solute carrier family 2,member 1	75.1	32.7	-2.1	
D12770_s_at	solute carrier family 25 (mitochondrial adenine translocator) member 4	1845.3	2183.3	1.2	Q01713
rc_AA892776_at	solute carrier family 25 (mitochondrial carrier; adenine adenine nucleotide translocator), member 3	939.7	2066.7	1.5	Q99MI5
U70476_at	solute carrier family 7, member 1	154.1	120.1	-1.2	P70565
rc_AA800787_at	Transferrin	702.8	559.8	-1.2	

Both solute carrier family 2 member 1 (GLUT1) and member 4 (GLUT4) changed in expression after linoleate incubation. The abundance of both these transporters is remarkably low. This gives less confidence in the magnitude of the change, and the low expression of these vital transporters also questions the glucose transporting proparlies of the L6 cell.

3.2.9 Combined search, muscle:

As described in ‘Methods and materials', a combined search was conducted on microarray data from two experiments comparing gene expression in muscle between high-fat-fed rats and chow fed rats and the comparison between linoleate treated and control L6 muscle cells. This search revealed that 11 probe sets showed increased gene expression and 3 probe sets showed a decrease in all three comparisons, representing a total of 12 genes.

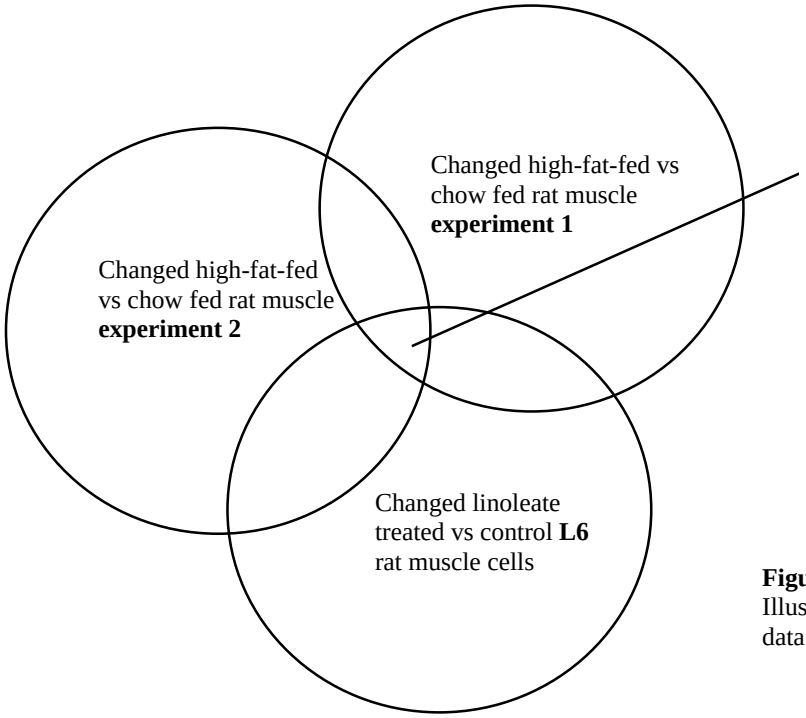

Figure 3.2.8.1
Illustration of combined gen-chip-data search

Of these 10 represent known genes and 2 unknown genes (presented in table 3.2.8.1). Of the 16 known genes, two genes, v-jun and immediate early gene transcription factor NGFI-B increased in two probe sets. V-jun differs from the related c-jun by a 27-amino acid deletion near the N-terminus and can not, unlike c-jun, be activated by upstream JNK signalling. V-jun belongs to the ‘bZIP’ proteins, and can form homodimers and heterodimers with various other ‘bZIP’ proteins, including c-fos, which can lead to regulation of transcription (87). NGFI-B is a nuclear receptor with structural features of ligand-activated transcriptional regulators, and together with Nurr1 and NOR-1 forms the NGFI-B superfamily. No specific ligands have been identified for

these receptors (93). Another interesting gene that decreased in expression both in rat muscle and in cultured cells is the insulin receptor substrate-1 (IRS1). IRS1 is involved in insulin signalling. Acetyl-CoA acyltransferase 2 is a key enzyme in β-oxidation of fatty acids and is, as expected, increased after increased lipid exposure. Early growth response 1, a member of the zinc finger transcription-factor family, has recently been reported to be regulated by insulin (109).

Table 3.2.8.1 Probe sets showing a change in expression after lipid exposure in both red gastroc rat muscle tissue and L6 rat muscle cells:

Gene ID	Name	Muscle1 (f-ch)	Muscle2 (f-ch)	L6 (f-ch)	swissprot
X05341	acetyl-Coenzyme A acyltransferase 2 (mitochondrial 3-oxoacyl-Coenzyme A thiolase)	1.6	1.5	1.7	P13437
rc_AA866452	actin alpha cardiac 1	-1.3	-1.3	-1.2	P03996
AF009329	basic helix-loop-helix domain containing, class B3	1.9	1.6	1.1	O35779
M18416	early growth response 1	2	1.6	1.4	P08154
U08976	enoyl coenzyme A hydratase 1	1.7	1.6	1.5	Q62651
U17254	immediate early gene transcription factor NGFI-B	2.1	1.7	1.5	P22829
U17254	immediate early gene transcription factor NGFI-B	3.5	2	1.7	P22829
X58375	Insulin receptor substrate 1	-1.9	-1.6	-1.4	P35570
D00729	Rattus norvegicus mRNA for delta3, delta2-enoyl-CoA isomerase, complete cds	1.9	1.6	2.6	Q64592
rc_AA945867	v-jun sarcoma virus 17 oncogene homolog (avian)	1.6	2.5	1.2	
rc_AI175959	v-jun sarcoma virus 17 oncogene homolog (avian)	1.4	1.9	1.1	
X06801cds	Rat mRNA for vaskular alpha-actin	-2.1	-1.9	-1.2	

3.2.10 Combined search, liver:

Compared to the control, the micro array data from linoleate treated L6 showed that genes involved in lipid synthesis (figure 3.2.1.1) and cholesterol biosynthesis (figure 3.2.1.2) were abundantly expressed in L6 cells. The data also revealed that mRNA expression of CPT1, liver isoform, and not the muscle isoform, increased after 1mM linoleate incubation. Based on this, a combined search where conducted on microarray data from two experiments comparing gene expression in liver from high-fat-fed- and chow-fed rats, and the comparison between linoleate treated and control L6 rat muscle cells.

This combined search showed that 18 common genes were increased and 19 were decreased in all three comparisons, encoding for a total of 34 known genes. Several genes involved in fatty acid synthesis where increased in all comparisons (including ATP-citrate lyase), and several

genes involved in β-oxidation (such as CPT1, liver isophorm and acyl-CoA dehydrogenase) and cholesterol synthesis were decreased (such as 7-cholesterol reductase).
Other genes of interest include the glucocoriticoid receptor (also known as nuclear receptor subfamily 3, group C, member 1), kruppel-like factor 9 (also known as basic transcription element binding protein, (BTEB)) and the insulin-induced growth response protein (CL-6) (94).

Table 3.2.9.1 Probe sets showing a change in expression after lipid exposure in both rat liver and L6 rat muscle cells:

Gene ID	Name	Swissprot	Liver#1	Liver#2	L6
AB016800	7-dehydrocholesterol reductase	Q9Z2Z8	-1.6	-1.6	-1.7
AB016800	7-dehydrocholesterol reductase	Q9Z2Z8	-1.5	-1.7	-1.5
J05029	acetyl-Coenzyme A dehydrogenase, long-chain	P15650	1.5	1.7	1.6
J05210	ATP citrate lyase	P16638	-2.3	-1.4	-1.5
J05210	ATP citrate lyase	P16638	-1.9	-1.7	-1.3
L07736	carnitine palmitoyltransferase 1	P32198	2.3	2.5	4.6
rc_AI237535	cysteine rich protein 1		-1.9	-1.9	-1.2
X13527cds	DnaJ-like protein	P12785	-2.0	-3.2	-1.2
U53922	dual specificity phosphatase 6	P54102	1.3	1.3	1.1
U08976	Eonyl coA hydratase 1		1.9	1.9	1.5
L13619	growth response protein (CL-6)	Q08755	-2.0	-1.9	-2.5
L13619	growth response protein (CL-6)	Q08755	-1.6	-1.6	-2.1
D12769	Kruppel-like factor 9	Q01713	2.0	1.7	1.3
D12769	Kruppel-like factor 9	Q01713	2.0	1.7	1.3
rc_AA946108	laminin 5 alpha 3	P70570	1.7	2.3	2.1
S45663	LPS-induced TNF-alpha factor		-1.1	-1.3	-1.2
M63485	matrin 3	P43244	1.3	1.7	2.1
rc_AI102562	Metallothionein	P02803	1.4	1.6	1.4
M14053	nuclear receptor subfamily 3, group C, m1	P06536	4.6	1.9	1.3
D00729	Rattus norvegicus mRNA for delta3, delta2-enoyl-CoA isomerase, complete cds	Q64592	2.3	2.5	2.6
J02585	stearoyl-Coenzyme A desaturase 1	P07308	-168.9	-48.5	-4.0
rc_AI175764	stearoyl-Coenzyme A desaturase 1	P07308	-22.6	-222.9	-4.6
AF036761	stearoyl-Coenzyme A desaturase 2	O54953	-18.4	-52.0	-3.5
U42627	synaptic glycoprotein SC2	Q64346	1.6	1.7	1.3
rc_AI176456	Transcribed sequence with strong similarity to METALLOTHIONEIN-II (MT-II)		2.8	2.5	1.1
rc_AA945867	v-jun sarcoma virus 17 oncogene homolog (avian)		2.5	2.3	1.2
rc_AI175959	v-jun sarcoma virus 17 oncogene homolog (avian)		1.9	1.9	1.1
L16995	Add1		-1.2	-1.6	-2.5

4. DISCUSSION

Although the link between increased lipid muscle content and insulin resistance is well established, the mechanisms behind this association are still not fully understood.
Gene array experiments on rat muscle tissue performed by the Diabetes group at the Garvan Institute of Medical Research, revealed that high-fat feeding increased expression of genes involved in stress associated pathways (such as c-jun, NFκB and IKK). Some of these genes have been linked to mechanisms involved in the development of insulin resistance (55-57). As discussed in the introduction chapter, some genes involved in providing cellular protection against oxidative stress are down regulated in skeletal muscle in people with type-2 diabetes, suggesting that oxidative stress has a role in development of the disease.
It is not known whether the increase in muscular expression of stress-genes observed in rats is a direct consequence of elevated muscular exposure to fatty acids, or whether the increased expression is a secondary effect of the high-fat diet. This change could for instance be due to an increase or decrease in secretion of a hormone by tissue other than muscle with an effect on skeletal muscle.
The main purpose of the study performed here was to use an *in vitro* rat muscle system to see if the *in vivo* effects of a high linoleate diet could be mimicked *in vitro*.

4.1 RT-PCR results

In this study, the relative expression of some genes involved in stress sensitive signalling was first measured in L6 rat muscle cells by conventional RT-PCR, after linoleate treatment. Transcripts of NFκB, IKK, c-jun were detected and abundantly expressed in all samples (measured at 29, 26 and 28 cycles respectively). The results revealed that neither c-jun, NFκB or IKK were significantly upregulated by 24 or 48-h 1mM linoleate incubation in differentiated L6 rat muscle cells, although there was a tendency for NFκB to be up-regulated by linoleate after 48-hour incubation. DNA binding protein, previously reported to be upregulated by >5 fold by high-fat feeding in rat muscle *in vitro* was also measured in L6 cells by RT-PCR. The result revealed that linoleate did not significantly change the gene expression of DNA binding protein

compared to control.
Surprisingly, TNF-α, reported to increase oxidative stress and stress associated gene expression in cultured skeletal muscle models, did not have an impact on the measured stress-related genes in L6 cells (100, 101). Also, the PPAR agonist rosiglitazone did not have any effect on the measured stress related gene expression. Rosiglitazone has previously, been demonstrated by the Diabetes Group at the Garvan Institute to reverse increased stress-related gene expression in high-fat-fed rats.

To ensure that the L6 muscle system was suitable for studies of gene expression in response to fatty acid exposure, we examined the literature for previous reports of genes upregulated by incubation with linoleate. UCP3 is reported to be upregulated by up to 10 fold in L6 cells incubated with linoleate, so we measured UCP3 expression in the linoleate treated L6 muscle cells to ensure that the linoleate had an impact on the cells compared to control. The conventional RT-PCR and real-time RT-PCR (LightCycler) results showed a convincing significant increase in expression after linoleate treatment (chapter 3.1.3 and 3.1.4). This demonstrated that the increase in linoleate concentration did have an impact on gene expression in L6 rat muscle cells.
Incubation with 1mM linoleate did not increase expression of the measured stress associated genes compared to control. This suggests that high dietary fat intake does not have a direct effect on expression of stress-associated genes in rat muscle, but that the observed change in expression is a secondary effect.
This secondary effect may be due to a change in secretion of a circulating cytokine or hormone from tissues other than skeletal muscle in response to increased dietary fat intake.
An example on a cytokine involved in energy homeostasis is leptin. Leptin correlates closely with fasting insulin concentrations and is known to be a marker of obesity and insulin resistance. Leptin has been reported to be upregulated by increased dietary fat intake, but it is not know whether leptin has an effect on stress-related gene expression in muscle (102). Other studies have shown that central administration of free fatty acids affect peripheral glucose metabolism independently of leptin (103, 104). This demonstrates that fatty acids can signal nutrient

availability to the CNS, but it is not known whether CNS can have an effect on stress-associated signalling in skeletal muscle.

Another explanation as to why no increase in stress-associated gene expression was detected in L6 rat muscle cells after linoleate exposure, could be that L6 rat muscle cells are substantially different from rat muscle cells *in vivo,* and therefore not a good model.

4.2 Gene chip results

To examine the degree of similarity in gene expression between red gastroc rat muscle tissue and cultured, differentiated L6 rat muscle cells, a micro array global gene expression experiment was conducted on mRNA pooled from five separate experiments on 24-h 1mM linoleate treated L6 rat muscle cells and their control.

4.2.1 Evaluation of L6 as a model of rat muscle cells in vivo

The data obtained from this global gene expression experiment showed that the linoleate treatment changed gene expression of several genes, including genes coding for enzymes involved in lipid metabolism (see table 3.2.1.1 in the result chapter). Unexpectedly, several genes involved in cholesterol and bile biosynthesis (for example HMG-CoA reductase and farnesyl diphosphate syntase) and fatty acid synthesis (for example ATP citrate lyse and fatty acid synthesis) were expressed in L6 rat muscle and were decreased after linoleate incubation. Expression of genes involved in cholesterol biosynthesis has also previously been demonstrated in L6 cells by Matzno et. al. (95). Although the mRNA expression level does not necessarily reflect the level of active protein this expression data clearly suggests that L6 myotubes have some properties usually associated with liver.

Interestingly, St-Amand et. al.found through serial analysis of gene expression that various genes, including genes involved in cholesterol synthesis, were differentially expressed in isolated immobilised skeletal rat muscle compared to control skeletal rat muscle *in vivo* (96). This may contribute to the explanation as to why genes involved in cholesterol synthesis are abundantly expressed in cultured L6 cells and not in rat muscle *in vivo*.

The results from the combined micro array search between data from the comparison of fatty acid treated L6 cells to control, and data from previously conducted experiments on global gene expression in liver from high-fat fed rats, also show similarities in gene expression changes between rat liver and L6 cells (for example the kruppel-like factor 9 and the glucocorticoid receptor). This, combined with the fact that L6 cells have low gene expression of GLUT4, no gene expression of CD36/FAT, and that they express the liver isoform of the key enzyme CPT1, may suggest that there is a substantial difference between cultured L6 rat muscle cells and rat muscle *in vivo*. This difference has to be accounted for in future *in vitro* experiments, and since CD36/FAT is not expressed and GLUT4 barely expressed in L6 cells this is particularly the case if the cells are to be used to reflect glucose and lipid metabolic pathways of muscle *in vivo.*

A gene chip experiment generates a lot of data, and all the differences in gene expression between linoleate treated L6 muscle cells and control will not be discussed here. The next section will review some linoleate-generated changes in L6 gene expression.

4.2.2 Genes involved in metabolism

Increased expression of genes involved in lipid mitochondrial transport, and β-oxidation suggests that linoleate has entered the cell and been metabolised. Interestingly, the micro array data revealed that the FAT/CD36 protein thought to have a central role in facilitated fatty acid transport is not expressed in L6 rat muscle. There is evidence that the uptake of fatty acids in L6 cells is the sum of passive diffusion plus a saturable component involving one or more protein structures (97). The finding that FAT/CD36 is not expressed in L6 cells suggests that there is another, or several other proteins involved in the active fatty acid transport in differentiated L6 rat muscle cells.

ADD1, also known as sterol regulatory element-binding transcription factor 1 (SREBP-1), is down regulated by 2.8 fold in the linoleate treated L6 cells compared to the control. This transcriptional activator regulates transcription of genes involved in lipid metabolism, including sterol biosynthesis (generally reduced after linoleate incubation, see figure 3.2.1.3.), the LDL receptor gene (reduced by 2.8 fold after linoleate incubation) and fatty acid synthesis (generally

reduced after linoleate incubation, see figure 3.2.1.2.). ADD1 is abundantly expressed in liver where it regulates fatty acid and cholesterol synthesis. Regulation of ADD1 occurs at two levels: transcriptional through a feed-forward loop, and post-transcriptional regulation (105). Insulin is known to regulate the activity of ADD1 in liver, and the fact that linoleate incubation leads to down regulation of this transcription factor is another result that may indicate that L6 cells share some properties normally associated with liver.

Linoleate incubation also had an impact on expression of genes involved in glucose metabolism. Glycogen phosphorylase (muscle isoform, gene id L10669), a key protein involved in glycogen breakdown (represented by two probe sets) showed increased gene expression in L6 cells after linoleate treatment. On the other hand, an enzyme in glycogen synthesis (glycogenin gene id U96130) is also increased after linoleate treatment, and drawing conclusions about the rate of glycogen synthesis based on these mRNA expressions observations would only be speculation.

Expression of two genes involved in glucose transport (GLUT1, solute carrier family 2, member 1 and GLUT4, solute carrier family 2, member 4) changed in mRNA expression after linoleate treatment. However, both genes, especially GLUT4, showed very low abundance in L6 cells. The micro array data also revealed that several ribosomal proteins (including ribosomal protein L4, L21, L13, S24, L22, L7a, L9 and S19, see appendix) were upregulated. Some of these proteins showed a large increase (ribosomal protein L4 gene expression was upregulated by 4.6 fold) This indicates that linoleate incubation also had an impact on protein biosynthesis in L6 cells.

Together these findings demonstrate that 24-hour 1mM linoleate incubation has a wide influence on expression of genes involved in L6 rat cell metabolism.

4.2.3 Genes involved in stress-protection and stress related signalling

Results from RT-PCR analysis and gene chip data revealed that linoleate did not up-regulate mRNA expression of the same stress associated genes as previously observed in high-fat rats.

This does not necessarily mean that these stress proteins were not activated in L6 cells after linoleate incubation, as NFκB is activated by degradation of the inhibitory unit and c-jun by phosphorylation, and not primarily via regulation of its transcription.
Some genes involved in cellular oxidative stress protection (including catalase) were increased after linoleate treatment (see figure 3.2.3.1). This may indicate that the concentration of free radicals was increased, although gene expression data is insufficient evidence to draw conclusions about the intracellular free-radical state of the linoleate treated L6 muscle cells.

Linoleate treatment also increased expression of some genes involved in stress sensitive signalling pathways (Results chapter 3.2.4). Although not all in the same signalling pathway, some of these stress proteins are known to interact, and cross-talk between pathways including JAK2 and NFκB signalling cascades has also been reported (98, 99). Some stress-sensitive genes of special interest include early growth responce-1 (EGR1, also known as Nerve growth factor-induced gene, increased by 1.4 fold in two probe sets) and v-Jun (also known as NURR77, increased by an average of 1.2 fold in three probe sets) both involved in regulation of transcription. EGR1 is a transcriptional regulator which activate the transcription of target genes whose products are required for mitogenesis and differentiation. EGR1 is induced by several growth factors. As discussed in the result chapter, v-jun is a leucine rich bZIP protein, which can form heterodimers or homodimers with other bZIP proteins, including c-fos.
It is interesting to note that v-jun is upregulated in two probe sets, both by linoleate incubation in L6 and by high-fat feeding in red gastroc rat muscle and by high-fat feeding in liver *in vivo*. Although the upregulation is relatively small, the fact that two probe sets encoding for the v-jun gene in a total of 10 gene chips all showed that v-jun is increased with linoleate incubation/high fat feeding, gives an increased confidence in the result.
Both EGR-1 and v-jun are relatively newly discovered transcription factors. Their function in regulating transcription is not fully understood, but they may play an important role in regulating gene transcription in muscle.

To compare the effect on gene expression of linoleate incubation on L6 cells with high-fat feeding on muscle cells *in vivo,* the data from the L6 gene chip experiment were compared to previously conducted gene chip experiments on rat muscle.

4.3 Comparison of L6 rat muscle cells with (red gastroc) rat muscle

The comparison between micro array data from cultured L6 and red gastroc rat muscle revealed that out of the 2734 probe sets present in rat muscle tissue 2476 probe sets were also present in the L6 cells. 258 probe sets were absent in the L6 cells. This comparison shows that the majority of the genes expressed in red gastroc rat muscle *in vivo* are also present in cultured L6 rat muscle cells *in vitro*. It is worth noting that a greater number of probe sets (and thus a greater number of genes) are expressed in L6 cells (4377) compared to red gastroc rat muscle cells *in vivo*. This may indicate that L6 cells express a wider range of genes compared to rat muscle cells *in vivo.* Another striking overall difference between the gene expression in rat muscle and cultured cells is the mRNA abundance (the signal) of genes involved in mitochondrial metabolism. The expression of genes involved in metabolism in the mitochondria is generally significantly lower in the L6 cells than in the rat muscle (examples include 3-ketoacyl-coA tiolase, medium and long chain acyl-CoA dehydrogenase and carnitine palmitoyl transferase 2). One explanation for this difference may be that rat muscle *in vivo* is more metabolically active and hence has a larger number of mitochondria and a larger enzyme density compared to L6 cells.

4.4 Comparison of L6 rat muscle cells with rat liver

The data obtained in the gene chip experiment clearly show that L6 myotubes abundantly expresses genes encoding for proteins normally associated with liver (such as genes involved in cholesterol biosynthesis and fatty acid synthesis). This observation lead us to comparing gene chip data from cultured L6 rat muscle cells with global gene expression data obtained from previous conducted experiments on liver from high-fat fed rats. The results revealed that out of the 2791 probe sets present in rat liver *in vivo* 2204 were also present, and 587 absent in L6 cells *in vitro*. In addition linoleate incubation of L6 cells upregulated expression of several genes also

upregulated by high fat feeding in rat liver. Some examples are given in table 4.4.1 (see table 3.2.9.1 for complete list).

Table 4.4.1 Examples on genes changed both in L6 cells (*in vitro*) and in rat liver (*in vivo*).

Gene ID	Name	Swissprot	Liver#1	Liver#2	L6
J05210	ATP citrate lyase	P16638	-2.3	-1.4	-1.5
L13619	growth response protein (CL-6)	Q08755	-2.0	-1.9	-2.5
J02585	stearoyl-Coenzyme A desaturase	P07308	-168.9	-48.5	-4.0
L16995	Add1		-1.2	-1.6	-2.5

Together, the comparisons of cultured L6 rat muscle cells, rat muscle cells (*in vivo*) and rat liver (*in vivo*) suggest that although L6 rat muscle cells share several properties with red gastroc rat muscle, they are also significantly different. The results from the comparisons above together with the results showing that genes involved in cholesterol biosynthesis, fatty acid synthesis and sterol regulation are abundantly present and decreased with linoleate incubation in L6 cells, suggests that in addition to properties similar to rat muscle *in vivo*, cultured L6 rat muscle cells also have properties associated with rat liver.

5. CONCLUSION AND FUTURE PERSPECTIVE

Conclusion:

This study has demonstrated that 24 and 48 h linoleate incubation does not induce any of the measured stress-associated genes in cultured L6 myotubes previously shown to be upregulated by high-fat feeding in rat skeletal muscle (*in vivo*).

Global gene expression analysis of L6 rat muscle cells revealed that there is a substantial difference between rat muscle cells *in vivo* and cultured L6 cells. Surprisingly, the global expression data also revealed that L6 myotubes has some properties normally associated with liver cells. This suggests that the L6 cell may not be a suitable model for further studies on fat-induced insulin resistance in rat skeletal muscle.

Future perspective:

To investigate the direct influence on stress associated gene expression in rat muscle further work is necessary to establish a cell-model that reflects lipid-induced insulin resistance in rat skeletal muscle *in vivo*. One way to test the direct effect of fatty acid on stress-associated gene expression could be to use isolated rat muscle (eg soleus or extensor degitorus longus) and measure gene expression, either by RT-PCR or by micro array after fatty acid incubation. However, the viability of isolated muscle could be a problem for long term (>6h) incubation with fatty acids. A primary rat muscle culture (from satellite cells) could also be established and used as a model for insulin resistance, although this cell-model could take a long time to grow/differentiate. However, imperfect simulation of perfusion and lack of electrical stimulation would also make this cell-model an imperfect imitation of rat muscle *in vivo*.

It would also be interesting to study the changes in lipid metabolism gene expression observed in fatty acid incubated L6 cells. By repeating the Affymetrix™ Gene Chip experiment on mRNA from 1mM linoleate incubated L6 cells and control for a shorter interval (for example 8h instead of 24h) one would be able to investigate the chronology in the gene expression changes imposed by fatty acid incubation. In this way early transcription factors central in regulating gene transcription could be identified.

REFERENCES

1. Molitch ME, Fujimoto W, Hamman RF, Knowler WC: The diabetes prevention program and its global implications. *J Am Soc Nephrol* 14:S103-107., 2003
2. King H, Aubert RE, Herman WH: Global burden of diabetes, 1995-2025: prevalence, numerical estimates, and projections. *Diabetes Care* 21:1414-1431., 1998
3. WHO: Obesity: Preventing and managing the global epidemic - Report of WHO consultation on obesity. *Geneva*, 1997
4. Quinn L: Type 2 diabetes: epidemiology, pathophysiology, and diagnosis. *Nurs Clin North Am* 36:175-192, v., 2001
5. Dostou J, Gerich J: Pathogenesis of type 2 diabetes mellitus. *Exp Clin Endocrinol Diabetes* 109:S149-156., 2001
6. Lovejoy JC: The influence of dietary fat on insulin resistance. *Curr Diab Rep* 2:435-440., 2002
7. Bogardus C, Lillioja S: Distribution of in vivo insulin action in Pima Indians as mixture of three normal distributions. *Diabetes* 38:, 1989`
8. Saltiel AR, Kahn CR: Insulin signalling and the regulation of glucose and lipid metabolism. *Nature* 414:799-806., 2001
9. DeFronzo R: Pathogenesis of type 2 diabetes: metabolic and molecular implications for identifying diabetes genes. *Diabetes Rev* 5:155-269, 1997
10. Petersen KF, Shulman GI: Pathogenesis of skeletal muscle insulin resistance in type 2 diabetes mellitus. *Am J Cardiol* 90:11G-18G., 2002
11. Powers A: Diabetes mellitus. *Harrison's Principles of Internal Medicine* 15:2109-2137, 2001
12. Goldstein BJ: Insulin resistance as the core defect in type 2 diabetes mellitus. *Am J Cardiol* 90:3G-10G., 2002
13. Zraika S, Dunlop M, Proietto J, Andrikopoulos S: Effects of free fatty acids on insulin secretion in obesity. *Obes Rev* 3:103-112., 2002

14. Bergman RN: Free fatty acids and pathogenesis of type 2 diabetes mellitus. *Trends Endocrinol. Metab.* 11:351-356, 2000
15. Ginsberg HN: Insulin resistance and cardiovascular disease. *J Clin Invest* 106:453-458., 2000
16. Kahn C: Insulin action, diabetogenes, and the cause og type II diabetes,. *Diabetes* 43:1066-1084, 1994
17. Carey D, Jerkins, Camobell L, Freund J, Chrisholm D: Abdominal fat and insulin resistance in normal and overweight women: Direct measurements reveal a strong relationship in subjects at both high and low risk of NIDDM. *Diabetes* 45:633-638, 1996
18. Randle PJ: The glucose fatty-acid cycle; its role in insulin sensiticity and the metabolic disturbances of diabetes mellitus. *Lancet* 785-789, 1963
19. Cooney GJ, Thompson AL, Furler SM, Ye J, Kraegen EW: Muscle long-chain acyl CoA esters and insulin resistance. *Ann N Y Acad Sci* 967:196-207., 2002
20. Boden G: Role of fatty acids in the pathogenesis of insulin resistance and NIDDM. *Diabetes* 46:3-10, 1997
21. Ellis BA, Poyten A, Lowy AJ, Furler SM, Chrisholm DJ, Kraegen EW, Cooney GJ: Long-chain acyl-CoA esters as indicators of lipid metabolism and insulin sensitivity in rat and human muscle. *Am J Endocrinol Metab* 279:E54-60, 2000
22. Thompson AL, Cooney GJ: Acyl CoA inhibition of hexokinase in rat and human skeletal muscle is a potential mechanism of insulin resistance. *Diabetes* 49:1761-1765, 2000
23. Schmitz-Peiffer C: Signalling aspects of insulin resistance in skeletal muscle: mechanisms induced by lipid oversupply. *Cellular Signalling* 12:583-594, 2000
24. Reynoso R, Salgado LM, Caldernon V: High levels of palmitic acid leads to insulin resistance due to changes in the level of phosphorylation of the insulin receptor and insulin receptor substrate-1. *Mol Cell Biochem* 246:155-162, 2003
25. Beeson M, Sajan MP, Dizon M, Grebenev D, Gomez-Daspet J, Miura A: Activation of protein kinase C-zeta by insulin and phospatidylinositol-3,4,5-(Po4)3 is defective in muscle in type 2 diabetes and impaired glucose tolerance: amelioration by rosiglitazone an exercise. *Diabetes* 52:1926-1934, 2003

26. Kim YB, Kotani K, Ciaraldi TP, Henry RR, Kahn BB: Insulin-stimulated protein kinase C lambda/zeta activity is reduced in skeletal muscle of humans with obesity and type 2 diabetes: reversal with weight reduction. *Diabetes* 52:1935-1942., 2003
27. Nishizuka Y: Protein kinase C and lipid signalling for sustained cellular responses. *FASEB J.* 9:484-496, 1995
28. Cutler RG, Mattson MP: Sphingomyelin and ceramide as regulators of development and lifespan. *Mech Ageing Dev* 122:895-908., 2001
29. Hegarty BD, Furler SM, Ye J, Cooney GJ, Kraegen EW: The role of intramuscular lipid in insulin resistance. *Acta Physiol Scand* 178:373-383., 2003
30. Merrill AH, Jr., Jones DD: An update of the enzymology and regulation of sphingomyelin metabolism. *Biochim Biophys Acta* 1044:1-12., 1990
31. Summers SA, Garza LA, Zhu H, Birnabum MJ: Regulation of insulin stimulated glucose transporter GLUT4 translocation and Akt kinase activity by ceramide. *Molecular Cell Biologi* 18:5457-5464, 1998
32. Muller G, Ayoub M, Storz P, Rennecke J, Fabbro D, Pfizenmaier K: PKC zeta is a molecular switch in signal transduction of TNF-alpha, bifunctionally regulated by ceramide and arachidonic acid. *Embo J* 14:1961-1969., 1995
33. Hawkins M, Barzilai N, Liu R, Hu M, Chen W, Rossetti L: Role of the glucosamine pathway in fat-induced insulin resistance. *J Clin Invest* 99:2173-2182., 1997
34. McKlain DA: Hexosamines as mediators of nutrient sensing and regulation in diabetes. *Journal of diabetes and its complications* 16:72-80, 2002
35. Patti ME, Virkamaki A, Landaker EJ, Kahn CR, Yki-Jarvinen H: Activation of the hexoamine pathway by glucosamine induces insulin resistance of early postreceptor insulin signalling events in skeletal muscle. *Diabetes* 48:1562-1571, 1999
36. Hart GW, Haltiwanger RS, Holt GD, Kelley WC: Glycosylation in the nucleus and cytoplasm. *Annual Review of Biochemistry* 58:841-874, 1989
37. Filippis A, Clark S, Proietto J: Increased flux through the hexosamine biosynthesis pathway inhibits glucose transport acutely by activation of protein kinase C. *J. Biochem* 324:981-985, 1997

38. Gagnon AM, Chabot J, Pardasani D, Sorisky A: Extracellular matirx induced by TGFbeta iympairs insulin signal transduction in 3T3-L1 preadipose cells. *Journal of cellular physiolog* 175:370-378, 1998
39. Shimomura I, Hammer RE, Ikemoto S, Brown MS, Goldstein JL: Leptin reverses insulin resistance and diabetes mellitus in mice with congenital lipodystrophy. *Nature* 401:73-76., 1999
40. Kubota N, Terauchi Y, Yamauchi T, Kubota T, Moroi M, Matsui J, Eto K, Yamashita T, Kamon J, Satoh H, Yano W, Froguel P, Nagai R, Kimura S, Kadowaki T, Noda T: Disruption of adiponectin causes insulin resistance and neointimal formation. *J Biol Chem* 277:25863-25866., 2002
41. Hong R, Harvey FL: Insulin resistance in adipose tissue: direct and indirect effects of tumor necrosis factor-alpha. *Cytokine & Growth Factor Reviews* 14:447-455, 2003
42. Steppan CM, Lazar MA: Resistin and obesity-associated insulin resistance. *Trends Endocrinol Metab* 13:18-23., 2002
43. Kahn BB, Flier JS: Obesity and insulin resistance. *The Journal of Clinical Investigation* 106:473-481, 2000
44. Uysal KT, Wiesbrock SM, Marino MW, Hotamisligil GS: Protection from obesity-induced insulin resistance in mice lacking TNF-alpha fuction. *Nature* 389:610-614, 1997
45. Begum N, Ragolia L: Effect of tumor necrosis factor-alpha on insulin action in cultured rat skeletal muscle cells. *Endocrinology* 137:2441-2446., 1996
46. Halse R, Pearson SL, McCormack JG, Yeaman SJ, Taylor R: Effects of tumor necrosis factor-alpha on insulin action in cultured human muscle cells. *Diabetes* 50:1102-1109., 2001
47. Evans JL, Goldfine ID, Maddux BA, Grodsky GM: Oxidative stress and stress-activated signalling pathways: a unifying hypothesis of type 2 diabetes. *Endocr Rev* 23:599-622., 2002
48. Yuan M, Konstantopoulos N, Lee J, Hansen L, Li ZW: Reversal of obesity- and diet-induced insulin resistance with salisylates of targeted disruption of IKKbeta. *Sience* 293:1673-1677, 2001

49. Ruan H, Hacohen N, Golub, T.R, Van Paroks L, Lodish HF: Tumor Necrosis Factor-alpha suppresses adipocyte-specific genes and activates expression of preadipocyte genes in 3T3-L1 adipocytes: nuclear factor-kappaB activation by TNF-alpha is obligatory. *Diabetes* 51:1319-1336, 2002
50. Yamauchi T, Kamon J, Ito Y, Tsuchida A, Yokomizo T, Kita S, Sugiyama T, Miyagishi M, Hara K, Tsunoda M, Murakami K, Ohteki T, Uchida S, Takekawa S, Waki H, Tsuno NH, Shibata Y, Terauchi Y, Froguel P, Tobe K, Koyasu S, Taira K, Kitamura T, Shimizu T, Nagai R, Kadowaki T: Cloning of adiponectin receptors that mediate antidiabetic metabolic effects. *Nature* 423:762-769., 2003
51. Haber CA, Lam TK, Gupta N, Goh T, Bogdanovic E: N-acetylcycsteine and taurine prevents hyperglycemia-induced insulin resistance in vivo: possible role of oxidative stress. *Am J Physiol Endoclinol Metab* 4:E-74-53, 2003
52. Paolisso G, Giugliano D: Oxidative stress and insulin action: is there a relationship? *Diabetologia* 39:357-363, 1996
53. Maddux BA, See W, Lawrence JC, Jr., Goldfine AL, Goldfine ID, Evans JL: Protection against oxidative stress-induced insulin resistance in rat L6 muscle cells by mircomolar concentrations of alpha-lipoic acid. *Diabetes* 50:404-410., 2001
54. Jacob S, Ruus P, Hermann R, Tritschler HJ: Oral adiministration of RAC-alpha lipoic acid modulates insulin sensitivity in patients with type-2 diabetes mellitus: a placebo-controlled pilot trial. *Free Radic Biol Med* 27:309-314, 1999
55. Bruce CR, Carey AL, Hawley JA, Febbratio MA: Intramuscluar Heat Shock Protein 72 and Heme Oxygenase-1 mRNA are reduced in patients with type 2 diabetes. *Diabetes* 52:2338-2345, 2003
56. Yuan M, Lee J, Konstantopoulos N, Hansen L, Shoelson SE: Salicylate inhibition of IKKbeta reverses insulin resistance in Zucker (fa/fa) rats. *Diabetes* 49:A292, 2000
57. Kim JK, Kim YJ, Fillmore JJ, Chen Y, Moore I, Lee J, Yuan M, Li ZW, Karin M, Perret P, Shoelson SE, Shulman GI: Prevention of fat-induced insulin resistance by salicylate. *J Clin Invest* 108:437-446., 2001

58. Kamp F, Guo W, Souto R, Pilch PF, Corkev BE: Rapid Flip-flop of Oleic Acid across the Plasma Membrane of Adipocytes. *The Journal of Biological Chemistry* 278:7988-7995, 2002
59. Luiken JJFP, Bonen A, Glatz JFC: Cellular fatty acid uptake is acutely regulated by membrane-associated fatty acid binding proteins. *Prostaglandins, Leukotreiens and Essential Fatty Acids* 67:73-78, 2002
60. van der Vusse GJ, van Blisen M, Glatz JF: Critical steps in cellular fatty acid uptake and utilization. *Mol Cel Biochem.* 239:9-15, 2002
61. Ibrahimi A, Bonen A, Blinn WD, Hajri T, Li X, Zhong K, Cameron R, Abumrad NA: Muscle-specific overexpression of FAT/CD36 enhances fatty acid oxidation by contracting muscle, reduces plasma triglycerides and fatty acids, and increases plasma glucose and insulin. *J Biol Chem* 274:26761-26766., 1999
62. Febbraio M, Abumrad NA, Hajjar DP, Sharma K, Cheng W, Pearce SF, Silverstein RL: A null mutation in murine CD36 reveals an important role in fatty acid and lipoprotein metabolism. *J Biol Chem* 274:19055-19062., 1999
63. Luiken JJ, Koonen DP, Willems J, Zorzano A, Becker C: Insulin stimulates long-chain fatty acid utilization by rat cardiac myocytes through cellular redistribution of FAT/CD36. *Diabetes* 51:3113-3119, 2002
64. Storlien LH, Jerkins AB, Chrisholm DJ, Pascoe WS, Khouri S, Kraegen EW: Influence of dietary fat composition on development of insuline resistance in rats. Relationship to muscle triglyceride and omega-3 fatty acids in muscle phospholipid. *Diabetes* 40:280-289, 1991
65. Kraegen EW, Clark PW, Jenkins AB: Development of insulin resistance after liver insulin resistance in high-fat-fed rats. *Diabetes* 40:1397-1403, 1991
66. Vila MC, Miligan G, Standaert ML, Farese RV: Insulin activates glycerol-3-phosphate acyltransferase (de novo phosphatic acid synthesis) through a phospholipid-derived mediator. Apparent involvment of Gi alpha and activation of a phospholipase C. *Biochemistry* 29:8735-8740, 1990

67. Goodpater BH, Kelley DE: Role of muscle in triglyceride metabolisn. *Curr. Opin. Lipidol.* 9:231-236, 1998
68. Turpeinen AK, Takala TO, Nuutila P: Impared free fatty acid uptake in skeletal muscle, but not in myocardium in patients with impaired glucose tolerance - studies with PET and 14(R,S)-[F-18]fluoro-6-thia-heptadecanoic acid. *Diabetes* 48:1245-1250, 1999
69. Ruderman NB, Saha AK, Vavvas D, Witters LA: Malonyl-CoA, fuel sensing, and insulin resistance. *Am J Physiol* 276:E1-E18., 1999
70. Otto DA, Baltzel JK, Wotten JT: Reduction in tracyleglycerol levels by fish oils correlates with free fatty acid levels in ad lib. itum fed rats. *Lipids* 27:, 1992
71. Kunau WH, Dommes V, Schulz H: Beta-oxidation of fatty acids in mitocondria, peroxisoes and bacteria: a century of continued progress. *Prog Lipid Res* 34:267-342, 1995
72. Willson TM, Lambert MH, Kliewer SA: Peroxisome proliferator-activated receptor gamma and metabolic disease. *Annu Rev Biochem* 70:341-367., 2001
73. Escher P, Wahli W: Peroxisome proliferator-activated receptors: insight into multiple cellular functions. *Mutat Res* 448:121-138, 2000
74. Frohnert BI, Bernlohr DA: Identification of a functional peroxisome proliferator-responsive element in the murine fatty acid transport protein gene. *J Biol Chem* 247:3970-3977, 1999
75. Schoonjans K, Watanabe M, Suzuki H: Induction of acyl-coenzyme A syntethase gene by fibrates and fatty acids is mediated by a peroxisome proliferator responce element in the C promoter. *J Biol Chem* 270:19269-19276, 1995
76. Brandt JM, Djouadi F, Kelley DP: Fatty acids activate transcription of the muscle carnitine palmitoyltransferase I gene in cardiac myocytes cia the peroxisome proliferator-activated receptor alpha. *J Biol Chem* 273:23786-23792, 1998
77. Chevilotte E, Rieusset J, Roques M, Desage M: The regulation of uncoupling protein-2 gene expression by omega-6 polyunsaturated fatty acids in human skeletal muscle cells involves multiple pathways, including the nuclear receptor peroxisome proliferator-activated receptor beta. *J Biol Chem* 276:10853-10860, 2002

78. Holst D, Luquet S, Kristiansen K, Grimaldi PA: Roles of peroxisome proliferator-activated receptors delta and gamma in myoblast transdifferentiation. *Exp Cell Res* 288:168-176., 2003
79. Wang YX, Lee CH, Tiep S, Yu RT, Ham J, Kang H, Evans RM: Peroxisome-proliferator-activated receptor delta activates fat metabolism to prevent obesity. *Cell* 113:159-170., 2003
80. Holst D, Luquet S, Nogueira V, Kristiansen K, Leverve X, Grimaldi PA: Nutritional regulation and role of peroxisome proliferator-activated receptor delta in fatty acid catabolism in skeletal muscle. *Biochim Biophys Acta* 1633:43-50., 2003
81. Schmidt DM, Ernst JD: A fluorometric assay for the quantification of RNA in solution wiht nanogram sensitivity. *Anal Biochem* 232:144-146, 1995
82. Affymetrix: U34 Rat Genome Data Sheet. *http://www.affymetrix.com/products/arrays/specific/rgu34.affx*, 2001
83. Doniger SW, Salomonis N, Dahlquist KD, Vranizan K, Lawlor SC, Conklin BR: MAPPFinder: using Gene Ontology and GenMAPP to create a global gene-expression profile from microarray data. *Genome Biol* 4:R7., 2003
84. Mitsumoto Y, Burdett E, Grant A, Klip A: Differential expression of the GLUT1 and GLUT4 glucose transporters during differentiation of L6 muscle cells. *Biochem Biophys Res Commun* 175:652-659., 1991
85. Mitsumoto Y, Klip A: Development regulation of the subcellular distribution and glycosylation of GLUT1 and GLUT4 glucose transporters during myogenesis of L6 muscle cells. *J Biol Chem* 267:4957-4962., 1992
86. Sumitani S, Ramlal T, Somwar R, Keller SR, Klip A: Insulin regulation and selective segregation with glucose transporter-4 of the membrane aminopeptidase vp165 in rat skeletal muscle cells. *Endocrinology* 138:1029-1034., 1997
87. Vogt PK: Jun, the oncoprotein. *Oncogene* 20:2365-2377, 2001
88. Nagase I, Yoshida S, Xavier C, Yukiko, Irie: Up-regulation of uncoupling protein 3 by thyroid hormone, peroxisome proliferator activated receptor ligands and 9-cis retinoic acid in L6 myotubes. *FEBS* 461:319-322, 1999

89. Costello A, Gray S, Donnelly R: Effects of rosiglitazone and oleic acid on UCP-3 expression in L6 myotubes. *Diabetes, Obesity and Metabolism* 6:136-138, 2003
90. Tamemoto H: Insulin resistance and growth retardation in mice lacking insulin resepror substrate 1. *Nature* 372:182-186, 1994
91. Garofalo RS, Orena SJ, Rafidi K: Severe diabetes, age-dependent loss of adipose tissue and mild growth deficiency in mice lacking Akt2/PKB beta. *Clin Invest* 12:197-208, 2003
92. Blair AS, Hajduch E, Litherland GJ, Hundal HS: Regulation of glucose transport and glycogen synthesis in L6 muscle cells during oxidative stress. Evidence for cross-talk between the insulin and SAPK2/p38 mitogen-activated protein kinase signalling pathways. *Biol Chem* 274:36293-36299, 1999
93. Maruyama K, Tsukada T, Ohkura N: The NGFI-B subfamily of the nuclear receptor superfamily. *Int J Oncol* 12:1237-1243, 1998
94. Foti D, Stroup D, Chiang JY: Basic transcription element binding protein (BTEB) transactivates the cholesterol 7 alpha-hydroxylase gene (CYP7A). *Biochem Biophys Res Commun* 253:109-113, 1998
95. Matzno S, Yamauchi T, Gohda M, Ishida N, Katsuura K, Hanasaki Y, Tokunaga T, Itoh H, Nakamura N: Inhibition of cholesterol biosynthesis by squalene epoxidase inhibitor avoids apoptotic cell death in L6 myoblasts. *J Lipid Res* 38:1639-1648., 1997
96. St-Amand J, Okamura K, Matsumoto K, Shimizu S, Sogawa Y: Characterization of control and immobilized skeletal muscle: an overview from genetic engineering. *Faseb J* 15:684-692., 2001
97. Marra CA, Giron MD, Suare MD: Evidence in favor of a facilitated transport system for FA uptake in cultured L6 cells. *Lipids* 37:273-283., 2002
98. Digicaylioglu M, Lipton SA: Erythropoietin-mediated neuroprotection involves cross-talk between Jak2 and NF-kappaB signalling cascades. *Nature* 412:641-647., 2001
99. Zhu T, Lobie PE: Janus kinase 2-dependent activation of p38 mitogen-activated protein kinase by growth hormone. Resultant transcriptional activation of ATF-2 and CHOP, cytoskeletal re-organization and mitogenesis. *J Biol Chem* 275:2103-2114., 2000

100. Langen RC, Schols AM, Kelders MC, Van Der Velden JL, Wouters EF, Janssen-Heininger YM: Tumor necrosis factor-alpha inhibits myogenesis through redox-dependent and -independent pathways. *Am J Physiol Cell Physiol* 283:C714-721., 2002
101. Reid MB, Li YP: Cytokines and oxidative signalling in skeletal muscle. *Acta Physiol Scand* 171:225-232., 2001
102. Havel PJ: Control of energy homeostasis and insulin action by adipocyte hormones: leptin, acylation stimulating protein, and adiponectin. *Curr Opin Lipidol* 13:51-59., 2002
103. Obici S, Rossetti L: Nutrient sensing and the regulation of insulin action and energy balance. *Endocrinology* 11:11, 2003
104. Obici S, Feng Z, Morgan K, Stein D, Karkanias G, Rossetti L: Central administration of oleic acid inhibits glucose production and food intake. *Diabetes* 51:271-275., 2002
105. Horton JD, Goldstein JL, Brown MS: SREBPs: activators of the complete program of cholesterol and fatty acid synthesis in the liver. *J Clin Invest* 109:1125-1131., 2002
106. Camps M, Nichols A, Arkinstall S: Dual specificity phosphatases: a gene family for control of MAP kinase function. *Faseb J* 14:6-16., 2000
107. Myokai F, Takashiba S, Lebo R, Amar S: A novel lipopolysaccharide-induced transcription factor regulating tumor necrosis factor alpha gene expression: molecular cloning, sequencing, characterization, and chromosomal assignment. *Proc Natl Acad Sci U S A* 96:4518-4523., 1999
108. Yamamoto H, Kurebayashi S, Hirose T, Kouhara H, Kasayama S: Reduced IRS-2 and GLUT4 expression in PPARgamma2-induced adipocytes derived from C/EBPbeta and C/EBPdelta-deficient mouse embryonic fibroblasts. *J Cell Sci* 115:3601-3607., 2002
109. Keeton AB, Bortoff KD, Bennett WL, Franklin JL, Venable DY, Messina JL: Insulin regulated expression of EGR-1 and KROX20 Dependence on ERK1/2 and interaction with p38 and PI3-kinase pathways. *Endocrinology* 11:11, 2003

APPENDIX I

Probe_set	name	Sig. Con	Sig.Lin	F.Ch	Swisprot
rc_AA859975_at	2-oxoglutarate carrier	371.4	447.3	1.1	O70603
rc_AI171090_g_at	3-hydroxy-3-methylglutaryl CoA lyase	54.4	84.4	1.9	
X55286_g_at	3-hydroxy-3-methylglutaryl-Coenzyme A reductase	50.5	22.3	-1.7	
rc_AI177004_s_at	3-hydroxy-3-methylglutaryl-Coenzyme A synthase 1	439.4	193.4	-2.3	
X52625_at	3-hydroxy-3-methylglutaryl-Coenzyme A synthase 1	804.5	449.8	-1.9	
X97772_at	3-phosphoglycerate dehydrogenase	470.8	400	-1.2	P25110
Y15748_at	3-phosphoinositide dependent protein kinase-1	39.1	53.7	1.4	Q63528
M77850_at	6-pyruvoyl-tetrahydropterin synthase	6.7	148.9	12.1	P19335
U48288_at	A-kinase anchoring protein	15.2	678.8	7.5	
U94904_s_at	abl-interactor 2	118.5	140.6	1.2	
X05341_at	acetyl-Coenzyme A acyltransferase 2	177.5	343.3	1.7	
	(mitochondrial 3-oxoacyl-Coenzyme A thiolase)				
J05029_s_at	acetyl-Coenzyme A dehydrogenase, long-chain	152.9	262.7	1.6	P10608
rc_AI070967_g_at	Acid nuclear phosphoprotein 32 (leucine rich)	10.8	16.2	1.6	
rc_AA866452_s_at	actin alpha cardiac 1	1147.9	902.9	-1.2	Q8CJH4
rc_AI104567_g_at	actin alpha cardiac 1	896.9	1038.8	1.2	
AF083269_at	actin related protein 2/3 complex, subunit 1B	840.8	714.6	-1.1	O88656
U19893_at	actinin alpha 4	553.4	433.3	-1.3	O35804
rc_AA964379_s_at	adaptor-related protein complex 2, beta 1 subunit	158	224	1.6	
rc_AI146195_at	adducin 3, gamma	14.5	32.5	2.1	
rc_AI176052_at	adenylate kinase 3	778.3	635	-1.1	
M80550_at	adenylyl cyclase 2	340	416.9	1.1	P04937
X80130cds_f_at	ADP-ribosylation-like 4	807.2	675	-1.1	Q63355
rc_AA964849_at	ADP-ribosyltransferase 1	19.3	115	4.0	P30009
J03024_at	adrenergic receptor, beta 2	100.9	134.1	1.1	P05982
rc_AA859702_at	afadin	9.6	20.9	2.0	
U89905_at	alpha-methylacyl-CoA racemase	61.6	84.2	1.2	P70616
rc_AA893158_at	annexin A7	63.4	48.8	-1.1	P40615
AA850219_at	Annexin III (Lipocortin III)	81.6	59	-1.3	P14669
U90829_at	APP-binding protein 1	469.3	359	-1.2	
AF026505_at	Arg/Abl-interacting protein ArgBP2	57.4	77	-1.2	O35413
rc_AA891194_s_at	Arg/Abl-interacting protein ArgBP2	176.9	141.4	-1.3	P03996
U07201_at	Asparagine synthetase	90.1	76.9	-1.3	Q07258
D13120_s_at	ATP synthase subunit d	1720.4	1909.2	1.1	Q01713
rc_AA799778_at	ATP synthase, H+ transporting, mitochondrial	99.6	1523.8	13.0	Q9Z2J3
	F0 complex, subunit b, isoform 1				
rc_AI230614_s_at	ATPase Na+/K+ transporting beta 1 polypeptide	20	105.3	6.1	
M99223_at	ATPase, Ca++ transporting, cardiac muscle,	61.5	119.6	1.5	P31232
	fast twitch 1				
AA799276_at	ATPase, Ca++ transporting, cardiac muscle,	1443.5	1708.1	1.1	
	slow twitch 2				
U29339_at	avian erythroblastosis oncogene B 3	107.4	131.3	1.3	
AF009329_at	basic helix-loop-helix domain containing, class B3	196.7	212.9	1.1	O35779
rc_AA859830_s_at	biglycan	207	475	2.3	
D49955_at	bone marrow stromal cell antigen 1	4.8	19.3	3.7	Q63714
S75359_s_at	bone morphogenetic protein receptor, type 1A	90.2	207.2	1.7	
D14441_at	brain acidic membrane protein	438.6	298.8	-1.2	
rc_AI030286_s_at	brain derived neurotrophic factor	23	14.2	-1.4	O70437
U68417_at	branched chain aminotransferase 2, mitochondrial	189.6	133	-1.3	P54844
rc_AI102839_g_at	calbindin 1	57.8	116	2.0	
M86621_at	calcium channel,voltage-dependent, alpha2/delta s.u.1	189.1	246.7	1.3	P26769
L13407_i_at	calcium/calmodulin-dependent protein kinase II, delta	17.5	13.8	-1.3	P15650
rc_AI180288_s_at	Caldesmon 1	151.1	145.3	-1.2	O08876
X53363cds_s_at	calreticulin	834.5	959.7	1.1	
AF037072_at	carbonic anhydrase 3	171.8	112.9	-1.6	P14141
rc_AA800851_s_at	carboxylesterase 3	44.8	36.1	-1.3	P19357
L07736_at	carnitine palmitoyltransferase 1	39.9	198	4.6	P09057
U22297_at	casein kinase 1 gamma 2 isoform	244	196.1	-1.2	P22829
M11670_at	Catalase	71.6	84.7	1.1	Q923V7
rc_AA926149_g_at	Catalase	127.5	138	1.2	
rc_AI235585_s_at	cathepsin D	663.7	956.9	1.2	
rc_AI043968_at	caveolin 3	1030	800	-1.2	P47198
rc_AI043968_g_at	caveolin 3	1448.1	1018.1	-1.3	Q63617
rc_AA946292_at	CCAAT/enhancerbinding, protein (C/EBP) delta	40.8	58.5	1.7	P04762

Probe_set	name	Sig. Con	Sig.Lin	F.Ch	Swisprot
rc_AI103957_g_at	CD 81 antigen	86.6	62.8	-1.3	P48317
D82928_at	CDP-diacylglycerol--inositol 3-phosphatidyltransferase (phosphatidylinositol synthase)	458.4	396.2	-1.1	Q63788
	(phosphatidylinositol synthase)				
rc_AA925473_g_at	cell division cycle 42 homolog (S. cerevisiae)	1134.4	941.9	-1.2	P16036
Y12178_at	Ceruloplasmin (ferroxidase)	4.3	9.4	1.6	
AJ010828_at	chemokine orphan receptor 1	108.6	127	1.2	O89039
X74402_at	choline transporter	177.2	131.2	-1.1	Q8K1F5
X74834cds_s_at	cholinergic receptor, nicotinic, alpha polypeptide 1	968.8	1282.9	1.3	Q63258
X74836cds_s_at	cholinergic receptor, nicotinic, delta polypeptide	43.8	104.1	1.5	P28570
X77235_at	cholinergic receptor, nicotinic, epsilon polypeptide	118.6	78.8	-1.3	P50398
X74835cds_at	cholinergic receptor, nicotinic, gamma polypeptide	558.1	706.3	1.3	Q63258
rc_AA892559_at	Ciliary neurotropic factor	7.5	21.2	2.0	O08622
rc_AA859757_at	collagen, type V, alpha 1	187.3	147.4	-1.2	
AJ005394_at	collagen, type V, alpha 1	471.8	426.8	-1.1	O70603
rc_AA859757_g_at	collagen, type V, alpha 1	924.1	695.7	-1.2	P50878
rc_AA894304_at	Complement component 3	694.4	521.9	-1.3	P40615
M10140_at	creatine kinase, muscle	1045.9	1408.4	1.3	P41135
X75207_s_at	cyclin D1	194.6	218.1	1.1	
rc_AI234146_at	cysteine rich protein 1	737.6	601.8	-1.2	P27817
rc_AA800784_at	cysteine rich protein 61	230.7	147.2	-2.0	O08589
Y12517cds_at	cytochrome b5,outer mitochondrial membrane isoform	96.2	99	-1.2	Q64346
rc_AA997614_s_at	cytochrome P450, subfamily 51	386.5	166.5	-2.3	P35281
AB004096_at	cytochrome P450, subfamily 51	405.5	193.3	-1.9	Q64654
rc_AA963449_s_at	cytochrome P450, subfamily 51	753.9	332.4	-2.0	Q62833
U17697_s_at	cytochrome P450, subfamily 51	805.4	497.5	-1.7	Q64536
AF038591_at	cytoplasmic aminopeptidase P	301.7	262.2	-1.1	O54975
X60328_g_at	cytosolic epoxide hydrolase	52.8	64.8	1.3	
Z36980_at	D-dopachrome tautomerase	260.7	212.6	-1.2	P04166
AF055884_s_at	DEAF-1 related transcriptional regulator (NUDR)	76.3	99.6	1.3	O88450
rc_AA963839_s_at	diaphorase 1	616.3	469.2	-1.2	Q03484
rc_AI229440_s_at	diaphorase 1	977.6	825.2	-1.1	Q01986
D00636Poly_A_Site#1_s	diaphorase 1	1889.8	1542.2	-1.2	Q9Z1K4
U49049_at	discs, large (Drosophila) homolog 2 (chapsyn-110)	19	16	-1.3	Q62809
U50717_s_at	discs, large (Drosophila) homolog 2 (chapsyn-110)	75	74.9	-1.2	Q64303
U67994_at	DNA primase, p49 subunit	4.4	166.9	48.5	P54102
rc_AI011998_at	dnaJ homolog, subfamily b, member 9	18.7	271.1	7.0	P53812
U53922_at	DnaJ-like protein	706.7	829.6	1.1	Q62920
X94185cds_s_at	dual specificity phosphatase 6	94.5	122.6	1.3	P18916
U42627_at	dual specificity phosphatase 6	159.2	209.6	1.3	Q62784
X54531mRNA_at	dynamin 1	137.8	174.9	1.2	
AF020210_s_at	dynamin 1-like	58.5	55.4	-1.2	O35303
rc_AA892562_g_at	dyskeratosis congenita 1, dyskerin	68.7	200.3	2.0	Q63413
rc_AA892562_at	dyskeratosis congenita 1, dyskerin	173.6	285.1	1.7	P00507
M18416_at	early growth response 1	58.6	75.9	1.4	P12369
AF023087_s_at	early growth response 1	287.1	416	1.4	P08154
U36482_g_at	endoplasmic retuclum protein 29	574.6	696.4	1.1	
U48247_g_at	enigma homolog	119.9	84.3	-1.3	P97659
rc_AA851223_at	enolase 3, beta	307.7	1339.9	2.5	P12346
U08976_at	enoyl coenzyme A hydratase 1	260.6	378.5	1.5	Q07258
rc_AA684631_at	ESTs, Weakly similar to ankycorbin; NORPEG-like protein [Mus musculus] [M.musculu	143.2	173.9	1.1	
U05014_at	eukaryotic translation initiation factor 4E binding protein 1	479.2	400	-1.1	Q64308
rc_AI180442_at	farensyl diphosphate synthase	470.5	207.6	-2.3	P29411
U72497_at	fatty acid amide hydrolase	72.2	93.1	1.2	P97577
rc_AA893242_g_at	fatty acid Coenzyme A ligase, long chain 2	101.3	72.1	-1.3	
rc_AI236284_s_at	fatty acid Coenzyme A ligase, long chain 4	209.1	136.5	-1.3	
X56551cds_at	fibroblast growth factor 7	28.3	82.1	2.5	
M28259cds_at	Fibronectin 1	151.8	112.4	-1.2	
rc_AA891769_at	Fibronectin 1	424	482.7	1.1	O88548
rc_AA799645_g_at	FXYD domain-containing ion transport regulator 1	32.7	78.6	1.7	P16632
rc_AA799645_at	FXYD domain-containing ion transport regulator 1	167.3	187.5	1.2	P54290
rc_AA946251_at	G protein-coupled receptor kinase 5	14.3	27.9	1.4	P30009
X74800_at	GDP-dissociation inhibitor 1	319.3	203	-1.4	Q8K1F5
rc_AA800912_at	general transcription factor II I repeat domain-containing 1	96.7	81.8	-1.2	P19511
X07467_at	glucose-6-phosphate dehydrogenase	365.2	290.4	-1.2	Q9Z1A5

Probe_set	name	Sig. Con	Sig.Lin	F.Ch	Swisprot
rc_AA892012_g_at	Glutamate oxaloacetate transaminase 2, mitochondrial (aspartate aminotransf	258.4	202.4	-1.3	
AF090113_g_at	glutamate receptor interacting protein 2	111.4	77.3	-1.3	O88961
J03914cds_s_at	Glutathione-S-transferase, mu type 2 (Yb2)	390.4	317.8	-1.2	P09495
U96130_at	glycogenin	309.1	365.6	1.2	
rc_AA859804_at	GM2 ganglioside activator protein	335.6	280.7	-1.2	Q62639
D25543_at	golgi-associated protein GCP360	111.9	99.1	-1.2	Q63429
D25543_g_at	golgi-associated protein GCP360	222.6	160.1	-1.3	
rc_AI070295_g_at	growth arrest and DNA-damage-inducible 45 alpha	279.4	319.1	1.1	
rc_AI070295_at	growth arrest and DNA-damage-inducible 45 alpha	261.6	350.6	1.2	
U77829mRNA_s_at	growth arrest specific 5	151	119.5	-1.2	P30823
U77829mRNA_i_at	growth arrest specific 5	403.3	303.8	-1.4	P70605
L13619_at	growth response protein (CL-6)	314.5	133.8	-2.5	
L13619_g_at	growth response protein (CL-6)	340.4	184.3	-2.1	P32198
AF077354_at	heat shock 70 kDa protein 4	48.5	65.4	1.4	O88600
M14050_s_at	heat shock 70kD protein 5	941.3	775.5	-1.2	P00388
U05013_at	heme oxygenase 2	114.7	156.4	1.1	
X62875mRNA_g_at	high mobility group AT-hook 1	117.8	258.9	2.5	
X62875mRNA_at	high mobility group AT-hook 1	224.6	642.2	2.1	
rc_AA944177_at	high mobility group box 1	18.7	23.4	1.2	P30009
rc_AI029805_at	high mobility group box 1	17.5	79.3	3.2	P70490
rc_AI232374_at	Histone H1-0	437.4	818.9	2.0	P20070
rc_AI232374_g_at	Histone H1-0	190.1	843.5	2.8	P41137
rc_AA892014_s_at	HLA-B-associated transcript 1A	515.8	422.8	-1.2	P16975
rc_AA799735_at	homer, neuronal immediate early gene, 1	319.4	271	-1.1	Q63139
M65251_s_at	human immunodeficiency virus type 1 enhancer	38.1	142.7	3.7	P20607
	-binding protein 2				
D37951UTR#1_at	human immunodeficiency virus type 1 enhancer-	131.9	151.7	1.1	Q63714
	binding protein 2				
rc_AI105448_at	hydroxysteroid 11-beta dehydrogenase 1	323.4	555.8	1.6	O08876
rc_AI236145_at	hydroxysteroid dehydrogenase 17 beta, type 7	27.9	21.5	-1.3	O55081
U21718mRNA_at	hypothetical RNA binding protein RDA288	647.4	557.8	-1.1	O35804
Y09507_at	hypoxia inducible factor 1, alpha subunit	84.6	67.1	-1.3	
U17254_at	immediate early gene transcription factor NGFI-B	32.5	48.6	1.5	Q62655
U17254_g_at	immediate early gene transcription factor NGFI-B	22.4	79.2	3.5	Q64536
rc_AI011179_at	immunoglobulin binding protein 1	82.9	87.7	1.4	
rc_AI230256_at	Inhibitor of DNA binding 2, dominant negative helix-loop-helix protein	54.7	67.5	1.2	Q62736
rc_AI171268_at	Inhibitor of DNA binding 3, dominant negative helix-loop-helix protein	24.4	98.1	2.8	Q62745
U26397_at	inositol polyphosphate-4-phosphatase, type 1	90.2	106.6	1.1	P22829
X58375_at	Insulin receptor substrate 1	36.9	24.7	-1.4	P14423
M17960_at	Insulin-like growth factor II (somatomedin A)	26	13.9	-1.6	P12369
X66494_at	integrin alpha 7	110.7	158.4	1.3	P80299
X65036_at	integrin alpha 7	1782.4	1487.5	-1.1	P35570
M26744_at	Interleukin 6 (interferon, beta 2)	39.5	33.8	-1.3	P06536
rc_AA892314_at	isocitrate dehydrogenase 1	193.8	138.2	-1.3	P04937
rc_AI102838_s_at	Isovaleryl Coenzyme A dehydrogenase	144	115	-1.2	
AJ000557cds_s_at	Janus kinase 2 (a protein tyrosine kinase)	78.2	49	-1.2	O35804
U13396_at	Janus kinase 2 (a protein tyrosine kinase)	111.2	59.8	-1.5	P49088
U13396_g_at	Janus kinase 2 (a protein tyrosine kinase)	120.2	95.8	-1.3	Q62651
U58858_at	junction plakoglobin	182.1	134.9	-1.2	Q62947
AF083330_at	kinesin family member 3C	87.4	66.1	-1.3	O55165
L26292_at	Kruppel-like factor 4 (gut)	285.7	227.7	-1.3	
D12769_at	Kruppel-like factor 9	45.9	62.4	1.3	P08461
D12769_g_at	Kruppel-like factor 9	204.7	272	1.3	P28677
U07181_at	lactate dehydrogenase B	111.8	146.3	1.3	P37140
U07181_g_at	lactate dehydrogenase B	93.6	188.7	1.9	Q62609
rc_AI232078_at	LanC (bacterial lantibiotic synthetase component C)-like 1	717.1	818.8	1.1	O70436
rc_AA859783_at	large subunit ribosomal protein L36a	720.8	1590	1.7	P15429
J02962_at	lectin, galactose binding, soluble 3	111.9	93.8	-1.1	O88548
X13722	Low density lipoprotein re -2.8	88	239	P35952	
rc_AA892810_at	low density lipoprotein receptor-related protein associated protein 1	67.8	78.9	1.1	P20294
rc_AI237535_s_at	LPS-induced TNF-alpha factor	283	238.3	-1.2	Q00918
X84039_at	lumican	968.2	1081.7	1.1	
rc_AI234060_s_at	lysyl oxidase	308.1	219.1	-1.3	
AF067727_s_at	MAD homolog 1 (Drosophila)	39.6	24.9	-1.4	P97588

Probe_set	name	Sig. Con	Sig.Lin	F.Ch	Swisprot
rc_AI228675_at	MAD homolog 2 (Drosophila)	37.8	26.4	-1.5	O70185
AB017912_at	MAD homolog 2 (Drosophila)	245.3	184.4	-1.1	O70436
rc_AI008639_at	MAD homolog 4 (Drosophila)	22.1	91.3	3.2	P20070
U09870_at	major vault protein	191	238.1	1.4	
rc_AI010480_g_at	malate dehydrogenase mitochondrial	1843.9	2039	1.1	
rc_AI171506_g_at	Malic enzyme 1, soluble	462.5	383.3	-1.1	
M63485_at	matrin 3	84.9	171.6	2.1	P14882
X83537_at	matrix metalloproteinase 14, membrane-inserted	359.8	474	1.2	
rc_AA891916_g_at	membrane interacting protein of RGS16	449.5	370.8	-1.1	Q63399
rc_AI102562_at	Metallothionein	74	103.7	1.4	
rc_AA924198_s_at	mevalonate kinase	117.9	76.7	-1.5	
U53706_at	mevalonate pyrophosphate decarboxylase	121.7	97.1	-1.3	Q64346
rc_AI008638_at	milk fat globule-EGF factor 8 protein	524.2	1038	1.4	Q64654
rc_AI639082_s_at	mini chromosome maintenance deficient 6 (S. cerevisiae)	52.7	412.2	6.1	P43278
U73142_g_at	mitogen activated protein kinase 14	188.7	244.3	1.2	O35854
rc_AI171630_s_at	mitogen activated protein kinase 14	190.6	278.5	1.3	P16232
rc_AI178835_at	mitogen activated protein kinase kinase 1	25.7	11.3	-1.9	O35532
AF004811_at	moesin	156	139.1	-1.2	O35763
rc_AI105076_s_at	Murine thymoma viral (v-akt) oncogene homolog 2	120.5	86.6	-1.3	P48317
M27151_at	myogenic factor 6	13.2	24.9	1.6	
L00370cds_s_at	myosin, heavy polypeptide 3	715.4	444.1	-1.5	P08010
rc_AA859896_at	myristoylated alanine rich protein kinase C substrate	2.3	23.7	5.7	Q62809
rc_AA925762_at	myristoylated alanine rich protein kinase C substrate	70.7	63.5	-1.2	Q99068
rc_AA955167_s_at	myristoylated alanine rich protein kinase C substrate	107.9	93.7	-1.2	
rc_AA899253_at	myristoylated alanine rich protein kinase C substrate	393	319.9	-1.2	
J02679_s_at	NAD(P)H dehydrogenase, quinone 1	1536.9	1980	1.3	
rc_AI137246_s_at	neural cell adhesion molecule 1	490.3	399.5	-1.2	Q64320
U88958_at	neuritin	122.2	152.2	1.3	
AJ007288_at	neutrophil collagenease	25.5	1.6	-14.9	O88766
rc_AA799423_at	nexilin	1001.7	800.8	-1.2	P13721
rc_AA859752_at	Noggin	31.5	21.9	-1.4	
U31203_at	Noggin	109.9	95.1	-1.2	Q62744
AF036335_at	NonO/p54nrb homolog	47.3	217.7	3.7	O54725
AF036335_g_at	NonO/p54nrb homolog	5.8	302.4	45.3	O54725
AF077338_at	norvegicus myosin binding protein H	1816.6	1579.1	-1.1	O88599
rc_AI176488_at	nuclear factor I/B	55.8	64.9	1.1	P70618
AF014503_at	nuclear protein 1	1179.6	1003.5	-1.1	O54842
M14053_at	nuclear receptor subfamily 3, group C, member 1	26.7	36.1	1.3	P00564
rc_AI230572_at	nuclease sensitive element binding protein 1	33.7	95.5	1.9	O55081
rc_AA944007_at	nucleobindin	219.7	598.7	1.9	
rc_AA891045_at	nucleoporin p58	12.1	15.9	1.2	P28480
U03416_at	olfactomedin related ER localized protein	352.4	283.4	-1.2	
J04792_at	ornithine decarboxylase 1	396.4	441.6	1.1	P08699
U41853_at	oxygen regulated protein (150kD)	60.8	43.5	-1.3	Q62762
rc_AI009098_at	oxygen regulated protein (150kD)	327.7	255.5	-1.1	Q64654
U35345_s_at	p21 (CDKN1A)-activated kinase 2	56.3	40.7	-1.3	Q8VHU3
X98490cds_at	p32-subunit of replication protein A	90.8	103.1	1.2	P09660
M10068mRNA_s_at	P450 (cytochrome) oxidoreductase	180.2	138.8	-1.2	
AF067790_s_at	palmitoyl-protein thioesterase 2	22.2	84.4	3.7	O70489
rc_H33491_at	phenylalkylamine Ca2+ antagonist (emopamil) binding protein	127.2	69.3	-1.6	P47875
AF080568_at	phosphate cytidylyltransferase 2, ethanolamine	435.9	307.9	-1.3	O88637
AF080568_g_at	phosphate cytidylyltransferase 2, ethanolamine	416.8	313.4	-1.2	O88637
D64046_at	phosphatidylinositol 3-kinase, regulatory subunit,	48.6	56.1	1.2	Q00900
	polypeptide 2				
D64046_g_at	phosphatidylinositol 3-kinase, regulatory subunit,	19.8	76.6	3.7	Q63072
	polypeptide 2				
D88666_at	phosphatidylserine-specific phospholipase A1	302.3	432.9	1.4	P70500
X51529_at	phospholipase A2, group IIA (platelets, synovial fluid)	28.6	46.9	1.4	
rc_AA998446_s_at	phosphotidylinositol transfer protein, beta	242	177.9	-1.2	Q15815
X64563cds_at	plasminogen activator inhibitor 2 type A	36.9	29.2	-1.4	Q02195
U72620_at	pleiomorphic adenoma gene-like 1	425.9	348	-1.2	P97599
AB020504_at	PMF32 protein	145.2	109.2	-1.3	Q9Z2X7
AB020504_g_at	PMF32 protein	239.7	166.2	-1.4	Q9Z2X7
U69884_at	potassium intermediate/small conductance	18.6	28.9	1.5	Q62981

Probe_set	name	Sig. Con	Sig.Lin	F.Ch	Swisprot
X17053mRNA_s_at	small inducible cytokine A2	261.9	432	1.5	
rc_AA799760_s_at	solute carrier family 2 , member 4	10	39.6	3.2	
S68135_s_at	solute carrier family 2,member 1	75.1	32.7	-2.1	
D12770_s_at	solute carrier family 25 (mitochondrial adenine	1845.3	2183.3	1.2	Q01713
	nucleotide translocator) member 4				
rc_AA892776_at	solute carrier family 25 (mitochondrial carrier; adenine	939.7	2066.7	1.5	Q99MI5
	nucleotide translocator), member 3				
U70476_at	solute carrier family 7, member 1	154.1	120.1	-1.2	P70565
rc_AA892557_at	spermidine synthase	148.6	185.8	1.1	Q9JL55
rc_AA955859_at	splicing factor, arginine/serine-rich	28.2	41.2	1.3	
	(transformer 2 Drosophila homolog) 10				
AJ004858_at	SRY-box containing gene 11	50.2	38.7	-1.2	Q04889
M81639_at	stannin	103.6	493.9	3.2	P18297
rc_AI175764_s_at	stearoyl-Coenzyme A desaturase 1	25.6	6.2	-4.6	
rc_AA875269_at	stearoyl-Coenzyme A desaturase 2	2173.3	1132.7	-1.9	
rc_AI172293_at	sterol-C4-methyl oxidase-like	1312.5	896.5	-1.4	P13596
U39546_at	surface protein MCA-32	12	29.9	2.3	
D78359_at	sushi-repeat-containing protein	236	191.3	-1.2	Q03527
S45663_g_at	synaptic glycoprotein SC2	1300.3	995.7	-1.2	
S45663_at	synaptic glycoprotein SC2	1679.6	1307.9	-1.2	Q62904
U90312_at	Synaptojanin II	86.4	104.3	1.2	P70618
X75785_at	Synaptonemal complex protein 3	2.8	4	2.1	
rc_AA892759_at	synaptosomal-associated protein, 23 kD	237.6	204	-1.1	P41562
rc_AI102079_at	Syntaxin binding protein 1	384.3	538.5	1.4	P51638
rc_AA859980_at	T-complex 1	734	350.5	-2.0	O70603
rc_AA859980_g_at	T-complex 1	1313.2	541.8	-2.1	P09896
rc_AI071299_at	TGFB inducible early growth response	21.6	33	1.3	P51638
rc_AI172476_at	TGFB inducible early growth response	79	133	1.5	P30120
rc_AI169327_g_at	tissue inhibitor of metalloproteinase 1	518.8	442	-1.1	
rc_AA799340_at	tissue inhibitor of metalloproteinase 2	1592.6	1863.3	1.1	P13721
rc_AA899854_at	topoisomerase (DNA) 2 alpha	427	502.1	1.2	
rc_AA926242_at	trans-golgi network protein 1	11.6	16.5	1.5	
U09228_at	transcription factor 4	105.2	76.5	-1.3	Q62622
U51583_at	transcription factor 8	82.6	173.1	1.4	Q63617
rc_AA800787_at	Transferrin	702.8	559.8	-1.2	
U03491_g_at	transforming growth factor, beta 3	194.8	284.4	1.4	P11167
U03491_at	transforming growth factor, beta 3	257.8	409	1.4	P35355
M83107_at	Transgelin (Smooth muscle 22 protein)	2340	1937	-1.1	P43244
Z14030_at	TRAP-complex gamma subunit	46.7	199.7	3.5	O35800
X68101_at	trg	114.8	136.6	1.1	
rc_AA891880_at	tricarboxylate carrier-like protein	221.8	172.6	-1.2	
rc_AA891880_g_at	tricarboxylate carrier-like protein	218.7	174.9	-1.2	
J02780_at	Tropomycin 4	441.4	365.2	-1.1	P97535
Y15054_at	tumor specific antigen 70 kDa	49.8	60.1	1.1	O08651
S55223_s_at	tyrosine 3-monooxgenase/tryptophan 5 monooxgenase	552.6	480.8	-1.1	Q62724
	activation protein, beta polypeptide				
rc_AI236721_r_at	tyrosine 3-monooxgenase/tryptophan 5-monooxgenase	103.8	79.7	-1.3	
	activation protein, gamma polypeptide				
rc_AI180424_at	Tyrosine 3-monooxygenase/tryptophan 5-monooxygenase	766.9	1563.3	2.1	
	activation protein, zeta polypeptide				
U75397UTR#1_s_at	U75397UTR#1 RNKROX2 Rattus norvegicus Krox-24	114.3	159.2	1.4	
U75404UTR#1_s_at	U75404UTR#1 RNU75404 Rattus norvegicus Ssecks 322	90	104.9	1.1	
U75927UTR#1_at	cytochrome oxidase subunit VIIa mRNA, 3'	61.8	89.7	1.4	
	untranslated region, partial sequence				
U95001UTR#1_s_at	developmentally-regulated cardiac factor (DRCF-5)	207.2	537.3	1.9	
D17296_at	ubiquitin C	1965.8	3290.3	1.3	P31399
U54632_g_at	Ubiquitin conjugating enzyme E2I	422.6	616.9	1.3	
AF047707_at	UDP-glucose:ceramide glycosyltransferase	233.5	315.3	1.4	Q9R0E0
rc_AI145931_at	UDP-N-acetylglucosamine-2-epimerase/	56.3	92.2	1.3	
	N-acetylmannosamine kinase				
rc_AI008423_at	unc-50 related protein (UNCL)	180.1	248.2	1.3	
X74832cds_at	unconventional myosin Myr2 I heavy chain	84.3	114.8	1.4	P29524
AB010743_at	Uncoupling protein 2, mitochondrial	92.2	261.2	3.0	P56500
U40628_at	unknown Glu-Pro dipeptide repeat protein	376.2	430.1	1.1	

Probe_set	name	Sig. Con	Sig.Lin	F.Ch	Swisprot
rc_AA850885_s_at	unknown Glu-Pro dipeptide repeat protein	2265.8	3650.5	1.6	
rc_AA944014_at	v-jun sarcoma virus 17 oncogene homolog (avian)	39	53.2	1.3	P01026
rc_AA945867_at	v-jun sarcoma virus 17 oncogene homolog (avian)	201.7	244.4	1.2	
rc_AI175959_at	v-jun sarcoma virus 17 oncogene homolog (avian)	792.2	913.9	1.1	P41138
U56242_at	v-maf musculoaponeurotic fibrosarcoma (avian) oncogene homolog	86	68	-1.2	Q63622
Y00396mRNA_g_at	v-myc avian myelocytomatosis viral oncogene homolog	132.1	110.9	-1.1	
X63722cds_s_at	Vascular cell adhesion molecule 1	75.7	122.9	1.9	
rc_AA850734_at	vascular endothelial growth factor	101.6	97.2	-1.2	
AF054826_at	vesicle-associated membrane protein 5	424.4	293.6	-1.4	Q9Z2J5
D10666_at	visinin-like 1	203.6	144.1	-1.3	
AF037272_at	wap four-disulfide core domain 1	47.5	36.1	-1.4	O70280
X07686cds_s_at	X07686cds RNLB6 Rat L1Rn B6 repetitive DNA element	13.6	68.3	2.6	
X07729exon#5_s_at	X07729exon#5 RNEN4 R.norvegicus gene encoding neuron-specif	62.6	155.3	2.5	
X13527cds_s_at	X13527cds RNFASACP Rat mRNA fragment for the acyl carrier pr	505.2	397.4	-1.2	
X14848cds#12_at	X14848cds#12 MIRNXX Rattus norvegicus mitochondrial genome	15.6	18.2	1.2	
X51536cds_g_at	X51536cds RRRPS3 Rat mRNA for ribosomal protein S3	3154.2	3906.2	1.1	
X54249mRNA_s_at	X54249mRNA RRATBP1 Rat mRNA for a zinc finger protein AT-BP1	36.8	50	1.2	
X56729mRNA_at	X56729mRNA RSCALPST Rat mRNA for calpastatin	33.1	83.9	1.9	
X60351cds_s_at	X60351cds RRLENSABC R.rattus mRNA for alpha B-crystallin (ocu	1040.6	1509.5	1.4	
X62951mRNA_s_at	X62951mRNA RNPBUS19 R.norvegicus mRNA (pBUS19) with repeti	90.3	111.2	1.3	
X76489cds_g_at	X76489cds RNCD9 R.norvegicus (Sprague Dawley) CD9 mRNA for	289.2	427.7	1.2	
X76489cds_at	X76489cds RNCD9 R.norvegicus (Sprague Dawley) CD9 mRNA for	139.3	440.9	2.8	
X89697cds_at	X89697cds RNTPCR07P R.norvegicus mRNA for TPCR07 protein	16.6	27.7	1.5	
X89698cds_at	X89698cds RNTPCR09P R.norvegicus mRNA for TPCR09 protein	19.6	29.3	1.7	
X89699cds_at	X89699cds RNTPCR10P R.norvegicus mRNA for TPCR10 protein	11.6	22.9	2.1	
X97374exon_g_at	X97374exon RNPPNEX2 R.norvegicus gene encoding prepronocice	106.7	128.2	1.1	
rc_AI171167_at	ZAP 36/annexin IV	76.9	270.1	3.2	
U27186_at	zinc finger protein 111	64.9	72.8	1.2	Q64654
U56862_at	zinc finger protein 260	69.5	51.2	-1.2	Q63622
L16995_at	ADD1/sterol regulatory element binding factor 1	170.3	73	-2.5	
AJ005023_at	MHC class Ia A1b antigen	144.6	102.8	-1.2	
D17521_at	protein kinase C-regulated chloride channel(ClC-3)	119	151.9	1.2	Q63555
S63521_i_at	glucose-regulated protein GRP78	388.4	299.8	-1.3	P41123
D87991_at	UDP-galactose transporter related isozyme 1	420	327.3	-1.2	Q63788
Z12158cds_at	pyruvate dehydrogenase E1 alpha form 1 subunit	546.6	424.9	-1.1	
X80130cds_i_at	alpha-actin cardiac protein	674.1	487.9	-1.4	P25108
D87991_g_at	UDP-galactose transporter related isozyme 1	748.4	636.4	-1.2	Q63769
U77931_at	rRNA promoter binding protein	1091.5	894.4	-1.2	P97612
X12367cds_s_at	glutathione peroxidase I	1626.2	1439.1	-1.1	O35823
X15013cds_at	ribosomal protein L7a	1783.2	1647.6	1.1	
X06801cds_i_at	vaskular alpha-actin	2869.4	2410.9	-1.2	P70473
X15013cds_g_at	ribosomal protein L7a	2210.9	2461.6	1.1	P05713
X51707cds_s_at	ribosomal protein S19	2163.2	2568.6	1.1	
X51706cds_at	ribosomal protein L9	2617.1	2967.5	1.1	
X51706cds_g_at	ribosomal protein L9	2573.6	2998.2	1.1	P20280

APPENDIX II

Probe_set	Name	Sig. Con	Sig.Lin	F.Ch
rc_AA799330_at	ESTs	176.9	218.5	1.1
rc_AA799396_g_at	ESTs	449.7	361.8	-1.2
rc_AA799406_at	ESTs	531.4	451.5	-1.1
rc_AA799467_at	ESTs	70.2	112	1.3
rc_AA799539_at	ESTs	85.4	68	-1.3
rc_AA799591_at	ESTs	188.4	196.4	1.1
rc_AA799601_at	ESTs	135.6	105.9	-1.2
rc_AA799616_at	ESTs	310.8	247.3	-1.1
rc_AA799637_at	ESTs	33.4	17.4	-1.2
rc_AA799637_g_at	ESTs	42.6	22.5	-1.3
rc_AA799680_at	ESTs	254.8	217.6	-1.1
rc_AA799691_at	ESTs	253.4	208.4	-1.2
rc_AA799721_g_at	ESTs	200.3	174.1	-1.2
rc_AA799751_at	ESTs	284.2	329.6	1.1
rc_AA799773_at	ESTs	1206.7	876.8	-1.3
rc_AA799773_g_at	ESTs	1456.6	1105.3	-1.3
rc_AA799832_at	ESTs	587.7	700.1	1.2
rc_AA799899_i_at	ESTs	3701.2	3163.1	-1.1
rc_AA800017_at	ESTs	102.3	122.2	1.1
rc_AA800034_at	ESTs	917.5	867.1	-1.1
rc_AA800036_at	ESTs	278.1	270.9	-1.2
rc_AA800039_s_at	ESTs	498.5	430	-1.1
rc_AA800176_at	ESTs	64.6	52.8	-1.2
rc_AA800199_at	ESTs	130.8	101.6	-1.2
rc_AA800200_at	ESTs	41.5	31.3	-1.3
rc_AA800202_at	ESTs	8.5	8.5	1.4
rc_AA800206_at	ESTs	76.3	60	-1.4
rc_AA800218_at	ESTs	250.9	231.3	-1.1
rc_AA800315_at	ESTs	69.2	62.2	-1.1
rc_AA800576_at	ESTs	606.7	417.9	-1.3
rc_AA800622_at	ESTs	313	273.6	-1.1
rc_AA800678_g_at	ESTs	812.6	687.8	-1.2
rc_AA800686_at	ESTs	73.9	34.2	-1.7
rc_AA800693_g_at	ESTs	137.2	114.6	-1.2
rc_AA800711_at	ESTs	66.8	45	-1.4
rc_AA800737_at	ESTs	140	109.5	-1.3
rc_AA800750_f_at	ESTs	110.2	139.1	1.1
rc_AA800772_at	ESTs	32.9	37.3	-1.3
rc_AA800850_at	ESTs	426.7	359.6	-1.2
rc_AA800881_at	ESTs	59.3	34.1	-1.6
rc_AA858588_g_at	ESTs	344.3	296.4	-1.1
rc_AA858617_at	ESTs	75.3	106.5	1.1
rc_AA859520_at	ESTs	87	135.4	1.5
rc_AA859536_at	ESTs	1147.4	881.9	-1.3
rc_AA859562_at	ESTs	118.3	129.3	1.2
rc_AA859585_at	ESTs	343.3	416.2	1.2
rc_AA859627_at	ESTs	11.4	15.7	1.4
rc_AA859633_at	ESTs	26.7	22.9	-1.3
rc_AA859633_g_at	ESTs	132.1	78.4	-1.3
rc_AA859690_at	ESTs	59.2	79.6	1.2
rc_AA859725_at	ESTs	24.3	40.3	1.5
rc_AA866234_at	ESTs	501.4	597.9	1.1
rc_AA866276_at	ESTs	1266.7	1021.4	-1.2
rc_AA866299_at	ESTs	219	219.9	-1.2
rc_AA866299_g_at	ESTs	224.7	181.9	-1.1
rc_AA866454_at	ESTs	378.2	277.4	-1.2
rc_AA874827_at	ESTs	91.1	123.9	1.2
rc_AA874912_at	ESTs	17.3	29.5	1.7
rc_AA874928_g_at	ESTs	317.2	358.3	1.1

Probe_set	Name	Sig. Con	Sig.Lin	F.Ch
rc_AA874943_at	ESTs	381	318.2	-1.3
rc_AA875098_at	ESTs	139.7	110	-1.2
rc_AA875126_at	ESTs	49.7	37	-1.2
rc_AA875215_at	ESTs	23.5	37.2	1.4
rc_AA875255_at	ESTs	33.9	21.6	-1.6
rc_AA875263_at	ESTs	368	298.7	-1.2
rc_AA875288_at	ESTs	46.2	32.3	-1.4
rc_AA875327_at	ESTs	449.5	366.7	-1.1
rc_AA875444_at	ESTs	20.1	13.4	-1.5
rc_AA875495_at	ESTs	152.2	114.5	-1.3
rc_AA875523_r_at	ESTs	284.5	224.4	-1.3
rc_AA875615_at	ESTs	15.5	11	-1.1
rc_AA875620_at	ESTs	173.5	113.2	-1.4
rc_AA875620_g_at	ESTs	301.6	215.4	-1.3
rc_AA875633_at	ESTs	390.1	320.6	-1.1
rc_AA891308_at	ESTs	136.7	92.5	-1.3
rc_AA891595_at	ESTs	140.1	101.9	-1.3
rc_AA891631_at	ESTs	11.4	19.1	1.3
rc_AA891669_g_at	ESTs	501.8	684.9	1.3
rc_AA891724_at	ESTs	440.4	274.9	-1.4
rc_AA891727_at	ESTs	315.9	250.6	-1.2
rc_AA891940_at	ESTs	588.8	595.5	1.1
rc_AA891944_at	ESTs	50.6	72.8	1.3
rc_AA892006_g_at	ESTs	268.3	217.9	-1.2
rc_AA892120_at	ESTs	145.7	184.8	1.2
rc_AA892154_g_at	ESTs	190.7	164.8	-1.1
rc_AA892238_at	ESTs	330.4	291	-1.1
rc_AA892248_at	ESTs	1555.4	1955.2	1.3
rc_AA892248_g_at	ESTs	2074.7	2504.1	1.2
rc_AA892273_at	ESTs	189.8	216.1	1.2
rc_AA892284_at	ESTs	139.3	162.5	1.1
rc_AA892300_at	ESTs	141.5	108.6	-1.2
rc_AA892310_at	ESTs	113.8	94.6	-1.2
rc_AA892364_at	ESTs	138.5	134	1.1
rc_AA892378_at	ESTs	326.5	274.6	-1.1
rc_AA892378_g_at	ESTs	802.2	656.5	-1.2
rc_AA892399_at	ESTs	63.9	58.8	-1.2
rc_AA892768_at	ESTs	282.1	235.1	-1.1
rc_AA892779_at	ESTs	97.8	86.6	-1.2
rc_AA892789_at	ESTs	196.9	243.7	1.1
rc_AA892832_at	ESTs	877.2	723.6	-1.1
rc_AA892847_at	ESTs	73.5	55.5	-1.3
rc_AA892851_g_at	ESTs	277.4	216.1	-1.2
rc_AA893022_at	ESTs	132.1	103.3	-1.2
rc_AA893032_at	ESTs	75.3	39.1	-2.0
rc_AA893172_at	ESTs	98.6	84.6	-1.1
rc_AA893183_g_at	ESTs	53	72.4	1.4
rc_AA893185_at	ESTs	528.4	619.4	1.1
rc_AA893230_at	ESTs	14	18.1	1.3
rc_AA893273_at	ESTs	85.1	44.5	-1.3
rc_AA893357_at	ESTs	267.1	323.6	1.2
rc_AA893493_i_at	ESTs	2656.9	2025.6	-1.2
rc_AA893641_at	ESTs	91.5	71.7	-1.2
rc_AA893641_g_at	ESTs	176.8	140	-1.2
rc_AA893659_at	ESTs	195.1	158.4	-1.2
rc_AA893717_at	ESTs	286.3	315.4	1.1
rc_AA893811_at	ESTs	341	263.3	-1.2
rc_AA893994_at	ESTs	13	11.8	-1.4
rc_AA894092_at	ESTs	41.1	38.4	-1.2
rc_AA894200_at	ESTs	175.7	139	-1.2
rc_AA894200_g_at	ESTs	2180.3	1821.3	-1.2
rc_AA894264_at	ESTs	55.9	28.9	-1.7
rc_AA894282_at	ESTs	284.5	193.6	-1.1
rc_AA894312_at	ESTs	166.5	138.8	-1.1
rc_AA894318_at	ESTs	356.9	260.5	-1.4
rc_AA894345_at	ESTs	464.7	373.2	-1.2
rc_AI007614_at	ESTs	22.8	30.4	1.4
rc_AI007824_at	ESTs	2553.8	2936.1	1.1
rc_AI010580_s_at	ESTs	165.8	217.7	1.3
rc_AI102868_g_at	ESTs	583.4	679.8	1.1

Probe_set	Name	Sig. Con	Sig.Lin	F.Ch
rc_AI176422_g_at	ESTs	117	189.5	1.3
rc_AI176456_at	ESTs	57.2	88.9	1.1
rc_AI177404_at	ESTs	104	240.4	2.0
rc_AI229924_at	ESTs	70.9	85.9	1.2
rc_AI236601_at	ESTs	359.3	465.7	1.2
rc_AI237007_at	ESTs	33.2	44.9	1.5
rc_AI638939_at	ESTs	54.3	70.4	1.2
rc_AI638949_s_at	ESTs	225.7	195.5	-1.1
rc_AI638989_at	ESTs	310.5	451.5	1.4
rc_AI639008_at	ESTs	79.8	313.3	4.3
rc_AI639042_at	ESTs	2.4	75.6	22.6
rc_AI639043_at	ESTs	4.3	31.6	6.1
rc_AI639045_at	ESTs	9.9	73.2	4.0
rc_AI639058_s_at	ESTs	1073.2	1332.6	1.2
rc_AI639119_at	ESTs	2.8	17.7	3.7
rc_AI639120_at	ESTs	85.1	173.4	4.9
rc_AI639148_at	ESTs	35.9	40.1	1.2
rc_AI639154_at	ESTs	22.8	53.7	2.1
rc_AI639155_at	ESTs	1.1	89.2	27.9
rc_AI639188_at	ESTs	49.5	334.6	4.9
rc_AI639255_at	ESTs	85.1	101.6	1.1
rc_AI639260_at	ESTs	2.7	16.2	3.2
rc_AI639289_at	ESTs	21.2	24.8	1.2
rc_AI639305_at	ESTs	9.8	36.4	3.0
rc_AI639305_g_at	ESTs	6.8	31.7	4.9
rc_AI639306_at	ESTs	44.8	84.5	2.0
rc_AI639308_at	ESTs	65.9	53.5	-1.3
rc_AI639336_at	ESTs	13.5	65.4	4.6
rc_AI639339_at	ESTs	0	18.8	194.0
rc_AI639371_at	ESTs	5.8	13.4	2.3
rc_AI639372_at	ESTs	22.6	96.3	2.6
rc_AI639381_at	ESTs	81.7	116	1.2
rc_AI639410_i_at	ESTs	0.8	48	48.5
rc_AI639410_s_at	ESTs	32.3	293.1	8.6
rc_AI639411_at	ESTs	7.7	183.3	27.9
rc_AI639411_g_at	ESTs	185.4	561.5	2.8
rc_AI639412_at	ESTs	5.6	45.6	4.0
rc_AI639447_at	ESTs	104.6	143	1.5
rc_AI639474_at	ESTs	39.4	223	6.1
rc_AI639475_at	ESTs	1.3	53.1	18.4
rc_AI639476_s_at	ESTs	240.4	271.6	1.2
rc_AI639510_at	ESTs	10.4	39.2	2.6
rc_H31351_at	ESTs	137.3	170	1.1
rc_H31479_at	ESTs	225.1	195.3	-1.3
rc_H31588_at	ESTs	38.9	70.6	1.6
rc_H31976_at	ESTs	213.8	205	-1.2
rc_H33426_at	ESTs	152.3	74.9	-1.9
rc_H33426_g_at	ESTs	114.6	67.7	-1.7